

AALBORG UNIVERSITY

Optimal Control for Water Distribution

Electronic & IT:
Control & Automation

Group:
CA-830

STUDENT REPORT

November 21, 2017

**First year of MSc study**

Electronic and IT

Fredrik Bajers Vej 7

DK-9220 Aalborg East, Denmark

<http://www.es.aau.dk>

AALBORG UNIVERSITY

STUDENT REPORT

Topic:

Optimal Control for Water Distribution

Project:

P8-project

Project time:

February 2017 - May 2017

Projectgroup:

17gr830

Participants:

Daniel Böhner Andersen
Ignacio Trojaola Bolinaga
Krisztian Mark Balla
Nicolaj Vinkel Christensen
Simon Bjerre Krogh

Supervisors:

Tom Nørgaard Jensen
Carsten Kallesøe

Synopsis:

This project covers the modelling and predictive control of a water distribution network with the aim of minimizing economic cost. The system consists of pipes, valves, pumps and additionally a water tower.

At first a non-linear model of the components and the dynamics of the system is modelled with a graph-based approach. System identification is carried out on the non-linear model due to the uncertainties in the network. The non-linear model is however linearized and a new parameter estimation is carried out with more acceptable results.

A model predictive controller is designed to minimize the running cost of the linearized model subject to constraints defined by measurements on a real-world test setup. Furthermore, PI controllers are designed to control the system with the reference set by the MPC.

Verification of the controller is attempted by simulation.

At the end, a discussion reflects on the results of the simulation and a conclusion sums up the possibilities of further improvements.

Number of pages: 113

Appendix: 38 + CD

Completed November 21, 2017

Preface

This report covers the 8th semester project at Control and Automation at Aalborg university for the Department of Electronic systems. The project is produced by group 17gr830.

The goal of this project is to control and optimize the running cost of a water distribution system, which is extended with a water tower.

The report starts with a small introduction to the system, how it is modelled and parameters are estimated. This is followed by the simulation, derivation of the controller and implementation. A discussion about ideas of improvement leads up to the final conclusion.

The reader can find a nomenclature at the beginning of the report which includes acronyms, a symbolic list and a notation list. In the appendix, detailed derivation, an assumption list, relevant measurements used for this project and a complete overview of the test setup can be found.

Aalborg University, 30th of May 2017

Daniel Böhner Andersen
dban13@student.aau.dk

Ignacio Trojaola Bolinaga
itroja16@student.aau.dk

Krisztian Mark Balla
kballa16@student.aau.dk

Nicolaj Vinkel Christensen
nvch13@student.aau.dk

Simon Bjerre Krogh
skrogh13@student.aau.dk

Nomenclature

Acronyms

PMA	Pressure Management Area
CP	Critical Point
WT	Water Tower
MP	Minimization Problem
OD	Opening Degree
KVL	Kirchhoff's Voltage Law
KCL	Kirchhoff's Current Law
MPC	Model Predictive Control
GT	Graph Theory
NRMSE	Normalized Root Mean Square Error
MNGB	Matlab Nonlinear Grey Box

Symbols

Symbol	Description	Unit
A	Cross sectional area	$[m^2]$
C_k	k^{th} component of the distribution network	$[\cdot]$
C	Electric capacitance	$[F]$
C_H	Hydraulic capacitance	$[m^3/(N/m^2)]$
D	Diameter	$[m]$
f	Moody friction factor	$[\cdot]$
$f(\mathbf{q}, \mathbf{OD})$	Vector field describing the pressure drops	$[bar]$
F	Force	$[N]$
g	Acceleration due to gravity	$[m/s^2]$
h	Height of the fluid in the water Tower	$[m]$
h_f	Pressure given in head	$[m]$
h_m	Form loss	$[m]$
I	Electric Current	$[A]$
\mathcal{I}	Identity matrix	$[\cdot]$
J_k	Inertia of the k^{th} component	$[kg/m^4]$
k_f	Form loss coefficient	$[\cdot]$
$k_v(\mathbf{OD})$	Conductivity function	$[\cdot]$
L	Length	$[m]$
m	Mass of body	$[kg]$
M	Linear momentum	$[kgm/s]$
n_{gl}	Valve characteristic curve factor	$[\cdot]$
OD	Opening Degree	$[\cdot]$
p_a	Atmospheric pressure	$[bar]$
P_e	Power consumption of the pumps	$[W]$
P_h	Hydraulic power	$[W]$
q_k	Flow through the k^{th} component	$[m^3/h]$
Re	Reynolds Number	$[\cdot]$
T	Temperature	$[^\circ]$
U	Electric voltage	$[V]$
$u(\cdot)$	Vector field describing inputs	$[bar]$
v	Velocity	$[m/s]$
V_t	Volume of water in the water tower	$[m^3]$
\mathbf{y}	Vector describing the model outputs	$[bar]$
z	Flow through the chords	$[m^3/h]$
$\alpha_k(\cdot)$	Pressure boost given by the k^{th} pump	$[bar]$
$\gamma_k(\cdot)$	Pressure drop across the WT-connection	$[bar]$
Δp_k	Pressure drop across the i^{th} component	$[bar]$
Δz_h	Head loss due to elevation.	$[m]$
ϵ	Average roughness	$[m]$
ζ	Pressure drop from elevation across the k^{th} component	$[bar]$
η	Efficiency of the pumps	$[\cdot]$
θ_{max}	Maximum angle of the valve opening degree	$[^\circ]$
θ_{off}	Minimum angle where the valve closes	$[^\circ]$
θ_{OD}	Angle of valve opening degree	$[^\circ]$
$\lambda_k(\cdot)$	Pressure drop across the k^{th} pipe	$[bar]$
$\mu_k(\cdot)$	Pressure drop across the k^{th} valve	$[bar]$
ν	Kinematic viscosity	$[kg/ms]$
ρ	Density	$[kg/m^3]$
Υ	Objective function for the minimization	$[DKK]$
ω_r	Pump impeller rotational speed	$[rad/s]$

Graph theory

Symbol	Description	Unit
e	Number of edges in the graph	$[\cdot]$
\mathbf{H}	Incidence matrix	$[\cdot]$
\mathbf{H}_c	Incidence matrix corresponding to the chords	$[\cdot]$
\mathbf{H}_f	Incidence matrix corresponding to the spanning tree	$[\cdot]$
\mathcal{G}	System Graph	$[\cdot]$
\mathcal{T}	Spanning tree	$[\cdot]$
l	Number of chords	$[\cdot]$
\mathbf{B}	Cycle matrix	$[\cdot]$
\mathbf{B}_c	Cycle matrix corresponding to the chords	$[\cdot]$
\mathbf{B}_f	Cycle matrix corresponding to the spanning tree	$[\cdot]$
n_i	i^{th} node of the distribution network	$[\cdot]$

Glossary of mathematical notation

This section sums up the mathematical notation and terminology used in this report.

Upper and lower bounds of a variable

$$\underline{x} < x < \bar{x} \quad (1)$$

Where $x \in \mathbb{R}$ and \bar{x} and \underline{x} are the upper and lower bounds, respectively.

Intervals

$$[a, b] = \{x \in \mathbb{R} | a \leq x \leq b\} \underline{x} < x < \bar{x} \quad (2)$$

Where \bar{x} and \underline{x} are the upper and lower bounds, respectively.

Vectors and matrices

Vectors and matrices are noted with bold fonts, such that \mathbf{v} is a vector:

$$\mathbf{v} = \begin{bmatrix} v_1 \\ v_2 \\ \vdots \\ v_n \end{bmatrix} \in \mathbb{R}^{(n \times 1)} \quad (3)$$

and \mathbf{M} is a matrix:

$$\mathbf{M} = \begin{bmatrix} m_{11} & m_{12} & \dots & m_{1k} \\ m_{21} & m_{22} & \dots & m_{2k} \\ \vdots & \vdots & \ddots & \vdots \\ m_{n1} & m_{n2} & \dots & m_{nk} \end{bmatrix} \in \mathbb{R}^{(n \times k)} \quad (4)$$

Continues vector variables are noted with $\mathbf{v}(\mathbf{t})$ such that:

$$\mathbf{v}(\mathbf{t}) = \begin{bmatrix} v_1(t) \\ v_2(t) \\ \vdots \\ v_n(t) \end{bmatrix} \in \mathbb{R}^{(n \times 1)} \quad (5)$$

While discrete vector variables are referred to as sequences and noted with $\mathbf{v}[\mathbf{k}]$, such that:

$$\mathbf{v}[\mathbf{k}] = \begin{bmatrix} v_1[k] \\ v_2[k] \\ \vdots \\ v_n[k] \end{bmatrix} \in \mathbb{R}^{(n \times 1)} \quad (6)$$

is a sequence, where k is the time step between two entries.

The pseudo inverse of a matrix is noted with \mathbf{M}^\dagger .

Small-signal and operating point values

Small-signals are noted with \hat{u} and the operating point values are noted with \bar{u} .

Derivatives

The partial derivative of a function is noted with

$$\frac{\partial f(x, y)}{\partial x} \quad (7)$$

The derivative of a vector by vector is noted with:

$$\frac{\partial \mathbf{v}}{\partial \mathbf{w}} = \begin{bmatrix} \frac{\partial v_1}{\partial w_1} & \frac{\partial v_1}{\partial w_2} & \cdots & \frac{\partial v_1}{\partial w_n} \\ \frac{\partial v_2}{\partial w_1} & \frac{\partial v_2}{\partial w_2} & \cdots & \frac{\partial v_2}{\partial w_n} \\ \vdots & \vdots & \ddots & \vdots \\ \frac{\partial v_k}{\partial w_1} & \frac{\partial v_k}{\partial w_2} & \cdots & \frac{\partial v_k}{\partial w_n} \end{bmatrix} \quad (8)$$

If the size of vector \mathbf{v} and \mathbf{w} are the same, the resulting matrix is referred to as a Jacobian.

The time derivative of a function is noted with

$$\dot{f} = \frac{df(t)}{dt} \quad (9)$$

Vector fields

Vector fields are introduced, and represent vector valued functions such that the mapping is the following:

$$\alpha(\mathbf{v}) : \mathbb{R}^{(n)} \rightarrow \mathbb{R}^{(n)} : [v_1, v_2, \dots, v_n] \rightarrow [\alpha(v_1), \alpha(v_2), \dots, \alpha(v_n)] \quad (10)$$

Contents

Nomenclature	v
1 Introduction	1
I Analysis	3
2 System Description	5
2.1 System overview	5
3 Requirements and Constraints	7
4 Modelling	9
4.1 Hydraulic modelling	9
4.1.1 Pipe model	9
4.1.2 Valve model	13
4.1.3 Pump model	16
4.1.4 Water Tower	17
4.1.5 Complete component model	18
4.2 Simplification and electrical analogy	19
4.3 Graph representation	21
4.3.1 Network model	22
4.3.2 Pressure drop across the nodes	26
4.4 Nonlinear Parameter identification	26
4.4.1 Measurements on the test setup	28
4.4.2 Estimation method	29
4.4.3 Nonlinear Estimation Outcomes	29
4.5 Linearization of the model	29
4.5.1 Taylor expansion on a simple example	30
4.5.2 Linear system model	31
4.5.3 State-space model for linear parameter estimation	32
4.6 Linear parameter estimation	35
4.6.1 Model Parameters	36
4.6.2 Measurements on the test setup	36
4.6.3 Linear Estimation Outcomes	37
4.7 State-space model for control	40
4.7.1 Discretization of state-space model	42
4.8 Verification of model	44
II Control Design	47
5 Controller	49
5.1 Control Problem	49
5.2 Model predictive control	51
5.3 Reformulation of the objective function	52
5.4 Constraints	57

5.5	Convexity	59
5.6	PI controller	61
6	Control System Implementation	63
6.1	Simulink implementation	63
6.2	Implementation goals	64
6.3	Implementation with input constraint	65
III	Conclusion and verification	69
7	Discussion	71
8	Conclusion	73
IV	Appendices	75
A	Unit Conversion	77
B	Assumption List	79
C	System Description	81
C.1	Components of the System	81
C.2	System Topology	83
C.3	System Graph	85
C.4	Spanning Tree	86
C.5	Incidence Matrix	87
C.6	Cycle Matrix	87
C.7	Mapping matrices	88
D	Linearization	89
E	Nonlinear estimation	91
F	Linear estimation	95
F.1	First linear parameter estimation	95
F.2	Second linear parameter estimation	96
G	Electrical price	99
H	Pump linearization and PI controller	101
I	Measurements	105
I.1	System time constant	105
I.2	System dynamics	106
J	Test considerations	109
	Bibliography	111

Water pressure management is a vital part of the water supply infrastructure all over the world. It ensures that an appropriate water pressure is present such that the consumers are supplied with water at all time. Maintaining a minimum pressure in the network is an important task as it ensures the end-user a decent water pressure and also minimizes the risk of contamination in the water system[1].

In the U.S alone, 4 % of the national energy consumption is used on moving and treating water or wastewater[2]. With an increasing focus on green energy, more renewable energy sources are added to the grid. Nevertheless, the intermittent behavior of renewable sources and time-dependent consumer preferences result in fluctuation of the available power. This means that the price for electric power also varies [3]. To minimize the cost of running a water distribution network, potential stored energy can be used to maintain a minimum pressure. When electric prices are low, water can be pumped to a higher altitude and stored in a water tower(WT), thereby storing energy for future use. The potential energy of the water stored in the WT can then be used to maintain a minimum pressure that is required at the end-consumers. However, when a WT is included in a water distribution network, the pressure in the system is defined by the water level and the physical properties of the WT. This means that in order to control pressure, the water level in the WT should be controlled.

The maximum allowed pressure in water distribution networks has to be considered as the risk of water leakage increases when pressure is increased[4]. Thus increased water losses due to leakage leads to a higher energy consumption. In [4] it is stated that the estimated world-wide water loss is at 30 %, so the energy used on cleaning the water from filth, bacteria and pressurizing it is therefore wasted. Another problem that should be highlighted regarding high pressure is that high pressure increases the wear on the pipes[5], which can lead to higher maintenance costs as pipes and fittings have to be replaced more frequently. Additionally, regular maintenance is not always possible, since pipes usually are placed underneath the ground and need to be dug up. Thereby the expense of maintenance is increased, especially in urban areas, where the operation can have a negative impact on significant infrastructures. Based on these facts, the maximum pressure in a water distribution network is a vital parameter of the profitability of the system. In a system with a WT, the maximum allowed pressure is defined by the maximum allowed water level in the WT, as the WT in most situations is able to provide a dominant pressure compared to the desired network pressure.

Some constraints regarding the solutions dealing with a WT are necessary to be taken into account. One of them being the quality of the water in the tower. If stored for too long, the quality starts to decrease due to decreasing oxygen level [6, 7]. Thus the water should not be stored for too long. The oxygen level of the water also depends on the water temperature and therefore the water should not be too warm. Furthermore, it is undesirable that the water remains stagnant in the tower or pipe as it also affects the water quality.

The considerations above lead to the following problem statement:

- *How can a water tower be implemented in a water distribution network and controlled to minimize the cost of running the distribution network without violating constraints and compromising the water quality.*

Part I

Analysis

System Description 2

This section gives an introduction to the available test system, including structure and components overview.

2.1 System overview

To develop and test different control methods for a water distribution system, a test setup is required. Such a setup is available at Aalborg university which is based on a real water distribution system, though as a 1:20 downscaled version.

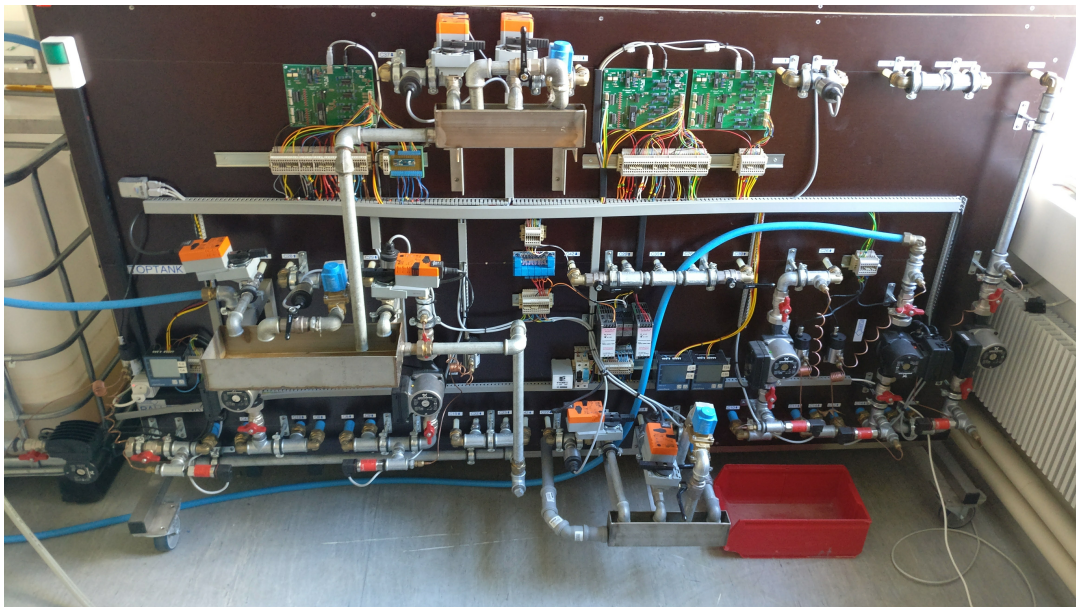


Figure 2.1. The available test setup used to represent a real water distribution system.

The test setup represents a real system, thus the same structure concerning piping, leveling and all the other components. In order to achieve different elevation levels between system parts, the setup is mounted on a wall. This also allows for a quick overview of the complete setup and eases access to the components. As the system is used for various test scenarios, other different equipment is also present in the test setup shown in *Figure 2.1*, enabling the test system to mimic a variety of different system types and scenarios. A simplified diagram representing the structure of the setup that is used in this project is shown in *Figure 2.2*.

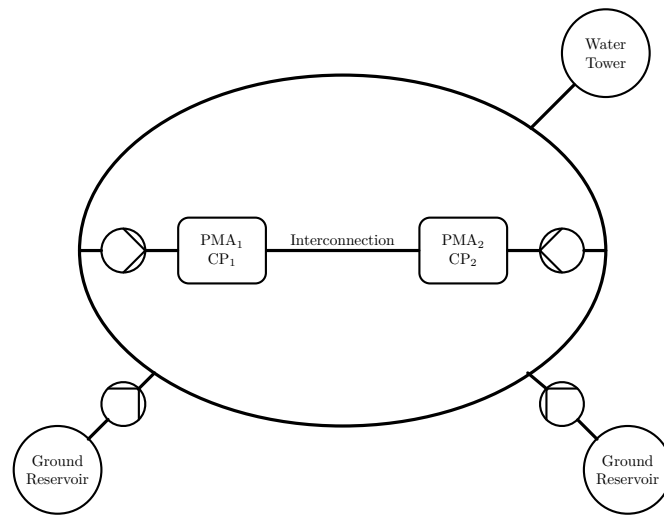


Figure 2.2. Overview of the reduced system that fulfills the scenario of this project.

The system can be split up into different parts, where the main part is a water reservoir placed at ground level, used to supply the system. Two pumps are connected to the reservoir and they supply water to a main water ring formed around the PMA's. A WT is also connected to the main water ring, and acts as an additional water reservoir pressurizes the ring due to the elevation of the WT. The direction of water flow, with respect to the WT, depends on the pressure in the main ring. The tower can thus be filled by pressurizing the ring or be used to pressurize and supply water to the ring instead of the pumps. From the water ring, two PMA's are connected, each via their own pump. In each PMA a measuring point, called the critical point (CP), is placed and the pressure at this point shall be kept to accommodate supply demands of the consumers. Furthermore, two consumers are placed in each PMA, these are simulated by valves with a variable opening degree where the water flows back to the main reservoir.

In the system two different types of Grundfos pumps are used. For supplying the water ring, two pumps, of the type UPMXL GEO 25-125[8], are used. Whereas the pumps used in each PMA are of the type UPM2 25-60[9], which is a smaller pump type and typically applied at the end-users.

In order to close off parts of the system that will not be used for a specific scenario or to simulate faulty behavior, manual rotary ball valves are placed throughout the system. To simulate a consumer, an electronically controlled Belimo valve is used. Thereby it is possible to vary the opening degree of the valves over time according to a specific consumer behavior. For the pipes two different material types are used. The pipes used in the main ring, which connect the reservoir and the WT, are made of polyethylene grade 80 called PE80[10]. The pipes used to connect the PMA's to the ring and the internal connections in the PMAs are made of polyethylene with cross-links called PEX. In addition, the pipes, fittings, bends, and elbows are also present and found in various metals as iron and brass.

The pressure measurement in each PMA is carried out with Jumo pressure sensors. The pressure is measured relative to the ground, Gnd, for the test system. Gnd is equal to the atmospheric pressure. Furthermore, both the differential pressure over each pump and the absolute pressure are measured with a Grundfos direct sensor DPI v.1 and a Danfoss mbs32/33 pressure sensor, respectively. The main reservoir has a volume of 700 L and the WT a volume of 200 L. The volume of the WT in this report is denoted as V_t . A full description of each component in the test setup, including type, naming and relevant technical information can be found in *Appendix: C* and a diagram of the entire test setup can be seen in *Appendix: C.2*.

Requirements and Constraints

3

Adding a WT to an existing water distribution network introduces new requirements and constraints on the system.

As mentioned in Section 1: *Introduction*, a minimum pressure must be maintained in the PMAs for the end-users. Furthermore, the pressure can not exceed a maximum level as this might increase the possibility of water leakage and increase the wear on the pipes. The system described in Section 2.1: *System overview*, is designed to operate at a pressure around 0.1 bar, relative to the environment [11]. For the purpose of this project the interval for which the CP pressure should be within, is chosen to be between $0.08 < \mathbf{y} < 0.18$ [Bar]. Where \mathbf{y} is the pressure at the CP's which for PMA 1 is chosen as node 10 and for PMA 2 is chosen as node 15. The upper limit is set high to allow that the pumps can provide a lot of pressure to fill the WT when the price is low.

Another important aspect when implementing a WT is water quality. If the water is stored in the WT for too long, the quality will decrease due to decreasing oxygen level. Thus a requirement for water quality has to be formulated. As described in Section 2.1: *System overview*, the WT has one combined input-output connection. Therefore a requirement for the flow is hard to formulate as the direction can change dependent on the usage. This could result in a flow based constraint being fulfilled by rapidly changing flow direction without actually replacing any significant water volume in the tower. Instead, a requirement for how often the content of the WT should be exchanged per time unit is discussed. It is important however to point out that formulating a constraint on the WT flow is over the limit of this project, therefore only discussion is considered. Minimum requirement for volume exchange can be chosen as 30% of the volume of V_t per day. This can be written as $\bar{q}_{wt} > 0.3 \cdot V_t [\frac{m^3}{day}]$. As stated in Section 2.1: *System overview* $V_t = 200 L$ so therefore $\bar{q}_{wt} > 0.06 [\frac{m^3}{day}]$.

These constraints, due to the scope of the project, are reduced and thus only contain a requirement for the pressure at each CP and a requirement to minimize the power consumption of the system. Thus, the requirement regarding water exchange in the WT is not investigated any further in this project. Therefore the following requirements and constraints are considered:

- Constraint on the output, $0.08 < \mathbf{y} < 0.18$ [bar]
- Constraint on the WT, $0.055 < \Delta p_{wt} < 0.127$ [bar]
- Constraint on the inputs, $0.05 < \mathbf{u} < 0.95$ [bar]
- Minimizing the total cost of running the system

4.1 Hydraulic modelling

Water distribution networks are designed to deliver water to consumers in terms of sufficient pressure and appropriate chemical composition. Distribution systems as such are generally consisting of four main components: pipes, pumps, valves and reservoirs. The common property is that they are all two-terminal components, therefore they can be characterized by the dynamic relationship between the pressure drop across the two endpoints and the flow through the element [12]. *Equation: (4.1)* shows the dual variables which describe one component.

$$\begin{bmatrix} \Delta P \\ q \end{bmatrix} = \begin{bmatrix} P_{in} - P_{out} \\ q \end{bmatrix} \quad (4.1)$$

Where

Δp is the pressure drop across the two endpoints, $\left[\frac{\text{Pa}}{\text{Pa}} \right]$
 and q is the flow through the element. $\left[\frac{\text{m}^3}{\text{s}} \right]$

In the following chapter, the hydraulic model of the system is derived by control volume approach [13]. The relationship between the two variables is introduced for each component in the hydraulic network.

4.1.1 Pipe model

Pipes are important components of water distribution systems since they are used for carrying pressurized water. A detailed model of the pipes has to be derived in order to understand the relationship of pressure and flow for each pipe component. The dynamic model of a pipe can be originated from Newton's second law. *Equation: (4.2)* describes the proportionality between the rate of change regarding the momentum of the water and the force acting on it.

$$\frac{d}{dt}M = \sum_i F_i \quad (4.2)$$

Where

M is the linear momentum of the water flow, $\left[\frac{\text{kgm}}{\text{s}^2} \right]$
 and F_i is the set of forces acting on the water. $\left[\text{N} \right]$

The dynamic model of a pipe component is derived under the assumption that the flow of the fluid is uniformly distributed along the cross sectional area of the pipe. In other words, all pipes in the system are filled up fully with water all the time. Thus, the density of water and the volume of the fluid is constant in time, as the mass of the water.

Rewriting *Equation: (4.2)*, due to the above-mentioned assumptions, the mass of the water can be taken out in front of the derivative.

$$\frac{d}{dt}M = \frac{d(m_w v)}{dt} = m_w \frac{dv}{dt} = \sum_i F_i \quad (4.3)$$

Where

m_w is the mass of the water, [kg]
 and v is the value of the velocity of the water at each point of the pipe. [$\frac{m}{s}$]

The sum of the forces acting on the control volume can be seen as input forces, acting on the inlet of the pipe and output forces acting on the outlet. Furthermore, resistance forces and the effect of gravitational force is present. These forces are expressed in terms of pressure in order to obtain the model of the pressure drop in the pipes. In *Figure 4.1*, all forces acting on a pipe segment are shown:

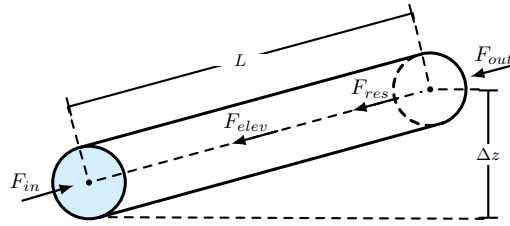


Figure 4.1. Free-body diagram describing the forces acting on a segment of a pipe.

The pipe is assumed to have a cylindrical structure. Furthermore, the cross section of the pipe, $A(x)$, is constant for every $x \in [0, L]$, where L is the length of the pipe:

$$A_{in} = A_{out} = \frac{1}{4}\pi D^2 \quad (4.4)$$

Where

A is the cross sectional area of a pipe, [m^2]
 and D is the diameter of the pipe. [m]

Water flow, q , can be expressed in terms of velocity, v , and cross sectional area, A , resulting in:

$$q = A \cdot v \quad (4.5)$$

In *Equation: (4.6)* the forces acting on the pipe are included. The difference between F_{in} and F_{out} defines the ideal pressure drop between the two endpoints, without taking into account the resistance forces F_{res} and the gravitational force effect due to change in elevation F_{elev} .

$$m_w \frac{dv}{dt} = F_{in} - F_{out} - F_{res} - F_{elev} \quad (4.6)$$

In order to obtain an equation consisting of only pressure variables, the relationship between forces and pressures is used.

$$AL\rho \frac{dv}{dt} = A(p_{in} - p_{out}) - F_{res} - F_{elev} \quad (4.7)$$

Where

m_w	is the mass of the water,	[kg]
L	is the length of a pipe,	[m]
ρ	is the water density,	$\left[\frac{\text{kg}}{\text{m}^3}\right]$
and p	is the pressure.	[Pa]

Rewriting the velocity in terms of volumetric water flow and cross sectional area according to *Equation: (4.5)*:

$$AL\rho \frac{d}{dt} \frac{q}{A} = A(p_{in} - p_{out}) - F_{res} - F_{elev} \quad (4.8)$$

By dividing the equation with the cross sectional area it can be seen that the equation is dependent on the pressure difference between two endpoints.

$$\frac{L\rho}{A} \frac{dq}{dt} = p_{in} - p_{out} - \frac{F_{res} - F_{elev}}{A} \quad (4.9)$$

Thus the desired pressure drop between two endpoint is obtained. The differential equation in *Equation: (4.10)*, describes the change in flow as a function of the pressure drops in the system.

$$\frac{L\rho}{A} \frac{dq}{dt} = \Delta p - \frac{F_{res} - F_{elev}}{A} \quad (4.10)$$

In *Equation: (4.10)*, the term F_{res} is the resistance force acting on the pipe, which consists of two parts: surface resistance(h_f) and the form resistance(h_m) due to the fittings.

Surface resistance (h_f)

The flow of liquid through pipes is affected by resistance from the turbulence occurring along the internal walls of the pipe, caused by the roughness of the pipe surface. The surface resistance is given by the Darcy-Weisbach equation [14].

$$h_f = \frac{fLv^2}{2gD} \quad (4.11)$$

Where

f	is the Moody friction factor,	[.]
h_f	is the pressure given in head,	[m]
and g	is the gravitational constant.	$\left[\frac{\text{m}}{\text{s}^2}\right]$

Equation: (4.11) is valid under the assumption that $v > 0$. Assuming that the flow is not unidirectional and substituting the velocity by the volumetric flow and pipe area:

$$h_f = \frac{8fL}{\pi^2 g D^5} |q|q \quad (4.12)$$

The unknown parameter in *Equation: (4.12)* is the Moody friction factor which is non-dimensional and is a function of the Reynold's number, Re . This friction factor depends on whether the flow is laminar, transient or turbulent, and the roughness of the pipe [15].

The Reynold's number can be used to determine the regime of the flow [15]. When $Re < 2300$ as laminar, if $2300 < Re < 4000$ as transient and if $Re > 4000$ as turbulent.

$$Re = \frac{vD}{\nu} \quad (4.13)$$

Where

ν is the kinematic viscosity. $\left[\frac{\text{kg}}{\text{ms}}\right]$

The kinematic viscosity according to [14] is given by :

$$\nu = 1.792 \cdot 10^{-6} \left[1 + \left(\frac{T}{25} \right)^{1.165} \right]^{-1} \quad (4.14)$$

Where

T is the water temperature. $[\text{°C}]$

In order to estimate the range of Reynolds numbers in a common water distribution, typical values for the temperature, velocity and the radius of the pipes are considered [16].

- $v \in [0.5, 1.5]$ $\left[\frac{\text{m}}{\text{s}}\right]$
- $D \in [50, 1500]$ $[\text{mm}]$
- $T \in [10, 20]$ $[\text{°C}]$

These values result in a Reynold's number between 19000 and 225000, which is considered as turbulent fluid flow through the pipes. For turbulent flow, the Moody friction factor is given by [14]:

$$f = 1.325 \left(\ln \left(\frac{\epsilon}{3.7D} + \frac{5.74}{Re^{0.9}} \right) \right)^{-2} \quad (4.15)$$

Where

ϵ is the average roughness of the wall inside the pipe. $[\text{m}]$

Form resistance (h_m)

Form resistance losses are present at any time the flow changes direction, due to elbows, bends, enlargers and reducers. It is a particular frictional resistance due to the fittings of a pipe. Form loss can be expressed as:

$$h_m = k_f \frac{v^2}{2g} \quad (4.16)$$

Applying the definition of volumetric flow:

$$h_m = k_f \frac{8}{\pi^2 g D^4} |q|q \quad (4.17)$$

Where

k_f is the form-loss coefficient. $[\cdot]$

The form-loss coefficient can be split into different losses depending on the fitting of the pipes.

Pipe bends are principally determined by the bend angle α and bend radius r . This is given by the following expression [14]:

$$k_f = \left[0.0733 + 0.923 \left(\frac{D}{r} \right)^{3.5} \right] \alpha^{0.5} \quad (4.18)$$

Pipe elbows are also used to change the direction of the flow, however providing sharp turns in pipelines. The coefficient for the losses in elbows is determined by the angle of an elbow α and is given by:

$$k_f = 0.442\alpha^{2.17} \quad (4.19)$$

Complete pipe model

In *Equation: (4.12)* and *Equation: (4.17)*, the head loss of the friction losses are determined. These terms are introduced in *Equation: (4.10)* in terms of pressure. The friction factors are multiplied by the water density and gravity. Nevertheless, the head loss due to elevation has to be added in the model, yielding the final expression:

$$\frac{L\rho}{A} \frac{dq}{dt} = \Delta p - h_f \rho g - h_m \rho g - \Delta z_h \rho g \quad (4.20)$$

Where

$$\Delta z_h \quad \text{the head loss due to elevation.} \quad [\text{m}]$$

Substituting the terms h_f and h_m with their respective values:

$$\frac{L\rho}{A} \frac{dq}{dt} = \Delta p - \frac{8fL}{\pi^2 g D^5} \rho g |q|q - k_f \frac{8}{\pi^2 g D^4} \rho g |q|q - \Delta z_h \rho g \quad (4.21)$$

Equation: (4.21) describes the rate of flow in terms of pressure losses due to pressure change, frictions and elevation. Introducing a function for the pressure drop due to friction in the pipes, the following expression can be written up for the k^{th} component:

$$J_k \dot{q}_k = \Delta p_k - \lambda_k(q_k) - \zeta_k \quad (4.22)$$

Where

$$\begin{aligned} J_k & \text{ is an analogous parameter as inertia for the water,} \\ \lambda_k(q_k) & \text{ is the friction as a function of flow,} \\ \text{and } \zeta_k & \text{ is the pressure drop due to elevation.} \end{aligned}$$

As can be seen in *Equation: (4.22)*, the flow dynamics of the k^{th} pipe is described by J_k , which is an analogous parameter as inertia in mechanical systems. \mathbf{J} is a diagonal matrix with zeros for the diagonal elements not related to pipe components, $\mathbf{J} = \text{diag}(J_k)$.

It is assumed, prior to the tests carried out on the system, that the presence of the WT in the system has a slow effect on the flow due to its slow integration behavior. This means that the WT assumed to have a relatively big time constant compared to the pipes. Due to this consideration, a fair assumption is that the parameter J_k does not influence the flow in the system significantly and therefore it could be neglected. However, the parameter is kept, until this assumption is verified by tests. The complete model of a pipe yields:

$$\Delta p_k = \lambda_k(q_k) + J_k \dot{q}_k + \zeta_k \quad (4.23)$$

4.1.2 Valve model

Valves in the water distribution system are modelled according to the assumption that the length of each valve, L , and the change in elevation, Δz_h , is zero. Therefore it is assumed that the length of the valve does not influence the flow and the pressure between the endpoints. The fact that the length of a valve is considerably smaller than the length

of a pipe makes this a fair assumption. Another assumption is that in case of a valve, elevation is not present.

In the given system, valves are considered as end-user components since they are placed only in the PMAs. These user valves have a variable Opening Degree(OD) which influences the pressure drop across the endpoints.

In case of valves, manufacturers provide a parameter which indicates the valve capacity. This coefficient is called the k_{v100} - factor that describes the conductivity of the valve at maximum OD. This parameter sets the relationship between the water flow through the valve in $[m^3]$ in one hour. The conductivity function is determined experimentally by the manufacturer with a pressure drop of $\Delta p = 1[bar]$ at a fully open state of the valve. According to [17], the experiments are carried out on water, therefore k_{v100} can be used for the valves in the water distribution system.

$$q = k_{v100} \sqrt{\Delta p} \quad (4.24)$$

Where

k_{v100} is the valve maximum capacity factor. $\left[\frac{m^3}{h} \right]$

Equation: (4.24) can be derived in detail using the law of continuity for each endpoint of the valve, however the exact derivations can be found in the datasheet [17]. In the further description and derivations, the coefficients and all the technical considerations are based on this datasheet.

Valve conductivity function $k_v(OD)$

Instead of k_{v100} , more generally $k_v(OD)$ can be used which is a function of the opening degree, where $OD \in [0, 1]$. In case of user-operated valves, k_v does not remain constant, it ranges over a compact set of values as the opening degree varies [12].

All valves in the system share the same characteristics, therefore the following characteristics of k_v are valid for all of them.

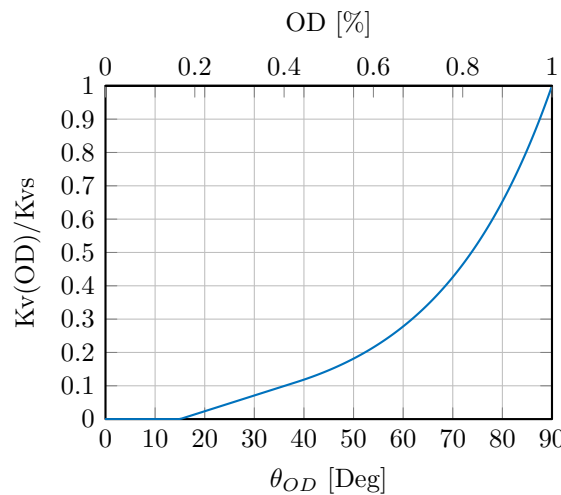


Figure 4.2. Valve characteristics - Valve conductivity in the function of OD.

According to [18], the following general definition can be written up for the conductivity function, $k_v(OD)$:

$$k_v(OD) = \begin{cases} k_{v100} \frac{\theta_{OD}}{\theta_{max}} n_{gl} e^{(1-n_{gl})}, & \text{if } \frac{\theta_{OD}}{\theta_{max}} \leq \frac{1}{n_{gl}}; \\ k_{v100} e^{(n_{gl}(\frac{\theta_{OD}}{\theta_{max}}-1))}, & \text{if } \frac{\theta_{OD}}{\theta_{max}} \geq \frac{1}{n_{gl}} \end{cases} \quad (4.25)$$

Where

θ_{OD}	is the opening degree,	[°]
θ_{max}	is the upper opening degree,	[°]
and n_{gl}	is the valve characteristic curve factor.	[.]

A new parameter, θ_{max} , is introduced which describes the maximum angle where the actuator closes the valve. The same can be stated for a minimum angle. The valve is closed when the position of the actuator $\in [0^\circ, 15^\circ]$. As a consequence, there is an offset in the curve as it is shown in *Figure 4.2*. Introducing the following angle:

$$\kappa = \frac{\theta_{OD} - \theta_{off}}{\theta_{max} - \theta_{off}} \quad (4.26)$$

Where

θ_{off}	is the minimum angle where the valve opens.	[°]
----------------	---	-----

In case of the water distribution system, *Equation: (4.25)* modifies to:

$$k_v(OD) = \begin{cases} k_{v100} \kappa n_{gl} e^{(1-n_{gl})}, & \text{if } \kappa \leq \frac{1}{n_{gl}}; \\ k_{v100} e^{(n_{gl}(\kappa-1))}, & \text{if } \kappa \geq \frac{1}{n_{gl}} \end{cases} \quad (4.27)$$

As it is shown, the conductivity function of the valve consists of two types of functions:

$$k_v(OD) = \begin{cases} k_v(\theta_{OD}) \sim linear(), & \text{if } \kappa \leq \frac{1}{n_{gl}}; \\ k_v(\theta_{OD}) \sim exponential(), & \text{if } \kappa \geq \frac{1}{n_{gl}} \end{cases} \quad (4.28)$$

Since exponential functions never cross the zero point, it is reasonable to use linear characteristics in the lower range. The transition from linear to exponential has to be continuously differentiable and predetermined by n_{gl} [12, 18].

Complete valve model

Using *Equation: (4.24)* with the conductivity function $k_v(OD)$ and expressing Δp yields:

$$\Delta p = \frac{1}{k_v(OD)^2} |q|q \quad (4.29)$$

Introducing a function for the pressure drop across the k^{th} valve, the model of the valves can be written as:

$$\Delta p_k = \mu_k(q_k, k_v(OD)) \quad (4.30)$$

In the further sections at any places where μ is mentioned, the input variable is considered as the OD . This is due to the fact that OD is the only input parameter for $k_v(OD)$. Hence, in notation only OD is written. Therefore the notation of the k^{th} valve, it yields:

$$\Delta p_k = \mu_k(q_k, OD_k) \quad (4.31)$$

4.1.3 Pump model

In order to move water from the reservoirs to the consumers, pumping is required. To guarantee that the water reaches every end-user with the appropriate pressure, different pumps can be used in the water distribution system.

Centrifugal pumps are suitable for this purpose, as the output is steady and consistent. A model describing the pressure drop is derived which is presented in detail in [19]. The pressure provided by the pump is given by:

$$\Delta p = -a_{h2}q_p^2 + a_{h1}\omega_r q_p + a_{h0}\omega_r^2 \quad (4.32)$$

Where

Δp	is the pressure produced by the pump,	[bar]
a_{h2}, a_{h1}, a_{h0}	are constants describing the pump,	[.]
q_p	is the volume flow through the impeller,	$\left[\frac{m^3}{h}\right]$
and ω_r	is the impeller rotational speed.	$\left[\frac{rad}{s}\right]$

The pump model is based on the parameters a_{h2} , a_{h1} , a_{h0} , which are provided in the data sheet and are scaled to units of pressure in [bar] and the unit for flow in $\left[\frac{m^3}{h}\right]$.

Hydraulic power and efficiency

In order to minimize the running cost of the pumps, it is necessary to know the power consumption. The electricity consumption of the pump, as a function of flow, q_p , is described in [11]. This expression can be used to calculate the efficiency η . By assuming η to be constant the expression becomes simpler, however η must be chosen within the operating area of the pump. The electrical power can then be calculated by taking the hydraulic power generated by the pumps and the efficiency of the pumps into account.

The hydraulic power generated by a pump can be described by an equivalent to Joule's law, that is in terms of the pressure difference across the pump, multiplied with the flow through it, see *Equation: (4.33)*.

$$P_h = \Delta p \cdot q_p \quad (4.33)$$

Where

P_h	is the hydraulic power.	[W]
-------	-------------------------	-----

The electrical power used for running the pump can then be described through the relation between the hydraulic power and the efficiency, η . This can be seen in *Equation: (4.34)*.

$$P_e = \frac{1}{\eta} \cdot \Delta p \cdot q_p \quad (4.34)$$

Where

P_e	is the power consumption of the pump,	[W]
and η	is the efficiency of the pump.	[.]

Equation: (4.34) is used in a *Section 5.1: Control Problem* to minimize the cost of running the system.

4.1.4 Water Tower

Water towers are used to maintain the correct pressure in different systems, ensure reliability and to improve the optimality of the water supply. The WT plays a determinative role in the control. Therefore it is dynamic model must be derived.

Similarly to the modelling of the other components, the relation between the two dual variables, pressure difference and flow is derived. The structure of the WT is illustrated in *Figure 4.3*.

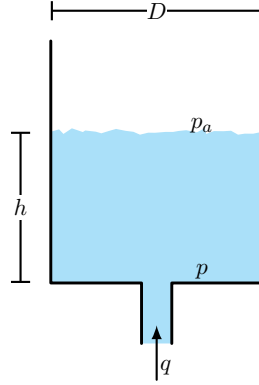


Figure 4.3. Sketch of the open water tower.

In *Figure 4.3*, p_a represents the pressure at the surface of the water, thus it always describes the atmospheric value. The variable p is used to describe the pressure value on the bottom of the tank.

The rate of change of the fluid volume in the WT is proportional to the volumetric flow at which water enters or leaves the tank.

$$q = \frac{dV_t}{dt} = A_{wt} \frac{dh}{dt} \quad (4.35)$$

Where

h	is the height of the fluid in the WT,	[m]
V_t	is the volume of the WT,	[m ³]
A_{wt}	is the cross section of the WT which is assumed to be constant for $y \in [0, h]$,	[m ²]
and q	is the volumetric flow.	[$\frac{m^3}{s}$]

The force on the bottom of the WT is due to the weight of water. According to Newton's second law:

$$F = m_w g = \rho g V_t \quad (4.36)$$

Where

ρ	is the density of water.	[$\frac{kg}{m^3}$]
--------	--------------------------	----------------------

Equation: (4.36) can be rewritten in terms of pressure such as:

$$\frac{F}{A_{wt}} = \rho g h = p - p_a = \Delta p \quad (4.37)$$

The total pressure on the bottom of the WT is a result of the pressure difference, p , and the atmospheric pressure, p_a . However, the model is derived in such a way that the atmospheric pressure is set to zero. Therefore, if the water is assumed to be incompressible, density does not change with pressure and *Equation: (4.35)* can be written as:

$$q = \frac{dV}{dt} = \frac{A_{wt}}{\rho g} \frac{d}{dt} \Delta p = C_H \Delta \dot{p} \quad (4.38)$$

Where

$$C_H \quad \text{is the hydraulic capacitance.} \quad \left[\frac{\text{m}^3}{\text{Pa}} \right]$$

This equation shows proportionality between pressure and the volume of water, which is the defining characteristic of a fluid capacitor. When the fluid capacitance is large, corresponding to a tower with a large area, a large increase in volume is accompanied by a small increase in pressure.

The model of the WT is described by a first order differential equation, consisting of the first time derivative of the pressure drop. The final expression is shown in *Equation: (4.39)*:

$$\Delta \dot{p}_{wt,k} = \frac{1}{C_{H,k}} q_k \quad (4.39)$$

Although *Equation: (4.39)* includes indexing for the pressure drops across the WTs, it is worth mentioning that the water distribution network in this project consists of only one WT.

4.1.5 Complete component model

Gathering the pressure drops across each type of component in the system, a complete system model is obtained.

The complete component model consists of the pipe model, valve model, pump model and the WT, see *Equation ((4.23), (4.31), (4.32), (4.39))*. For the pressure drop across the k^{th} component the following expression can be written:

$$\Delta p_k = \underbrace{\lambda_k(q_k) + \zeta_k + J_k \dot{q}_k}_{\text{Pipe}} + \underbrace{\mu_k(q_k, OD)}_{\text{Valve}} - \underbrace{\alpha_k(\omega_k, q_k)}_{\text{Pump}} + \underbrace{\Delta p_{wt,k}}_{\text{Water tower}} \quad (4.40)$$

The complete component model, *Equation: (4.40)*, is used to represent the pressure loss or contribution across each component. In order to describe every part of the system by *Equation: (4.40)*, the functions corresponding to the specific part of the system are selected. The remaining expressions are set to zero if the model does not match the specific part of the network e.g. if the k^{th} element of the system is a pump, then only $\alpha_k(u_k)$ is taken into account and the rest of the expressions are set to zero. *Table: 4.1* shows the parametrization of the system:

Component	J_k	λ_k	μ_k	α_k	ζ_k	$\Delta p_{wt,k}$
Pipe	J_k	λ_k	0	0	ζ_k	0
Valve	0	0	μ_k	0	0	0
Pump	0	0	0	$-\alpha_k$	0	0
Water tower	0	0	0	0	0	$\Delta p_{wt,k}$

Table 4.1. Complete model parametrization.

Unit transformation

During the derivation of the dynamic model, the units of the physical variables are considered as pascals and seconds. The flow will however be significantly small compared to the pressure if these SI-units are kept.

The pressure sensors fitted on the test setup can measure up to 0.16 [bar] equal to $18 \cdot 10^3$ [Pa] according to the data sheet found at `CD:/References/t40.4327da`. Inserting this maximum measurable pressure in the fully open valve model given by *Equation: (4.29)* and setting $k_v = 1$ yields a maximum flow of $1.11 \cdot 10^{-4} [\frac{m^3}{s}]$ equal to $0.4 [\frac{m^3}{h}]$. Therefore an unit conversion is carried out from [Pa] to [bar] and from seconds[s] to hours[h] resulting in numerically closer flow and pressure values.

Another reason which makes this conversion reasonable is that the conductivity function, k_{v100} in Section 4.1.2: *Valve model*, is derived under the condition that the pressure drop is one [bar] [18]. Furthermore, the pressure sensors are set up to provide measurements in [bar] and with the conversion the data can be used without further scaling.

In addition, the pump equation, see *Equation: (4.32)*, is given by a set of parameters which values are calculated for $[\frac{m^3}{h}]$ flow conditions and [bar] pressure conditions.

The detailed derivation of the unit conversion can be found in *Appendix: A*. The result is stated here:

$$\frac{L\rho}{A \cdot 10^5} \frac{d}{dt} \frac{q}{3600} = \frac{\Delta p}{10^5} - \left(\frac{8fL}{\pi^2 g D^5 \cdot 10^5} + k_f \frac{8}{\pi^2 g D^4 \cdot 10^5} \right) \rho g \frac{|q|}{3600} \frac{q}{3600} - \frac{\Delta z_h \rho g}{10^5} \quad (4.41)$$

4.2 Simplification and electrical analogy

After deriving the dynamics of all elements in the network, the complete system is drawn. In *Appendix: C.2*, the topology of the test system is described in detail. In the following section, all conclusions and notations are based on the system diagram placed in the appendix.

The way of modelling a hydraulic system is in some way analogous to an electric circuit. Hydraulic components can be represented as electronic equivalents with some restrictions. It should be emphasized that in hydraulic networks there are not such phenomenon as magnetic flux.

In the block diagram of the system, nodes are introduced which represent different potential points in the system. This is equivalent to hydraulic pressures. Nodes represent points in the system where pressure have different values due to the pressure drop across the elements e.g. pipes, valves and pumps, placed between them. These points represent interconnection between hydraulic components and take into account the fact that each individual component in the system has an effect on the pressure drop across their corresponding endpoints.

In the network, volumetric flow is equivalent to current and the quantity of water has similar representation as charge in an electric circuit.

Although nodes can be placed across all the component endpoints, some simplifications are introduced in the network. These simplifications do not change the way the system is described. There are two different types of simplifications in the network.

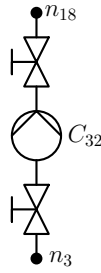


Figure 4.4. Simplifications: The rotational speed of the pump, $\omega_r = 0$ and therefore this part is modelled differently.

The WT is connected to the rest of the system with three components, a pump, C_{32} , and two valves. This is shown in *Figure 4.4*, where the components are shown between n_3 and n_{18} , which also connects the WT to the system. In this particular case the pump is turned off, however contributes to the pressure drop due to its resistance. The same can be said for the valves, except that they are fully open at all time but they modify the flow. Extra nodes are not introduced between the valves and the pump, instead the series connection is seen as one component. This can be modelled by lumping the resistance of the valve, *Equation: (4.29)*, into the model of the pump, *Equation: (4.32)*, when the rotational speed is zero. Thus the following model yields for the case when $\omega_r = 0$:

$$\Delta p = \left(\frac{2}{k_{v100}^2} - a_{h2} \right) |q|q \quad (4.42)$$

For the case where $\omega \neq 0$, a model including the pump and both valves can also be made. This is done in the same manner:

$$\Delta p = \left(\frac{2}{k_{v100}^2} - a_{h2} \right) |q|q + a_{h1}\omega_r q + a_{h0}\omega_r^2 \quad (4.43)$$

The case when $\omega_r = 0$ applies to one component between (n_3-n_{18}) . The case when $\omega_r \neq 0$ applies to the components between (n_1-n_2) , (n_1-n_7) , (n_4-n_8) and (n_5-n_{13}) . It should be mentioned however that all these subsystems inside this simplified model are modelled as described in Section 4.1.5: *Complete component model*.

Since the components influence the pressure between the endpoints, they behave similar to electric components. Valves are considered as nonlinear resistors, since the pressure is the quadratic function of the flow and they have a resistance depending on the OD. The model of the pipes is equivalent to a series connection of a linear inductor and a non-linear resistor. The pumps provide pressure and therefore drive flow through the system. They can be seen as voltage generators. The WT acts as a capacitor in the network. Deriving the relationship between the voltage and the charge of the capacitor:

$$I = C \frac{dU}{dt} \quad (4.44)$$

Where

I	is the current,	[A]
U	is the voltage,	[V]
and C	is the capacitance.	[F]

In *Equation: (4.38)* the volumetric flow, q , is equivalent to the current, I , in a circuit and the constant term, $\frac{A_{wt}}{\rho g}$, is equivalent to the capacitance of an electric capacitor, C . The voltage drop is analogous to the pressure drop in the water system.

The equivalence between the hydraulic and electric system is summarized in *Table: 4.2*.

Hydraulic system	Electrical system
Valve	Nonlinear resistor
Pipe	Linear inductor with a nonlinear drift term
WT	Capacitor
Pressure	Voltage
Flow	Current
Pump	Voltage source

Table 4.2. Equivalence of an electrical and hydraulic network.

4.3 Graph representation

A graph is a formal mathematical way for representing a network, which can be applicable among others in engineering or scientific context such as in mechanical systems, electrical circuits and hydraulic networks [20].

The modelling of the water distribution network is done with the help of Graph Theory(GT). Each terminal of the network is associated with a node and the components of the system correspond to edges [21].

Incidence matrix

The incidence matrix, \mathbf{H} , of a graph with n nodes and e edges is defined by $\mathbf{H} = [a_{ij}]$. Where the number of rows and columns are defined by the amount of nodes and edges respectively. Additionally, the particular node and edge is noted with the indices i and j .

In case of a hydraulic networks, the edges are directed in order to keep track of the direction of the flows in the system. This results in a directed incidence matrix as described below:

$$a_{ij} = \begin{cases} 1 & \text{if the } j^{th} \text{ edge is incident out of the } i^{th} \text{ node} \\ -1 & \text{if the } j^{th} \text{ edge is incident into the } i^{th} \text{ node} \\ 0 & \text{otherwise} \end{cases} \quad (4.45)$$

In *Appendix: C.5* the corresponding incidence matrix of the system is shown.

Cycle matrix

A spanning tree, $T \in \mathcal{G}$ is a subgraph which contains all nodes of \mathcal{G} but has no cycles [22]. In order to obtain the spanning tree, it is necessary to remove an edge from each cycle of the graph. The removed edges are called chords. The number of chords, l , is governed by the following expression:

$$l = e - n + 1 \quad (4.46)$$

By adding a chord to T , a cycle is created which is called a fundamental cycle. A graph is conformed by as many fundamental cycles as there are chords[22]. The set of fundamental cycles correspond to the fundamental cycle matrix \mathbf{B} , such that the number of rows and columns are defined by the amount of chords and edges, respectively.

The cycle matrix of a directed graph can be expressed with $\mathbf{B} = [b_{ij}]$ where i and j denote the chords and edges:

$$b_{ij} = \begin{cases} 1 & \text{if the edges } j^{th} \text{ is in the cycle } i^{th} \text{ and the directions match} \\ -1 & \text{if the edges } j^{th} \text{ is in the cycle } i^{th} \text{ and the directions are opposite} \\ 0 & \text{otherwise} \end{cases} \quad (4.47)$$

In *Appendix: C.6* the corresponding cycle matrix of the system is shown.

Kirchhoff's Law

In the same way as it is described in Section 4.1: *Hydraulic modelling*, the graph of a hydraulic network assigns dual variables to every edge: the pressure, $\Delta p_k(t)$, and the flow, $q_k(t)$. These two variables can be set as vectors containing the individual flows through the edges and the pressure drop across them:

$$\Delta \mathbf{p}(t) = \begin{bmatrix} \Delta p_c \\ \Delta p_f \\ \vdots \\ \Delta p_e \end{bmatrix} \text{ and } \mathbf{q}(t) = \begin{bmatrix} q_c \\ q_f \\ \vdots \\ q_e \end{bmatrix} \quad (4.48)$$

Where the subscript c denotes the chords and the subscript $f...e$ denotes all the edges in the spanning tree. In order to derive a model for the hydraulic network, a set of independent flow variables are identified [23]. These flow variables have the property that their values can be set independently from other flows in the network and they coincide with the flows through the chords. Therefore it is convenient to choose the column indexing of the \mathbf{H} and \mathbf{B} matrix, such as:

$$\mathbf{H} = [\mathbf{H}_c \quad \mathbf{H}_f] \text{ and } \mathbf{B} = [\mathbf{B}_c \quad \mathbf{B}_f] = [\mathbf{I} \quad \mathbf{B}_f] \quad (4.49)$$

Where

\mathbf{H}_c and \mathbf{B}_c are the matrices corresponding to the chords,
 \mathbf{H}_f and \mathbf{B}_f are the matrices corresponding to the spanning tree.

Since the edge variables are governed by elements interconnected in the network, they must obey the law of conservation of mass and pressure [22].

Kirchhoff's Current Law (KCL) states that the net sum of all the flows leaving and entering a node is zero. Formulating this statement in matrix form:

$$\mathbf{H}\mathbf{q}(t) = 0 \quad (4.50)$$

Furthermore, regarding Kirchhoff's Voltage Law (KVL) it is stated that at any time the net sum of the pressure drops in a cycle is zero. In terms of matrix form:

$$\mathbf{B}\Delta \mathbf{p}(t) = 0 \quad (4.51)$$

where the fundamental loops have a reference direction given by the direction of the chords.

4.3.1 Network model

Once the corresponding incidence and cycle matrices are identified, and the analogy between hydraulic and electrical circuits is concluded, the hydraulic network is described as a set of differential equations. In this section a general form of the network model is

derived using all the previously obtained expressions.

In *Appendix: C.5*, the incidence matrix is shown. The last column of \mathbf{H} represents the edge that belongs to the WT.

Hence, the \mathbf{H} matrix can be written as:

$$\mathbf{H} = [\mathbf{H}_1 \quad \mathbf{H}_0] \quad (4.52)$$

Where

$\mathbf{H}_1 \in \mathbb{R}^{n \times (e-1)}$ is the \mathbf{H} matrix without the edge corresponding to the WT,
and $\mathbf{H}_0 \in \mathbb{R}^{n \times 1}$ is the \mathbf{H} matrix with the column corresponding to the WT.

Similarly, the fundamental cycle matrix, \mathbf{B} , is structured such that the last column agrees with the edge representing the WT.

$$\mathbf{B} = [\mathbf{B}_1 \quad \mathbf{B}_0] \quad (4.53)$$

Where

$\mathbf{B}_1 \in \mathbb{R}^{l \times (e-1)}$ is the \mathbf{B} matrix without the edge corresponding to the WT,
and $\mathbf{B}_0 \in \mathbb{R}^{l \times 1}$ is the \mathbf{B} matrix with the column corresponding to the WT.

As mentioned in Section 4.3: *Kirchhoff's Law*, \mathbf{q} is a vector containing all the flows, which can be structured as follows:

$$\mathbf{q} = \begin{bmatrix} \mathbf{q}_1 \\ \mathbf{q}_0 \end{bmatrix} \quad (4.54)$$

Where

$\mathbf{q}_1 \in \mathbb{R}^{(e-1) \times 1}$ is the flow through all edges expect for WT,
and $\mathbf{q}_0 \in \mathbb{R}^{1 \times 1}$ is the flow through the edge belonging to the WT.

The vector containing the pressures at the nodes can be structured as

$$\mathbf{p} = \begin{bmatrix} \mathbf{p}_1 \\ \mathbf{p}_0 \end{bmatrix} \quad (4.55)$$

Where

$\mathbf{p}_1 \in \mathbb{R}^{(n-1) \times 1}$ is the pressure at all nodes expect for the WT,
and $\mathbf{p}_0 \in \mathbb{R}^{1 \times 1}$ is the pressure in the WT.

In *Equation: (4.50)* KCL is applied, which states that the sum of all flows entering into a node must be equal to the sum of the flows leaving the node. By choosing independent set of flows corresponding to the chords of a spanning tree, the flow through every edge of the hydraulic system can be expressed in terms of the flow through the chords, \mathbf{z} [22]. The chord flows make it possible to deal with less variables, thus making the set of differential equations easier to handle. The elements of \mathbf{z} are called the free flows of the system and are independent from each other[21].

$$\mathbf{q} = \mathbf{B}^T \mathbf{z} \quad (4.56)$$

Where

$\mathbf{z} \in \mathbb{R}^{(1 \times l)}$ is the chord flow vector and l is the number of chords.

Before writing up an expression that describes all parts, the component model, *Equation: (4.40)*, needs to be modified with the simplifications introduced in Section 4.2: *Simplification and electrical analogy*. As specified, there are four pumps in the system,

two main pumps and two PMA pumps, which provide a pressure according to the input signals. However, there is one case between (n_3-n_{18}) , see *Appendix: C.2*, where the pump acts as a resistance for the series connection. This is because the pump is inactive in the system. In this case the corresponding edge does not act as an input but can be described by *Equation: (4.42)*. Therefore *Equation: (4.40)* is structured in such a way that the edge corresponding to the connection between the WT and the system is represented separately, thus *Equation: (4.40)* can be rewritten as:

$$\Delta p_k = \underbrace{\lambda_k(q_k) + \zeta_k + J_k \dot{q}_k}_{\text{Pipe}} + \underbrace{\mu_k(q_k, OD_k)}_{\text{Valve}} + \underbrace{\Delta p_{wt,k}}_{\text{Water tower}} + \underbrace{\gamma_k(q_k)}_{\text{WT connection}} - \underbrace{\tilde{\alpha}_k(\omega_k, q_k)}_{\text{Pump+valves}} \quad (4.57)$$

Where

$$q_k$$

is the k^{th} element of \mathbf{q}

$$\lambda_k(q_k) + \zeta_k = C_{p,k} q_k |q_k|$$

is the k^{th} element of the vector field which describes the pressure drop around the pipe elements and $C_{p,k}$ is the resistance of the pipe,

$$\mu_k(q_k, OD_k) = C_{v,k} q_k |q_k|$$

is the k^{th} element of the vector field which describes the pressure drop around the valve elements and $C_{v,k}$ is the resistance of the valve,

$$\tilde{\alpha}_k(\omega_k, q_k) = \left(\frac{2}{k_{v100}^2} - a_{h2k} \right) |q_k| q_k + a_{h1k} \omega_k q_k + a_{h0k} \omega_k^2$$

is the k^{th} element of the vector field which describes the pressure contribution of the k^{th} pump,

$$\gamma_k(q_k) = \left(\frac{2}{k_{v100}^2} - a_{h2k} \right) |q_k| q_k$$

is the k^{th} element of the vector field which describes the pressure drop around the WT connection.

Gathering the functions of the pipes, valves, the WT and its connection the following vector field is introduced:

$$f(\mathbf{q}, \mathbf{OD}) = \lambda(\mathbf{q}) + \boldsymbol{\zeta} + \mu(\mathbf{q}, \mathbf{OD}) + \gamma(\mathbf{q}) + \Delta \mathbf{p}_{wt} \quad (4.58)$$

Where $f(\mathbf{q}, \mathbf{OD})$ is a vector field describing the pressure drops, due to friction and the WT capacitance, across each corresponding component.

Where

$$f_k = \lambda_k(q_k) + \zeta_k \quad \text{for } k = 2, 3, 4, 5, 6, 7, 10, 11, 12, 14, 17, 18, 19, 21, 23 \quad (4.59)$$

$$f_k = \mu_k(q_k, OD_k) \quad \text{for } k = 13, 15, 20, 22 \quad (4.60)$$

$$f_k = \gamma_k(q_k) \quad \text{for } k = 24 \quad (4.61)$$

$$f_k = \Delta p_{wt,k} \quad \text{for } k = 25 \quad (4.62)$$

It is important to point out that in *Equation: (4.58)* the functions for the different components take the flow as a vector in their arguments. It means that the right hand-side of the equation returns a vector with a size of \mathbf{q} . The elevation and the pressure drop across the WT therefore are also treated as vector that returns the appropriate value only for edges where elevation or the WT is present.

Taking the newly introduced vector field, $f(\mathbf{q}, \mathbf{OD})$ into account, the model for the network, *Equation: (4.57)*, can be written up such that:

$$\Delta \mathbf{p} = \mathbf{J} \dot{\mathbf{q}} + f(\mathbf{q}, \mathbf{OD}) - \tilde{\alpha}(\boldsymbol{\omega}, \mathbf{q}) \quad (4.63)$$

In *Equation: (4.63)* the hydraulic network model is described in terms of the independent flows through all the nodes and shows the inputs to the system separately. The vector field, $f(\mathbf{q}, \mathbf{OD})$, represents the pressure drops across elements as one vector. The k^{th} element of the vector, e.g. represents a pressure drop accross a valve only if $\mu(\mathbf{q}, \mathbf{OD})$ is nonzero, which is the case if the k^{th} edge is a valve. The same can be said in case of pipes, the WT and the connection.

In order to reduce the order of the model and hence, the amount of unknowns, chord flows are introduced according to *Equation: (4.56)*.

$$\Delta \mathbf{p} = \mathbf{J} \mathbf{B}^T \dot{\mathbf{z}} + f(\mathbf{B}^T \mathbf{z}, \mathbf{OD}) - \tilde{\alpha}(\boldsymbol{\omega}, \mathbf{B}^T \mathbf{z}) \quad (4.64)$$

Making use of *KVL* shown in *Equation: (4.51)*, the following is obtained

$$\mathbf{B} \Delta \mathbf{p} = \mathbf{B} \mathbf{J} \mathbf{B}^T \dot{\mathbf{z}} + \mathbf{B} f(\mathbf{B}^T \mathbf{z}, \mathbf{OD}) - \mathbf{B} \tilde{\alpha}(\boldsymbol{\omega}, \mathbf{B}^T \mathbf{z}) = 0 \quad (4.65)$$

Isolating the inertia matrix to the left side

$$\mathbf{B} \mathbf{J} \mathbf{B}^T \dot{\mathbf{z}} = -\mathbf{B} f(\mathbf{B}^T \mathbf{z}, \mathbf{OD}) + \mathbf{B} \tilde{\alpha}(\boldsymbol{\omega}, \mathbf{B}^T \mathbf{z}) \quad (4.66)$$

It is desired to know the value of the flow through the chords, hence the equation above is solved for $\dot{\mathbf{z}}$. In order to invert $(\mathbf{B} \mathbf{J} \mathbf{B}^T)$ it has to be non-singular i.e. invertible.

Defining $\mathcal{J} = \mathbf{B} \mathbf{J} \mathbf{B}^T$, then for the term \mathcal{J} in order to be positive-definite it has to be a square matrix and its determinant has to be non-zero. Note that \mathcal{J} is

$$\mathcal{J} = \begin{pmatrix} \mathbf{I} & \mathbf{B}_f \end{pmatrix} \begin{pmatrix} \mathbf{J}_c & \mathbf{0} \\ \mathbf{0} & \mathbf{J}_f \end{pmatrix} \begin{pmatrix} \mathbf{I} \\ \mathbf{B}_f^T \end{pmatrix} = \mathbf{J}_c + \mathbf{B}_f \mathbf{J}_f \mathbf{B}_f^T \quad (4.67)$$

Where

$\mathbf{J}_c \in \mathbb{R}^{l \times l}$ is the inertia in the chord components,
and $\mathbf{J}_f \in \mathbb{R}^{f \times f}$ is the inertia in the components of the spanning tree.

\mathbf{J}_c is a diagonal inertia matrix containing the chord elements. Since all the components corresponding to a chord in \mathcal{G} are pipes, all the diagonal terms are positive. Thus, $\mathbf{J}_c > 0$.

Nevertheless, if there is a chord corresponding to a non-pipe element, *Equation: (4.67)* would still be positive-definite as long as it is possible to create a spanning tree containing all chords as pipe elements from \mathcal{G} [23].

For the remaining term $\mathbf{B}_f \mathbf{J}_f \mathbf{B}_f^T$, \mathbf{J}_f is a non-negative matrix as all its elements are zero or describe the inertia of a pipe. Multiplying $\mathbf{B}_f \mathbf{J}_f \mathbf{B}_f^T$ by a non-zero vector column \mathbf{x} and its transpose \mathbf{x}^T

$$\mathbf{x}^T \mathbf{B}_f \mathbf{J}_f \mathbf{B}_f^T \mathbf{x} \quad (4.68)$$

Creating a new variable $\mathbf{y} = \mathbf{B}_f^T \mathbf{x}$ and applying the definition of positive semi-definiteness [24]

$$\mathbf{y}^T \mathbf{J}_f \mathbf{y} \geq 0 \quad (4.69)$$

Thus, *Equation: (4.67)* is positive-definite and it provides a sufficient condition for \mathcal{J} being invertible.

Therefore, the system can be described as follows

$$\dot{\mathbf{z}} = -\mathcal{J}^{-1} \left[\mathbf{B}f(\mathbf{B}^T \mathbf{z}, OD) + \mathbf{B}\tilde{\alpha}(\omega, \mathbf{B}^T \mathbf{z}) \right] \quad (4.70)$$

4.3.2 Pressure drop across the nodes

Equation: (4.63) describes the system by the pressure across each element. The dynamics are determined by the inertia of the pipes while the pressure drop relation is described by the vector field f and the input pressure is provided by the pumps, $\tilde{\alpha}$. The flow rate through the chords is found in *Equation: (4.70)*, thus an expression for $\Delta \mathbf{p}$ can be expressed by substituting the flow rate into *Equation: (4.64)*:

$$\Delta \mathbf{p} = -\mathbf{J} \mathbf{B}^T \mathcal{J}^{-1} \left[\mathbf{B}f(\mathbf{B}^T \mathbf{z}, OD) + \mathbf{B}\tilde{\alpha}(\omega, \mathbf{B}^T \mathbf{z}) \right] + f(\mathbf{B}^T \mathbf{z}, OD) - \tilde{\alpha}(\omega, \mathbf{B}^T \mathbf{z}) \quad (4.71)$$

Writing in short form:

$$\Delta \mathbf{p} = (\mathcal{I} - \mathbf{J} \mathbf{B}^T \mathcal{J}^{-1}) f(\mathbf{B}^T \mathbf{z}, OD) - (\mathcal{I} + \mathbf{J} \mathbf{B}^T \mathcal{J}^{-1}) \tilde{\alpha}(\omega, \mathbf{B}^T \mathbf{z}) \quad (4.72)$$

a general form of the pressure across all elements of the network is obtained. \mathcal{I} is the identity matrix.

4.4 Nonlinear Parameter identification

The behavior of the complete water distribution system is governed by the previously derived model. Certain parameters of the system are either unknown or can vary significantly from the assumed design values. Furthermore, the obtained model of the system gives nonlinear relations between flows and pressures in each individual components.

In case of the valves, the conductivity function is dependent on the OD, therefore the parameter of these elements are considered to be known. The centrifugal pumps are fully described by their models and by the coefficients provided by the manufacturer. The hydraulic capacity is also considered as known in case of the WT. However, parameters in the model of the pipes are uncertain. Even though the necessary friction parameters can be found in the data sheet provided by the manufacturer. These values are only acceptable for new pipes, as over time material can build up on the inside of the pipes, since the laboratory setup to a large extent is built from PEX/PEM (plastic) pipes. Furthermore, the physical parameters of the pipe volumes are assumed to be known to an accuracy where there is not any benefits from estimating it. Therefore the inertia matrix is known.

The aim of the system identification in case of the water distribution system is to estimate the missing parameters which describe the frictions and form losses in the pipes. Therefore, defining the additional pressure losses and thus obtain a model that precisely describes the system. This is especially important in order to ensure correct behavior when applying the MPC, which will be based on the parameter estimated model to the actual system. Due to these considerations, the importance of obtaining accurate parameters is additionally essential in order to setup a simulation that represents the real test setup.

The block diagram of a general parameter identification method is shown in *Figure 4.5*.

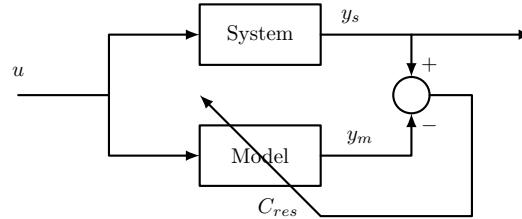


Figure 4.5. Parameter identification block diagram.

As it is shown in the figure, the measurements from the real life system are compared to the output of the simulation introducing the same input for both systems. In the figure, C_{res} denotes the unknown resistance parameters.

In order to obtain measurements from the real life test setup, the system has to be excited by various input signals. The inputs to the system are the input signals to the pumps, however in case of the parameter estimation the OD of the valves are also considered as inputs. Therefore, it is reasonable to reformulate the equation describing the network in *Equation: (4.70)* into such a form where the terms for the inputs and states are isolated. Recalling *Equation: (4.66)*, the system equation is in such a form, except that the input only considers the two main and two PMA pumps:

$$BJB^T \dot{z} = -Bf(B^T z, OD) + B\tilde{\alpha}(\omega, B^T z) \quad (4.73)$$

Reformulating *Equation: (4.73)* such that all valves and pumps are isolated in the input, the following yields:

$$BJB^T \dot{z} = -B\tilde{f}(B^T z) + Bu(\omega, B^T z, OD) \quad (4.74)$$

where the vector field $u(\omega, B^T z, OD)$ contains all the functions for the elements, which are dependent on the inputs. The vector field $\tilde{f}(B^T z)$ describes the rest of the resistance terms which are responsible for the pressure drops in the network. Although $u(\omega, B^T z, OD)$ takes the inputs as ω and OD , during the estimation and the control, the inputs to the pumps are specified as pressure differences, Δp .

In the system, outputs are defined as differential pressures according to the available sensors on the test setup. From the system setup 8 different relative pressures can be measured. Following the notation of *Figure C.2*, sensors are placed in: $n_2, n_4, n_5, n_7, n_{10}, n_{11}, n_{15}$, and n_{16} . During the parameter identification, these measurements are compared to the output from the simulation and the parameters are varied until the model fits the data.

It is important to point out that the estimation is applied for steady state, since the unknown parameters are the resistances and form losses. The inertia and the capacitance

only affect the dynamics, therefore have no influence during steady-state. The inertia of the pipes, and the capacitance of the WT are considered as known parameters.

Taking the steady state into account, the system equation for the nonlinear parameter estimation can be rewritten as:

$$0 = \underbrace{-B\tilde{f}(B^T z) + Bu(\omega, B^T z, OD)}_{\mathcal{X}_p} \quad (4.75)$$

The aim of the parameter identification is to obtain a minimum difference between the outputs by adjusting the parameters of the resistance terms in $\tilde{f}(\cdot)$. The general parameter estimation problem is a minimization problem with the following objective function:

$$\min_p \left(\mathcal{X}_p^T \mathcal{X}_p + (y_s(B^T z) - y_m(B^T z))^T (y_s(B^T z) - y_m(B^T z)) \right) \quad (4.76)$$

Where

$y_s(B^T z)$	is the vector of pressure measurements on the system,	[bar]
$y_m(B^T z)$	is the vector of outputs in the model,	[bar]
and \mathcal{X}_p	is the term defined in Equation: (4.76).	[bar]

4.4.1 Measurements on the test setup

On the system setup, *Figure C.2*, 8 different relative pressures can be measured. The measurements obtained from the pressure sensors placed in these nodes are relative to the atmospheric pressure. In order to compare the measurements from the system setup and the data obtained from the simulation in Matlab, an atmospheric pressure node, n_1 , is set as reference point. Thus, the relation between the measured outputs and the reference point can be set, resulting in:

Node 2

$$y_1 = \Delta p_{C2} \quad (4.77)$$

Node 7

$$y_2 = \Delta p_{C16} \quad (4.78)$$

Node 4

$$y_3 = \Delta p_{C18} + \Delta p_{C19} + \Delta p_{C23} + \Delta p_{C24} \quad (4.79)$$

Node 5

$$y_4 = \Delta p_{C25} + \Delta p_{C26} + \Delta p_{C30} + \Delta p_{C31} \quad (4.80)$$

Node 10

$$y_5 = \Delta p_{C24} \quad (4.81)$$

Node 11

$$y_6 = \Delta p_{C20} + \Delta p_{C21} \quad (4.82)$$

Node 15

$$y_7 = \Delta p_{C31} \quad (4.83)$$

Node 16

$$y_8 = \Delta p_{C28} + \Delta p_{C27} \quad (4.84)$$

4.4.2 Estimation method

In order to carry out the parameter estimation of the water distribution, Matlab NonLinear Grey Box (MNGB) toolbox[25], is used. This toolbox estimates previously defined coefficients of nonlinear differential equations, to fit with the desired data. Thereby, a nonlinear model has to be implemented in Matlab to carry out the simulation.

The comparison between the test setup measurements and the model output is done with the Matlab function *compare*. Together with the comparison plot, the normalized root mean square (NRMSE) measure is also added which measures the quality of the fit. This fit is calculated as a percentage [26] using:

$$fit = 100 \left(1 - \frac{\|y_s - y_m\|}{\|y_s - \text{mean}(y_s)\|} \right) \quad (4.85)$$

Where

y_s	is the validation data, the outcome of the measurement,	[Bar]
and y_m	is the output of the model.	[Bar]

4.4.3 Nonlinear Estimation Outcomes

The results of the nonlinear parameter estimation are shown in *Appendix: E*. It is concluded that the estimation has been unsuccessful, seeing that the model and the measured data follow different behaviors. This might be due to the incapability to excite the system sufficiently in order to estimate the pipe parameters correctly due to limited information in the measured data. Moreover, the dynamics of the valves are slower in comparison with dynamics of the pipes, resulting in the information of the pipes being hidden into the dynamics of the valves. Thus preventing the estimation process from obtaining the correct values for the resistance as only the valves dynamics are present in the output data.

An alternative could be to only use the pumps as inputs without affecting the valves dynamics. However in order to obtain accurate values for the parameters, different scenarios have to be simulated which include varying the water consumption of the end-users as the pumps cannot excite the system sufficiently on their own. Furthermore, it is indicated that the dynamics of the pipes are faster than the pumps, this is shown in *Appendix: I.2*.

Therefore, after seeing that the nonlinear approach is not suitable to estimate the unknown parameters for this test setup, the model will be linearized in order to perform a linear parameter estimation.

4.5 Linearization of the model

As it is shown in *Equation: (4.74)*, both $\tilde{f}(\mathbf{B}^T \mathbf{z})$ and $u(\boldsymbol{\omega}, \mathbf{B}^T \mathbf{z}, \mathbf{OD})$ are vector fields. Since the flows, the ODs and the differential pressure inputs, Δp , are all functions of time, it can be stated that the differential equation describing the system is a first order nonlinear system of differential equations. The number of equations are defined by the number of free variables, therefore the number of states, as mentioned in *Section 4.3.1: Network model*.

In this section the results are shown of how the model, describing the network, is linearized with the use of Taylor expansion.

4.5.1 Taylor expansion on a simple example

The method of linearization is introduced on a simple one state, one input variable system. The consideration behind the example is analogous to the method applied for the water distribution system. In *Equation: (4.86)* the system with one state variable and one input can be seen:

$$\frac{d}{dt}x = f(x, u) \quad (4.86)$$

$f(x, u)$ can be written up with Taylor series with the assumption that it is continuously differentiable, therefore the partial derivatives exist in the operating point:

$$f(x, u) = f(\bar{x}, \bar{u}) + \frac{\partial f}{\partial x|_{\bar{x}, \bar{u}}} \hat{x} + \frac{\partial f}{\partial u|_{\bar{x}, \bar{u}}} \hat{u} + \text{higher order terms} \quad (4.87)$$

Where

\bar{x} and \bar{u} are the operating points,
and \hat{x} and \hat{u} are the deviations from the operating points.

The aim of the linearization is to describe the function $f(x, u)$ around an operating point as a linear function. It should be noted that the approximation around this point is only valid for cases when the deviation from this point is small. Therefore, the linearized version of a dynamic model is often called the small-signal model of the system.

In *Equation: (4.87)*, the linearized term of $f(x, u)$ is expressed. The operating point is chosen such that $f(\bar{x}, \bar{u}) = 0$, hence an equilibrium for the system is given with input \bar{u} . The higher order terms are not taken into account in the approximation. Since the model is described by small-signals, quadratic and higher order terms result in very small values, therefore they are negligible.

The following expression in *Equation: (4.88)* gives the approximation of the function:

$$\frac{d}{dt}x = f(x, u) \approx \frac{\partial f}{\partial x|_{\bar{x}, \bar{u}}} (x - \bar{x}) + \frac{\partial f}{\partial u|_{\bar{x}, \bar{u}}} (u - \bar{u}) \quad (4.88)$$

In case of a pipe or a valve component, the pressure drop across the element is described by a quadratic function of the flow, if steady state is considered and the dynamics are neglected. *Figure 4.6* describes a nonlinear function, $f(q)$, and its linearized interpretation for the operating values of pressure and flow.

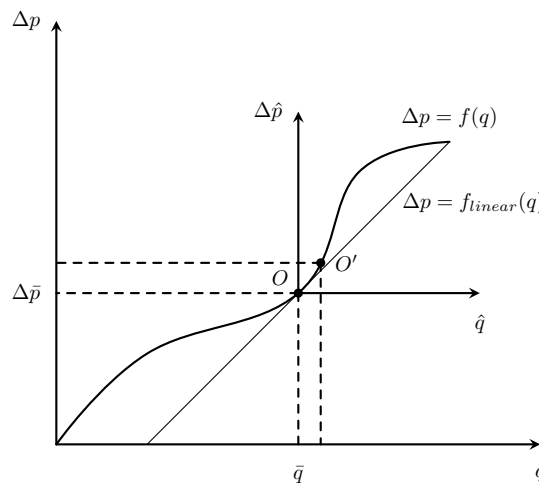


Figure 4.6. Linearization of a nonlinear function $f(q)$.

As can be seen, the line inserted in the operating point, O , describes the model accurately only if the deviation is very small from this point, e.g. O' . Therefore the linearized model describes the system behavior in the new coordinate system $(\bar{q}, \Delta\bar{p})$. It is important to mention that in *Figure 4.6*, the function $f(q)$ is an illustration of a non-linear function and not the exact same as for a pipe element.

4.5.2 Linear system model

Recalling *Equation: (4.57)* to show how the pressure drop is obtained for each element in the network:

$$\Delta p_k = \underbrace{\lambda_k(q_k) + \zeta_k + J_k \dot{q}_k}_{\text{Pipe}} + \underbrace{\mu_k(q_k, OD_k)}_{\text{Valve}} + \underbrace{\Delta p_{wt,k}}_{\text{Water tower}} + \underbrace{\gamma_k(q_k)}_{\text{WT-connection}} - \underbrace{\tilde{\alpha}_k(\omega_k, q_k)}_{\text{Pump+valves}} \quad (4.89)$$

Among these functions, the pipes, valves, pumps and the edge describing the WT connection are nonlinear functions of the edge flows, therefore they need to be linearized. The linearization is carried out according to Taylor expansion as it is described in *Equation: (4.88)*.

The expression describing the pipes consists of three terms, the resistances and form losses, λ_k , the dynamics, $J_k \dot{q}_k$, and the elevation, ζ_k , if there is any present.

Applying the KVL as in *Equation: (4.65)*, the expression describing the pipes is approximated by its linear model as follows:

$$\mathbf{B}_1 \lambda(\mathbf{B}_1^T \mathbf{z}) \approx \mathbf{B}_1 \lambda(\mathbf{B}_1^T \bar{\mathbf{z}}) + \mathbf{B}_1 \left[\frac{\partial \lambda(\mathbf{B}_1^T \mathbf{z})}{\partial \mathbf{B}_1^T \mathbf{z}} \right]_{\bar{\mathbf{z}}} \mathbf{B}_1^T \hat{\mathbf{z}} \quad (4.90)$$

where the partial derivatives are first order derivatives of the vector field, λ , in the operating point $\bar{\mathbf{z}}$. Since the derivation is according to $\mathbf{B}_1^T \mathbf{z}$ the derivative is multiplied by \mathbf{B}_1^T , due to the chain rule. The reason for only $\lambda(\mathbf{B}_1^T \mathbf{z})$ being expressed is because the elevation is constant and the inertia term is a linear function of the flows.

In case of the valves, $\mu(\mathbf{B}_1^T \mathbf{z}, OD)$ is not only the function of the independent flows, but also the opening degree. The conductivity function, k_v , which is a function of OD, can vary over time. Therefore the linearization has to be done according to the flow and the OD:

$$\begin{aligned} \mathbf{B}_1 \mu(\mathbf{B}_1^T \mathbf{z}, OD) \approx & \mathbf{B}_1 \mu(\mathbf{B}_1^T \bar{\mathbf{z}}, \bar{OD}) + \mathbf{B}_1 \left[\frac{\partial \mu(\mathbf{B}_1^T \mathbf{z}, OD)}{\partial \mathbf{B}_1^T \mathbf{z}} \right]_{(\bar{\mathbf{z}}, \bar{OD})} \mathbf{B}_1^T \hat{\mathbf{z}} \\ & + \mathbf{B}_1 \left[\frac{\partial \mu(\mathbf{B}_1^T \mathbf{z}, OD)}{\partial OD} \right]_{(\bar{\mathbf{z}}, \bar{OD})} \hat{OD} \end{aligned} \quad (4.91)$$

The Taylor expansion is carried out in the same manner as in *Equation: (4.90)*, however the linearized valve model is in the function of two small-signal variables, the flow and the OD. Therefore the partial derivatives are calculated in the operating point defined by the operating value of \mathbf{z} and OD .

For the WT connection, the same is applied as for the pipe model.

$$\mathbf{B}_1 \gamma(\mathbf{B}_1^T \mathbf{z}) \approx \mathbf{B}_1 \gamma(\mathbf{B}_1^T \bar{\mathbf{z}}) + \mathbf{B}_1 \left[\frac{\partial \gamma(\mathbf{B}_1^T \mathbf{z})}{\partial \mathbf{B}_1^T \mathbf{z}} \right]_{\bar{\mathbf{z}}} \mathbf{B}_1^T \hat{\mathbf{z}} \quad (4.92)$$

The pumps are operating according to the model described in *Equation: (4.43)*, where the valves around each pump are taken into account. Although this model is both dependent on the OD of the valves and the flow through the pumps, it is unnecessary to linearize it for the following reason, explained with the help of *Figure 4.7*.

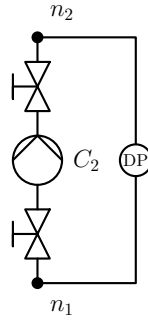


Figure 4.7. Block representing the extended pump model.

As it is shown, there is a differential pressure sensor around every pump in the system. The angular velocity is therefore not used directly as input to the system, rather the measured differential pressure is used. It is shown in a later chapter, Chapter *II: Control Design*, that around the pumps a cascade control is designed. The pumps are chosen to be controlled by PI controllers in an inner loop with the control variable as the differential pressure. This inner control loop linearizes the pumps and therefore the differential pressure becomes the control input.

The input, in case of the parameter estimation, is defined by the four pumps and four valves. Therefore, it is convenient to define an input vector which consists of the four opening degrees controlling the valves and the four differential pressures controlling the pumps:

$$\mathbf{u} = \left[OD_{e13}, OD_{e15}, OD_{e20}, OD_{e22}, \Delta p_{e01}, \Delta p_{e08}, \Delta p_{e09}, \Delta p_{e16} \right]^T \quad (4.93)$$

It should be noted here that this control input representation is valid only for the parameter estimation. It is shown in a later chapter, Chapter *II: Control Design*, that for the control, the structure of the model and the input vector is structured differently. However, in this case it is convenient to handle all pumps and valves as input terms. In order to build up such an input vector, linear mapping between the corresponding edges and the input is required. The vector field describing the pumps, $\tilde{\alpha}$ can be used to show this mapping, although it is important to mention that $\tilde{\alpha}$ consists of the nonlinear terms of the pump pressure contribution. However, the terms are nonzero at edges where a pump is present, therefore it is only used to show how the resulting differential pressure contribution of these terms can be mapped into \mathbf{u} .

$$\mathbf{B}_1 \tilde{\alpha}(\omega, q) = \mathbf{B}_1 \mathbf{G}_p \mathbf{u} \quad (4.94)$$

Where

$\mathbf{G}_p \in \mathbb{R}^{(e \times u)}$ is a matrix representing a linear mapping where the dimension u is the number of inputs and e is the number of edges without the WT.

\mathbf{G}_p is an extended matrix for the eight inputs which means that the first four columns consist of zeros, since the first four elements of the input vector are the valve ODs. \mathbf{G}_p can be found in *Appendix: C.7*.

4.5.3 State-space model for linear parameter estimation

For the sake of clearance, the nonlinear model describing the water distribution system in *Equation: (4.74)* is shown again:

$$\mathbf{B} \mathbf{J} \mathbf{B}^T \dot{\mathbf{z}} = -\mathbf{B} \tilde{f}(\mathbf{B}^T \mathbf{z}) + \mathbf{B} u(\omega, \mathbf{B}^T \mathbf{z}, \mathbf{O} \mathbf{D}) \quad (4.95)$$

The behavior of the WT is described by the equation below:

$$\Delta \dot{p}_{wt} = \frac{1}{C_H} q_0 \quad (4.96)$$

These two differential equation systems give a full description of the pressures in the whole network, and describe the effect of the WT on the system. However, due to the linearization, it is desired to reformulate the linear system into the general state-space representation with inputs, outputs and states separated.

Before setting up the state-space form of the system, the following relation should be considered:

$$\mathbf{H}_1 \mathbf{q}_1 + \mathbf{H}_0 q_0 = 0 \quad (4.97)$$

In *Equation: (4.97)*, the current law is shown for the WT and for the rest of the system. The two current laws sum up to zero taking into account the whole system. Expressing the flow in the WT yields:

$$q_0 = -\mathbf{H}_0^\dagger \mathbf{H}_1 \mathbf{q}_1 \quad (4.98)$$

Where \mathbf{H}_0^\dagger is the pseudoinverse of \mathbf{H}_0 . Inserting *Equation: (4.98)* into *Equation: (4.96)*, the original model of the WT, results in:

$$\Delta \dot{p}_{wt} = -\frac{1}{C_H} \mathbf{H}_0^\dagger \mathbf{H}_1 \mathbf{q}_1 = -\frac{1}{C_H} \underbrace{\mathbf{H}_0^\dagger \mathbf{H}_1 \mathbf{B}_1^T}_{\mathbf{S}} \mathbf{z} \quad (4.99)$$

Therefore the dynamic of the WT can be expressed with the incidence matrix for the whole system in terms of the independent chord flow variables as follows:

$$\Delta \dot{p}_{wt} = -\mathbf{S} \mathbf{z} \quad (4.100)$$

In order to formulate a linear standard state-space representation, the linearized terms in vector fields $\tilde{f}(\mathbf{B}^T \mathbf{z})$ and $u(\omega, \mathbf{B}^T \mathbf{z}, \mathbf{O} \mathbf{D})$ should be separated according to the small-signal values of the chord flows, the inputs and the pressure contribution from the WT. The representation is shown in *Equation: (4.101)*:

$$\mathbf{B} \mathbf{J} \mathbf{B}^T \dot{\hat{\mathbf{z}}} = -\mathbf{M}_p \hat{\mathbf{z}} + \mathbf{N}_p \hat{\mathbf{u}} - \mathbf{B}_o \Delta \hat{p}_{wt} \quad (4.101)$$

In *Equation: (4.101)*, the \mathbf{M}_p matrix consists of the following terms:

$$\mathbf{M}_p \approx \mathbf{B}_1 \left[\frac{\partial \lambda(\mathbf{B}_1^T \mathbf{z})}{\partial \mathbf{B}_1^T \mathbf{z}} \right]_{\bar{\mathbf{z}}} \mathbf{B}_1^T + \mathbf{B}_1 \left[\frac{\partial \mu(\mathbf{B}_1^T \mathbf{z}, \mathbf{O} \mathbf{D})}{\partial \mathbf{B}_1^T \mathbf{z}} \right]_{(\bar{\mathbf{z}}, \mathbf{O} \mathbf{D})} \mathbf{B}_1^T + \mathbf{B}_1 \left[\frac{\partial \gamma(\mathbf{B}_1^T \mathbf{z})}{\partial \mathbf{B}_1^T \mathbf{z}} \right]_{\bar{\mathbf{z}}} \mathbf{B}_1^T \quad (4.102)$$

And the \mathbf{N}_p matrix consists of the following terms:

$$\mathbf{N}_p \approx -\mathbf{B}_1 \left[\frac{\partial \mu(\mathbf{B}_1^T \mathbf{z}, \mathbf{O} \mathbf{D})}{\partial \mathbf{u}} \right]_{(\bar{\mathbf{z}}, \bar{\mathbf{u}})} + \mathbf{B}_1 \mathbf{G}_p \quad (4.103)$$

Where \mathbf{B}_o is the cycle matrix belonging to the WT. As it can be seen, the linearized terms, which are represented in the element wise model description in *Equation: (4.57)*, are separated if they are multiplied by the small-signal values of flows or inputs.

In order to find a good state-space representation for the system, extended with the WT, the dynamics of the system have to be considered. The pipes, compared to the WT, are assumed to have a considerably faster response time, which means that their time constants are small, therefore the settling time is short. According to [27], in cases like this, the dynamics with the small time constant does not effectively take part in the dynamics of the system, therefore they can be neglected. Due to this consideration, *Equation: (4.101)* is rewritten in steady-state form, where the derivative of the states are set to zero:

$$0 = -\mathbf{M}_p \hat{\mathbf{z}} + \mathbf{N}_p \hat{\mathbf{u}} - \mathbf{B}_o \Delta \hat{p}_{wt} \quad (4.104)$$

The small-signal value of the state vector can be expressed on the left side of the equation only if \mathbf{M}_p is invertible. In *Equation: (4.102)*, the equation can be rewritten as follows:

$$\mathbf{M}_p \approx \mathbf{B}_1 \left[\left[\frac{\partial \lambda(\mathbf{B}_1^T \mathbf{z})}{\partial \mathbf{B}_1^T \mathbf{z}} \right]_{\bar{\mathbf{z}}} + \left[\frac{\partial \mu(\mathbf{B}_1^T \mathbf{z}, OD)}{\partial \mathbf{B}_1^T \mathbf{z}} \right]_{(\bar{\mathbf{z}}, OD)} + \left[\frac{\partial \gamma(\mathbf{B}_1^T \mathbf{z})}{\partial \mathbf{B}_1^T \mathbf{z}} \right]_{\bar{\mathbf{z}}} \right] \mathbf{B}_1^T \quad (4.105)$$

In *Equation: (4.105)*, the \mathbf{M}_p matrix is invertible for the same reason as it is described in Section 4.3.1: *Network model*, for the inertia matrix. Expressing the the state vector the following yields:

$$\hat{\mathbf{z}} = (\mathbf{M}_p^{-1} \mathbf{N}_p) \hat{\mathbf{u}} - (\mathbf{M}_p^{-1} \mathbf{B}_o) \Delta \hat{p}_{wt} \quad (4.106)$$

Equation: (4.106) shows the relation between flows and inputs. If the input is increased then the flow increases.

Having the independent states expressed, *Equation: (4.106)* can be inserted in the previously derived WT model with the \mathbf{S} matrix in *Equation: (4.100)*.

$$\Delta \dot{\hat{p}}_{wt} = \underbrace{(\mathbf{S} \mathbf{M}_p^{-1} \mathbf{B}_o)}_{\mathbf{A}_p} \Delta \hat{p}_{wt} - \underbrace{(\mathbf{S} \mathbf{M}_p^{-1} \mathbf{N}_p)}_{\mathbf{B}_p} \hat{\mathbf{u}} \quad (4.107)$$

Equation: (4.107) represents the linear system with the pressure drop across the WT as a state, and the input vector consisting of differential pressures from the pumps and OD values from the end-user valves. The general formulation of the small-signal state equation can be written as follows:

$$\Delta \dot{\hat{p}}_{wt} = \mathbf{A}_p \Delta \hat{p}_{wt} + \mathbf{B}_p \hat{\mathbf{u}} \quad (4.108)$$

Where

$\mathbf{A}_p \in \mathbb{R}^{(1 \times 1)}$ is the system matrix for the parameter estimation, which in this case is a scalar,
and $\mathbf{B}_p \in \mathbb{R}^{(1 \times g)}$ is the input matrix for the parameter estimation.

An output equation is defined, which represents the pressure difference available from the system setup. In this way, the output equation can be compared to the data measured in the setup and proceed to estimate the unknown parameters.

$$\hat{\mathbf{y}} = \mathbf{C}_{p,1} \hat{\mathbf{z}} + \mathbf{C}_{p,2} \hat{\mathbf{u}} \quad (4.109)$$

By substituting the expression for the state vector in *Equation: (4.106)* into the output equation, the following yields:

$$\hat{\mathbf{y}} = \mathbf{C}_{p,1}((\mathbf{M}_p^{-1}\mathbf{N}_p)\hat{\mathbf{u}} - (\mathbf{M}_p^{-1}\mathbf{B}_o)\Delta\hat{p}_{wt}) + \mathbf{C}_{p,2}\hat{\mathbf{u}} \quad (4.110)$$

Reorganizing the terms:

$$\hat{\mathbf{y}} = \underbrace{\mathbf{C}_{p,1}(\mathbf{M}_p^{-1}\mathbf{B}_o)}_{\mathbf{C}_p} \Delta\hat{p}_{wt} + \underbrace{(\mathbf{C}_{p,1}(-(\mathbf{M}_p^{-1}\mathbf{N}_p)) + \mathbf{C}_{p,2})}_{\mathbf{D}_p} \hat{\mathbf{u}} \quad (4.111)$$

$$\hat{\mathbf{y}} = \mathbf{C}_p\Delta\hat{p}_{wt} + \mathbf{D}_p\hat{\mathbf{u}} \quad (4.112)$$

The equation above shows how the output equation includes a feedforward matrix due to the outputs being affected directly by the inputs, as the opening degree of the PMA valves are assumed as inputs.

4.6 Linear parameter estimation

The method that describes the linear parameter estimation is shown in *Figure 4.8*.

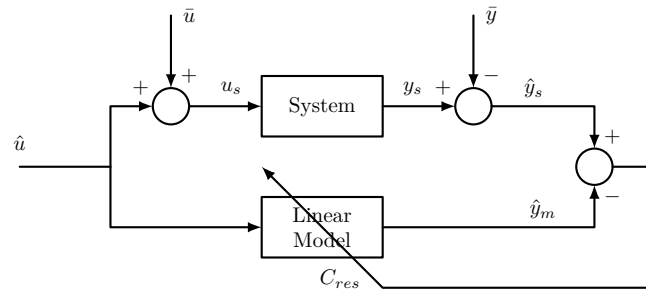


Figure 4.8. Parameter identification block diagram for the linear system.

The small-signal inputs are applied to both the test setup and the model. The linearized model is compared to the real system, therefore the operating point is taken into account as the model is small-signal. Since the linear model is only valid for small deviations around the operating point, the real system has to be excited around the same operating point to stay within the limits of the model. In order to achieve it, the operating values are added to both the input and the output such as:

$$u_{sys} = \bar{u} + \hat{u} \quad (4.113)$$

Where

\hat{u}	is the small-signal input,	[bar]
\bar{u}	is the operating value of the input,	[bar]
and u_s	is the input to the real-life system.	[bar]

And:

$$y_s = \bar{y} + \hat{y}_{sys} \quad (4.114)$$

Where

\hat{g}_s	is the small-signal output from the real-life system,	[bar]
\bar{u}_s	is the operating value of the output,	[bar]
and y_s	is the output from the real-life system.	[bar]

For the linear parameter estimation, the same problem is solved as it is shown in *Equation: (4.76)*. In this case, the parameters are varied according to the comparison of the small-signal outputs.

4.6.1 Model Parameters

In order to obtain a complete model of the physical setup, all the parameters describing the components have to be defined. In Section 4.4: *Nonlinear Parameter identification* a detailed description of the known parameters of the system has been done. In the linearized state-space model, more parameters have to be identified due to the introduction of the operating points. Hence, in the current chapter a detailed description of the unknown parameters of the physical water distribution setup is carried out.

Unknown Parameters

The unknown parameters are related with the form losses, k_f , and form friction, f , of the pipes. Despite they are provided by the manufactures they need to be estimated. The form losses depend on the fittings and bends of the pipes, which are not always known. The friction losses depend on the average inside roughness of the pipes, ϵ , which can change its value due buildups inside pipes or fittings or material change over time.

The operating points of the flow through the chords, \bar{z} , is also unknown. These values, which correspond to the 8 flow chords, are introduced in the linearized expression of both pipes and valves, see *Equation: (4.90)* and *Equation: (4.91)*. Thus, not only pipe parameters introduce uncertainties into the system model but also the lack of knowledge of the chord operating points.

Consequently, it has been decided to estimate the total expression for the pressure across the pipes and valves in order to reduce the amount of unknowns in the system.

The system has 15 pipes in total, from *Equation: (4.90)*, it can be seen that either tuning for k_f , f or \bar{z} will have the same result for the total value of the pressure across the pipes, $\lambda(\mathbf{B}_1^T \mathbf{z})$. For this reason the pressure across the 15 pipes are estimated.

The linearized valve expression, see *Equation: (4.91)*, consists of the term depending on the chord flows, z , and the one depending on the *OD*. Both terms include the operating point of the chord flows inside them, thus the pressure difference given by both terms, has to be estimated. In the system four valves are used, resulting in eight unknowns in total.

The WT connection edge, see *Equation: (4.94)*, is conformed by two valves and one pump. Although the parameters corresponding to the pump are considered as known, the ones corresponding to the valves have to be estimated. Resulting in two more unknowns for the system.

In total, the system has 24 unknown terms which is calculated following the estimation process described in the next section.

4.6.2 Measurements on the test setup

In order to adjust the state-space model, derived in Chapter 4.5.3: *State-space model for linear parameter estimation*, according to physical setup, an estimation for the parameters

defined in Section 4.6.1: *Model Parameters* is carried out.

From the system setup, nine different relative pressures can be measured, following *Figure C.2* notation the sensors are placed in: n_2 n_4 n_5 n_7 n_{10} n_{11} n_{15} n_{16} n_{18} . The estimation will be done only regarding the four PMA pressures and the pressure in the WT. This is chosen since those are the outputs that will be controlled in Section 4.7: *State-space model for control*. Thus, the estimation will only focus on obtaining the best fit for the outputs relevant in the control part.

The relationship between pressures, where Δp_{CXX} describes the pressure difference for the XX component, is obtained in the same way as in Section 4.4: *Nonlinear Parameter identification* and are defined as:

Node 10

$$y_1 = \Delta p_{C24} \quad (4.115)$$

Node 11

$$y_2 = \Delta p_{C20} + \Delta p_{C21} \quad (4.116)$$

Node 15

$$y_3 = \Delta p_{C31} \quad (4.117)$$

Node 16

$$y_4 = \Delta p_{C28} + \Delta p_{C20} \quad (4.118)$$

There is no need to define a relation with a referent point for the WT node, since the pressure across the WT is the state of the state-space model.

4.6.3 Linear Estimation Outcomes

Obtaining a precise model from parameter estimation that describes all aspects of the system well, has been proven challenging. A number of different parameter estimation approaches concerning estimation parameters and data choices has been performed.

The first attempt is based on a relative short data set with both valve and pump input variations and a complete duration of approximately 15 minutes. Here the 24 terms defining the pressure across the unknowns edges are estimated. In *Appendix: F.1* the results of the estimation are presented. From the tests a different behavior between the model and the data from the setup is observed at some time intervals. This dissimilar behavior showing up at some time samples deems it incorrect to be used in a model based control scheme.

In light of the above observations, a different approach for the parameter estimation is attempted. In Section 4.6.1: *Model Parameters* it is described how the unknown pressures across the edges are estimated in order to build up the state-space matrices of the system. As the estimation did not succeed it is decided to estimate the final values of the state-space matrices stated in *Equation: (4.101)*, where M is a symmetric matrix.

Altogether these matrices sum up to 28 unknown parameters, which are the ones to be estimated, furthermore the data duration is extended to approximately 38 minutes to capture more of the system dynamics. In *Appendix: F.2* the results of this estimation technique is displayed. The obtained model now fits the behavior of the system during

the whole dataset and the fit is significantly better than the previous model. However the model fit is in the case of note 16 still not satisfying. Furthermore are the model dynamics of the system too fast compared to real world measurements found in *Appendix: I.1*. The time constant of the system is 19.25 minutes based on step response measurements, where the obtained model based on the parameter estimated matrices has a settling time under 15 seconds.

Due to these model misbehaviors it is chosen to change the used estimation data. The new data has a duration of eight hours in order to catch more of the dynamics. Furthermore, only one input is changed at a time and the system inputs are returned to their respective operating point values before a new input step is applied. Thus can each type of input change be distinguished from each other in the output data.

The model outputs to be compared with the test data are reduced to the WT, note 10 and note 15, in order to facilitate the data gathering due to connection problems at the test setup when running longer tests. The toolbox used for estimating remains the same.

To obtain satisfying results by this approach the estimation process is divided into two parts. The first part estimates the system matrices from *Equation: (4.101)* to fit only the behavior of the WT. From this estimation the final result for these matrices are thus obtained, as the state in this part is the only output from the model.

The next part consists of estimating the remaining system matrices from *Equation: (4.110)* to fit the output behavior described by note 10 and 15. From this the final result for $C_{p,1}$ and $C_{p,2}$ is obtained.

In the following both the inputs and the results obtained by this approach is shown.

Estimation Data

As the estimation is based on a linearized model an operating point for the system is chosen. This point is based on the WT being approximately half full which allows for an equal amount of deviation in both directions. For the chosen operating point, data is gathered from the system while small steps are individually applied to the two main pumps and the opening degree of the PMA valves. In order to use the data for parameter estimation the operating point is subtracted, leaving only small-signal values.

The operating point of the PMA valves is placed at 70% opening corresponding to 63° and the small-signal values for the estimation can be seen in *Figure 4.9*.

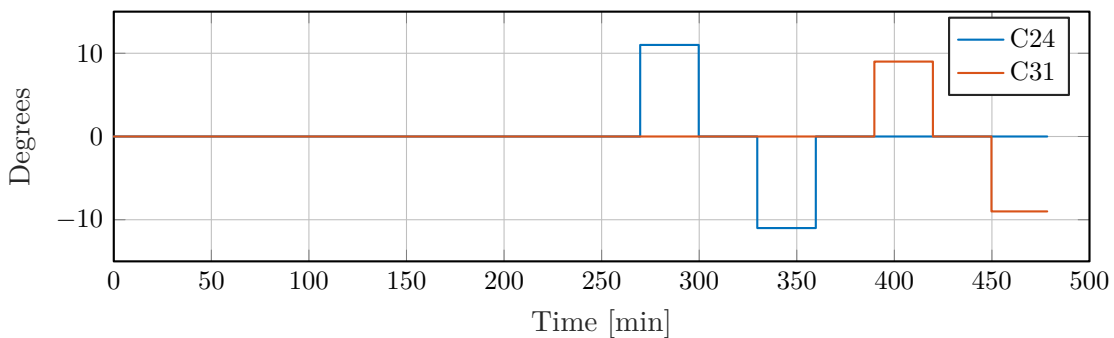


Figure 4.9. Small-signal values of the opening degrees of the PMA valves.

To achieve a 50% fill level of the WT in steady state combined with the chosen operating point of the valves, the operating point of the two inlet pumps, C2 and C16, has to be

set at a differential pressure of $\Delta p = 0.2[\text{bar}]$. The required operating point is found by experimental tests made on the setup. The small-signal values used in the estimation are shown in *Figure 4.10*.

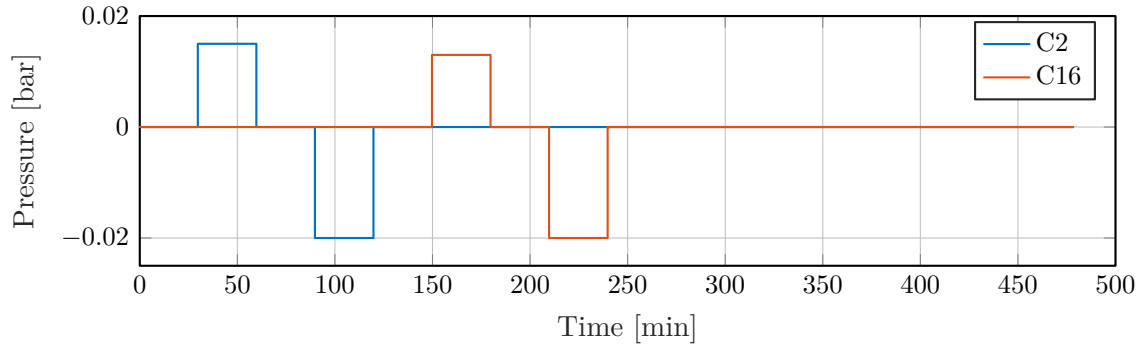


Figure 4.10. Small-signal values of the differential pressure of the two main pumps.

Estimation Result

The following figures show the comparison between the data obtained from the lab and the outputs of the model with the estimated parameters.

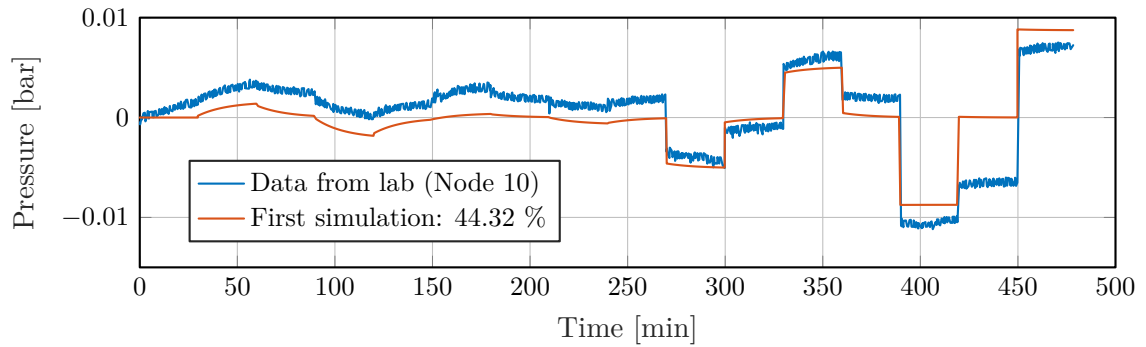


Figure 4.11. Estimation comparison for node 10.

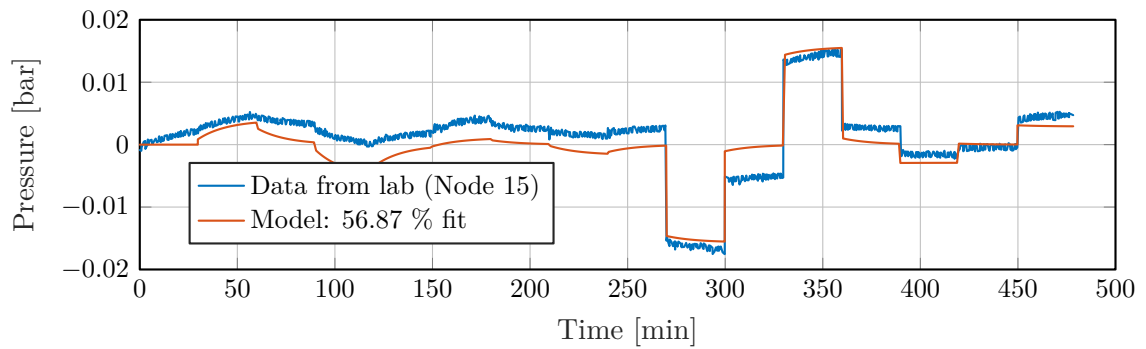


Figure 4.12. Estimation comparison for node 15.

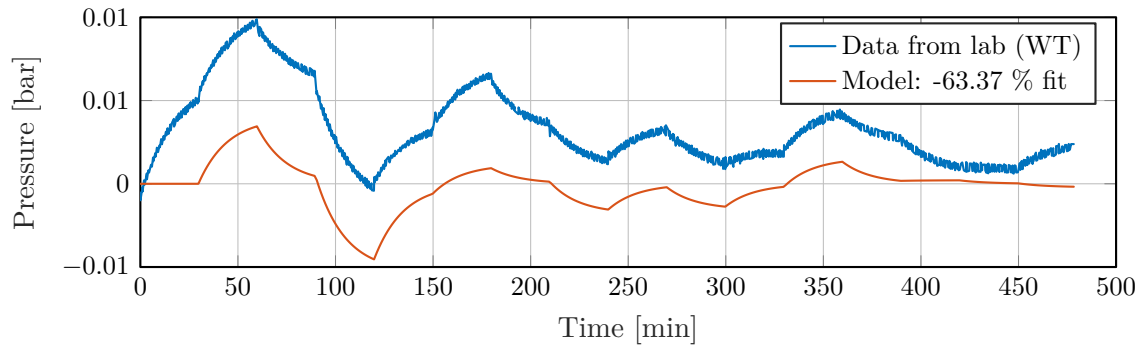


Figure 4.13. Estimation comparison for WT.

With the estimated parameters it is seen that the model follows the behavior of the measured data and that the fit percentage is within a decent margin. Based on these results, the system model and the parameters contained inside can now be used for control purposes, as a description approximating the system is obtained.

4.7 State-space model for control

For reference, the steady state, state-space representation of the parameter estimation for small-signal values is restated here:

$$0 = -M_p \hat{z} + N_p \hat{u} + -B_o \Delta \hat{p}_{wt} \quad (4.119)$$

The equation for the outputs:

$$\hat{y} = C_p \Delta \hat{p}_{wt} + D_p \hat{u} \quad (4.120)$$

And the dynamic model of the WT pressure:

$$\Delta \dot{\hat{p}}_{wt} = \frac{1}{C_H} \hat{q}_0 \quad (4.121)$$

Although *Equation: (4.119)*, *Equation: (4.120)* and *Equation: (4.121)* include all the linearized terms that are necessary to describe the system, for the control it is restructured. The input vector for the parameter estimation consists of four pump differential pressures along with four valve opening degrees. For the control, only the two main pumps are considered as inputs. The control input for the system is therefore defined as $\hat{u} \in \mathbb{R}^{(2 \times 1)}$ as follows:

$$\hat{u} = \begin{bmatrix} \Delta p_{e01} \\ \Delta p_{e08} \end{bmatrix} \quad (4.122)$$

This distinction between the parameter estimation and the control is due to different purposes. For the parameter estimation the inputs are set to excite the system in order to make different pressure scenarios in the network. Therefore, the valve ODs and all pumps are controlled manually to create appropriate output measurements. These measurements are then used to achieve a fit with the output of the simulation by changing its parameters. However in the control this is not desired. Here the inputs are chosen for the control and therefore neither the valve ODs, nor the pump signals are varied manually. Instead the OD is treated as a disturbance.

The mapping for the two main pump pressures yields:

$$\mathbf{B}_1 \tilde{\alpha}(\omega, q) = \mathbf{B}_1 \mathbf{G} \hat{\mathbf{u}} \quad (4.123)$$

Where

$\mathbf{G} \in \mathbb{R}^{(e \times u)}$ is a matrix representing a linear mapping between the vector field $\tilde{\alpha}(\omega, q)$, describing the pressure contribution of the pumps, and between the input vector defined in *Equation: (4.122)* where the dimension u is the number of inputs and e is the number of edges without the WT.

\mathbf{G} is now a mapping matrix for only the two inputs for the main pumps. \mathbf{G} can be found in *Appendix: C.7*.

The input matrix for the control system can be written in the form:

$$\mathbf{N}_c = \mathbf{B}_1 \mathbf{G} \quad (4.124)$$

Compared to the input matrix, in *Equation: (4.103)*, it is seen that the linearized terms belonging to the valves are not part of the matrix since valves are not considered as control inputs.

However, the end-user valves are considered as known disturbances in the control system. Therefore, the disturbance is defined as $\mathbf{d} \in \mathbb{R}^{(2 \times 1)}$:

$$\mathbf{d} = \begin{bmatrix} OD_{e15} \\ OD_{e22} \end{bmatrix} \quad (4.125)$$

It is shown that the PMA pumps are neither considered as inputs nor as disturbances. The inputs for the PMA pumps are excluded from the linearized model. It means that if the PMA pumps were included as disturbances, they would not have an effect on the linearized system because they are kept constant all the time.

The disturbance matrix for the state-space model consists of the linearized terms of the end-user valves. The matrix can be formulated as follows:

$$\mathbf{Q}_c = \mathbf{B}_1 \left[\frac{\partial \mu(\mathbf{B}_1^T \mathbf{z}, OD)}{\partial \mathbf{d}} \right]_{(\bar{\mathbf{z}}, \bar{\mathbf{u}})} \quad (4.126)$$

Taking the same considerations into account as for the parameter estimation, see *Equation: (4.75)*, the steady state equation for small-signals can be formulated as:

$$0 = -\mathbf{M}_c \hat{\mathbf{z}} + \mathbf{N}_c \hat{\mathbf{u}} - \mathbf{Q}_c \hat{\mathbf{d}} - \mathbf{B}_o \Delta \hat{p}_{wt} \quad (4.127)$$

where the system matrix, \mathbf{M}_c is the same as the system matrix, \mathbf{M}_p , for the parameter estimation.

The matrix \mathbf{M}_c is invertible for the same reason as described in *Equation: (4.67)*, thus:

$$\hat{\mathbf{z}} = (\mathbf{M}_c^{-1} \mathbf{N}_c) \hat{\mathbf{u}} - (\mathbf{M}_c^{-1} \mathbf{Q}_c) \hat{\mathbf{d}} - (\mathbf{M}_c^{-1} \mathbf{B}_o) \Delta \hat{p}_{wt} \quad (4.128)$$

Inserting the states into *Equation: (4.100)*:

$$\Delta \hat{p}_{wt} = (\mathbf{S} \mathbf{M}_c^{-1} \mathbf{B}_o) \Delta \hat{p}_{wt} - (\mathbf{S} \mathbf{M}_c^{-1} \mathbf{N}_c) \hat{\mathbf{u}} + (\mathbf{S} \mathbf{M}_c^{-1} \mathbf{Q}_c) \hat{\mathbf{d}} \quad (4.129)$$

Which in standard state-space form can be written as:

$$\Delta \dot{\hat{p}}_{wt} = A_c \Delta \hat{p}_{wt} + B_c \hat{u} + E_c \hat{d} \quad (4.130)$$

Where

$$\begin{aligned} A_c &= -SM_c^{-1}B_o && \text{is the system matrix for the control,} \\ B_c &= -SM_c^{-1}N_c && \text{is the input matrix for the control,} \\ \text{and } E_c &= SM_c^{-1}Q_c && \text{is the disturbance matrix for the control.} \end{aligned}$$

The output of the control model is defined as the two CP corresponding to node 10 and 15. Therefore the output vector is defined as:

$$\mathbf{y} = \begin{bmatrix} \Delta p_{e15} \\ \Delta p_{e22} \end{bmatrix} \quad (4.131)$$

Since the outputs are pressures around two end-user valves, the output expression should be written in the form:

$$\hat{\mathbf{y}} = C_{c,1} \hat{\mathbf{z}} + C_{c,2} \hat{\mathbf{d}} \quad (4.132)$$

Where

$$\begin{aligned} C_{c,1} & \text{ is the matrix consisting of the mapping between the vector field, } \mu, \\ & \text{ and the output vector. Furthermore it includes the partial derivative} \\ & \text{ matrix of the vector field according to the independent states,} \\ \text{and } C_{c,2} & \text{ is the matrix consisting of the mapping between the vector field, } \mu, \\ & \text{ and the output vector. Furthermore it includes the partial derivative} \\ & \text{ matrix of the vector field according to the ODs.} \end{aligned}$$

The output equation includes feedforward from the measured disturbances.

Expressing the independent flow variables with *Equation: (4.128)*, the following yields:

$$\hat{\mathbf{y}} = C_{c,1}[(M_c^{-1}N_c)\hat{\mathbf{u}} - (M_c^{-1}Q_c)\hat{\mathbf{d}} - (M_c^{-1}B_o)\Delta \hat{p}_{wt}] + C_{c,2}\hat{\mathbf{d}} \quad (4.133)$$

And the output equation in standard state-space form:

$$\hat{\mathbf{y}} = C_c \Delta \hat{p}_{wt} + D_c \hat{\mathbf{u}} + K_c \hat{\mathbf{d}} \quad (4.134)$$

Where

$$\begin{aligned} C_c &= -C_{c,1}M_c^{-1}B_o && \text{is the output matrix for the control,} \\ D_c &= C_{c,1}M_c^{-1}N_c && \text{is the feedforward matrix for the control,} \\ \text{and } K_c &= C_{c,2} - C_{c,1}M_c^{-1}Q_c && \text{is the disturbance matrix affecting the output.} \end{aligned}$$

The continuous state-space representation given by *Equation: (4.130)* and *Equation: (4.134)*.

4.7.1 Discretization of state-space model

The dynamics of the water distribution system are described. In order to use this linear model subjected to MPC, the model needs to be discretized. The aim is to have a linear discrete time state-space model with piecewise constant $\Delta \hat{p}_{wt}[k]$, $\hat{\mathbf{u}}[k]$ and $\hat{\mathbf{d}}[k]$ signals. The method used for discretization is the forward Euler-method [27], which can be formulated as follows:

$$\Delta \dot{\hat{p}}_{wt} \approx \frac{\Delta \hat{p}_{wt}[k+1] - \Delta \hat{p}_{wt}[k]}{T_s} \quad (4.135)$$

In order to carry out the discretization, the time constant of the first order system has to be considered. Recalling the dynamic equation:

$$\Delta \dot{\hat{p}}_{wt} = A_c \Delta \hat{p}_{wt} + \mathbf{B}_c \hat{\mathbf{u}} + \mathbf{E}_c \hat{\mathbf{d}} \quad (4.136)$$

The time constant is determined by showing the output and input relation between the WT pressure, the inputs to the main pumps and the disturbance. The frequency component is described by the constant A_c , see *Equation: (4.138)*, where the time constant is $\frac{1}{A_c}$.

$$s \Delta \hat{p}_{wt}(s) = A_c \Delta \hat{p}_{wt}(s) + \mathbf{B}_c \hat{\mathbf{u}}(s) + \mathbf{E}_c \hat{\mathbf{d}}(s) \quad (4.137)$$

After Laplace transforming *Equation: (4.137)*, due to superposition law the time constant of the system can be shown as follows:

$$\Delta \hat{p}_{wt}(s) = \frac{\mathbf{B}_c}{s - A_c} \hat{\mathbf{u}}(s) + \frac{\mathbf{E}_c}{s - A_c} \hat{\mathbf{d}}(s) \quad (4.138)$$

According to the Nyquist-Shannon sampling theorem [27], the sampling frequency has to be at least twice as fast as the highest frequency that is to be sampled. Therefore the sampling time is defined such that:

$$T_s \geq \frac{1}{2A_c} \quad (4.139)$$

However this is the minimum for fulfilling the Nyquist criterion. Therefore, for this project a sample frequency ten times faster has been chosen.

By inserting *Equation: (4.136)* into *Equation: (4.135)*, the discretization of the continuous model can be derived as:

$$\Delta p_{wt}[k+1] \approx (A_c T_s + 1) \hat{p}_{wt} + \mathbf{B}_c T_s \hat{\mathbf{u}} + \mathbf{E}_c T_s \hat{\mathbf{d}} \quad (4.140)$$

where the discrete model is defined as seen in *Equation: (4.141)*.

$$\Delta p_{wt}[k+1] \approx A_d \Delta \hat{p}_{wt}[k] + \mathbf{B}_d \hat{\mathbf{u}}[k] + \mathbf{E}_d \hat{\mathbf{d}}[k] \quad (4.141)$$

Where

$A_d = A_c T_s + 1$ is the discrete state matrix,
 $\mathbf{B}_d = \mathbf{B}_c T_s$ is the discrete input matrix,
 and $\mathbf{E}_d = \mathbf{E}_c T_s$ is the discrete disturbance matrix.

and the output equation:

$$\hat{\mathbf{y}}[k] = \mathbf{C}_d \Delta \hat{p}_{WT}[k] + \mathbf{D}_d \hat{\mathbf{u}}[k] + \mathbf{K}_d \hat{\mathbf{d}}[k] \quad (4.142)$$

Where

\mathbf{C}_d is the discrete output matrix, which is the same as in the continuous case,
 \mathbf{D}_d is the discrete feedforward matrix, which is the same as in the continuous case,
 and \mathbf{K}_d is the discrete disturbance matrix affecting the output, which is the same as in the continuous case.

4.8 Verification of model

A model of the water distribution system is obtained, linearized, Section 4.5: *Linearization of the model*, the parameters are estimated, Section 4.6: *Linear parameter estimation*, the model is arranged on state-space form, Section 4.7: *State-space model for control*, and finally discretized, Section 4.7.1: *Discretization of state-space model*. In this section the model is excited in different ways, to consider if the behavior can be deemed reasonable compared to the test setup. First the time constant for the system is compared to real measurements, then an input is applied to both pumps in order to see how the pressure at the CP changes and then the disturbance, given as OD of the valves, is changed to see how the pressure at the CP changes.

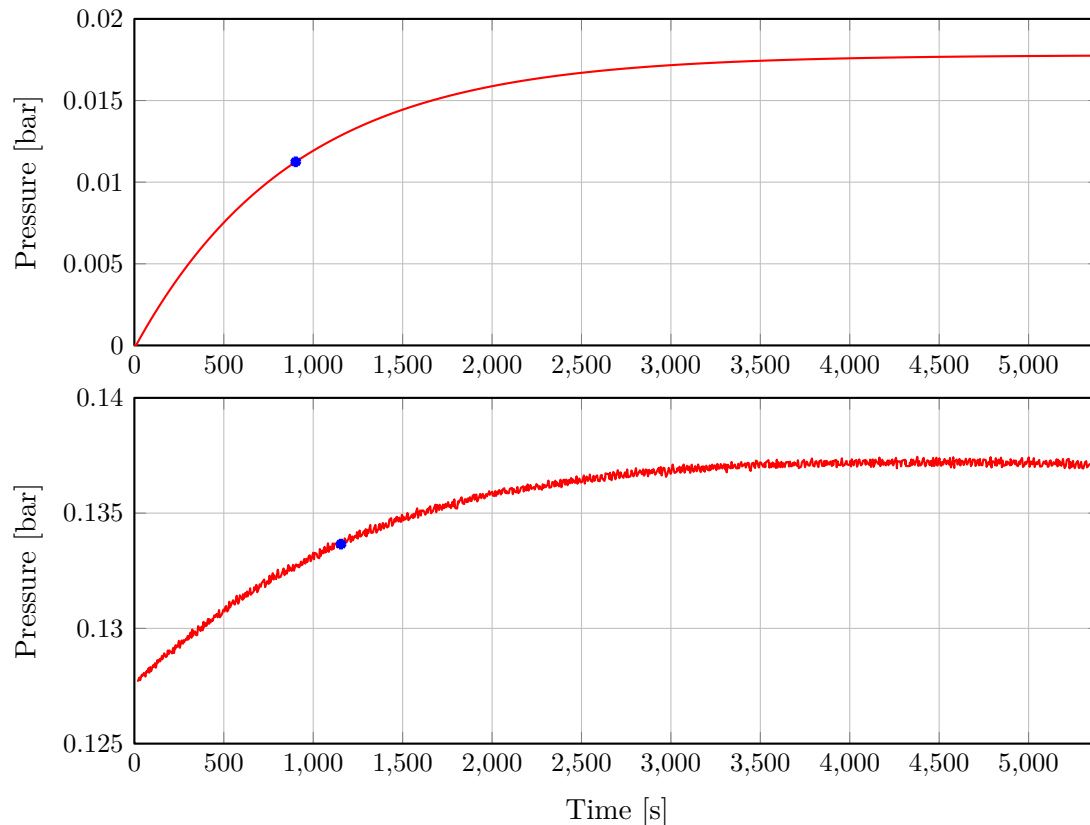


Figure 4.14. The first plot shows a small-signal simulation where a step is applied to both pumps in the final model. The second plot shows the measurement described in *Appendix: I.1*.

At *Figure 4.14* a positive step is applied to both the model and the real system. As it can be seen the pressure rises, meaning that the level of the WT rises. Furthermore the time constant is marked with a blue dot on both plots. From this a time constant for the simulation of 903 seconds, and a time constant for the real system of 1155 seconds are obtained. Thus the model is faster than the system but within a reasonable range.

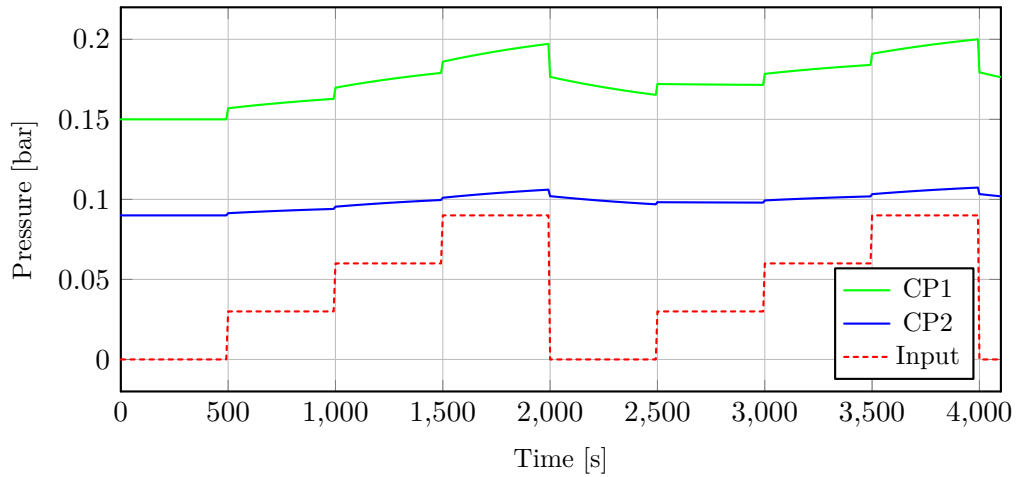


Figure 4.15. A series of steps are applied to the main pumps and it can be seen that the PMA pressure follows as expected.

At Figure 4.15, a series of steps is applied to the model of the main pumps and the pressure change at the CP is plotted. Here it is seen that when a positive step is applied, the pressure at the PMAs increases positively, and the opposite with a negative step. Furthermore, it is seen that there is a pressure different between CP1, node 10, and CP2, node 15. This is also expected because of the physical height difference.

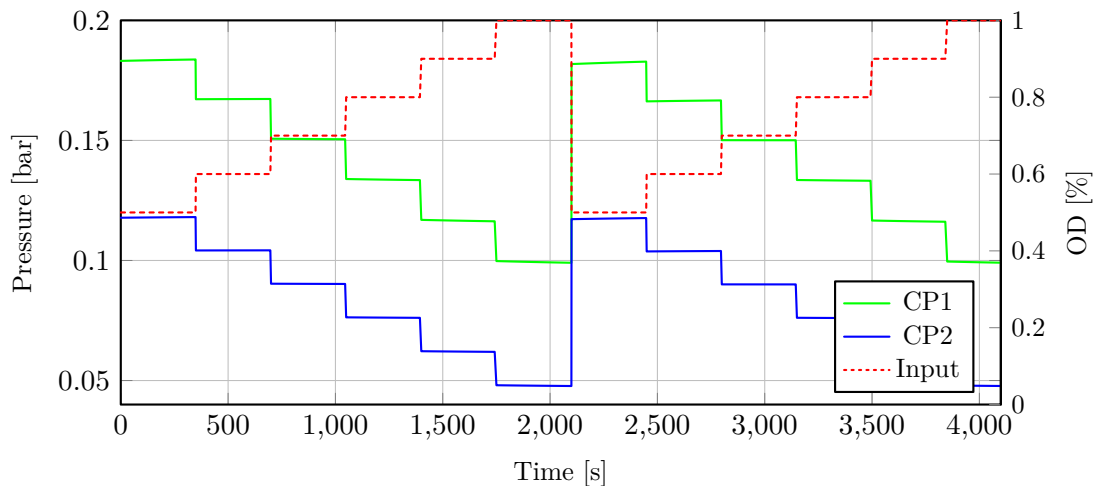


Figure 4.16. A series of steps are applied to the valves and it can be seen that the PMA pressure follows as expected.

At Figure 4.16 a series of steps are applied to the valves, in order to see how a change in disturbance affects the pressure at the CP. Here a pressure drop is seen when OD is increased and an increase in pressure when OD is lowered. This behavior corresponds to the expected as opening a valve at constant differential pump pressure should decrease the PMA pressure and vice versa.

Based on these three tests the overall behavior of the model is validated as the model behaves correctly and consists of the same dynamic properties as the test setup.

Part II

Control Design

In this chapter the design of the controller is explained, including the control problem, optimality and structure. The chosen control approach is then described and leads up to a section where the implementation is discussed.

5.1 Control Problem

The water distribution system described in Section 2.1: *System overview* is to be controlled with respect to the requirements and constraints stated in Section 3: *Requirements and Constraints* and the dynamics of the system described in Section 4.7: *State-space model for control*. For a better clearance, the requirements and constraints are stated again:

- Consumer pressure requirements
- Minimizing the total running costs
- Performance constraints on the pumps

The system consists of four pumps and is controlled by the two placed in the main ring. The two pumps in the PMAs influence only the operating point with a fixed pressure lift.

The project deals with a control scheme that minimizes the cost of running the system, by controlling the main pumps and using the WT, such that the pressure at the end-users is maintained. In other words, the use of the main pumps and the WT is controlled according to the constraints and requirements stated above.

In order to achieve such an optimal behavior, Model Predictive Control (MPC) is considered. With MPC, the dynamics of the model, knowledge about prices and end-user consumption are used to predict the system behavior subject to the constraints in the system.

Apart from the MPC control, all pumps are controlled by PI controllers in order to deliver the required differential pressure. The MPC could be used to control the main pumps directly, but to mimic a real world scenario, without PMA pumps, it is chosen to let the MPC set differential pressure references to the main pumps. As a consequence of the chosen control method, the following cascade structure is formulated for the two main pumps as it is shown in *Figure 5.1*:

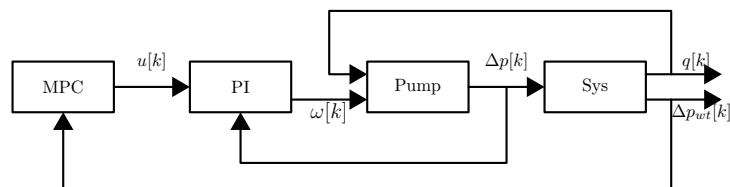


Figure 5.1. Cascade control structure with MPC and PI controllers.

The PI controllers are responsible for setting the control inputs to the main pumps, using the feedback from the differential pressure output. It should be noted that typically the

flow out of the pumping station is controlled instead of the pressure. Here the use of pressure feedback has the advantage that in case of system failure the pressure is what matters. The flow would typically either lead to high or low pressure or it will make the WT overflow. The reference to the PI controllers is set by the MPC algorithm, which takes the measurements from the output into account. The references are set as differential pressures. One of the advantages of such a cascade control is that the pump controllers are present at each pump, also including the PMA pumps. At the event of implementation or communication failure between the MPC and the pump controllers, the pumping remains operational.

In order to define an objective function for the MPC problem, the cost of running the system has to be taken into account based on the power consumption of the pumps and the electrical price. Such an objective function can be written in the form:

$$\Upsilon(\mathbf{u}[k], \mathbf{q}_p[k], c_p[k]) = \frac{1}{\eta} \sum_{i=1}^{H_p-1} \left(\mathbf{u}^T[k+i|k] \cdot \mathbf{q}_p[k+i|k] \right) \cdot c_p[k+i|k] \quad (5.1)$$

Where

Υ	is the price of running the system,	[DKK]
H_p	is the prediction horizon,	[·]
\mathbf{u}	is the differential pressure input to the main pumps,	[bar]
\mathbf{q}_p	is the flow through the main pumps,	[m ³ /h]
η_i	is the efficiency of the main pumps,	[·]
and c_p	is the electricity price cost sequence.	$\left[\frac{\text{DKK}}{\text{MWh}} \right]$

It should be pointed out that the input and flow variables of the objective function are not small-signal values since the energy is to be optimized. Therefore the deviation from the operating point would not result in the total amount of energy consumed by the pumps.

The efficiency of the two main pumps is assumed to be the same as the pumps are of the same type. Furthermore, the efficiency is considered to be constant since the operating point is the same for the main pumps and it is assumed that for small deviations in flow and pressure the efficiency does not vary significantly. The control problem is formulated as a minimization problem of the form:

$$\min_{\mathbf{u}} \Upsilon(\mathbf{u}[k], \mathbf{q}_p[k], c_p[k]) = \min_{\mathbf{u}} \frac{1}{\eta} \sum_{i=0}^{H_p-1} \left(\mathbf{u}^T[k+i|k] \cdot \mathbf{q}_p[k+i|k] \right) \cdot c_p[k+i|k] \quad (5.2)$$

$$\text{s.t.} \quad \Delta \hat{p}_{wt}[k+i+1|k] = A_d \Delta \hat{p}_{wt}[k+i|k] + B_d \hat{\mathbf{u}}[k+i|k] + E_d \hat{\mathbf{d}}[k+i|k] \quad (5.3)$$

$$\hat{\mathbf{y}}[k+i|k] = C_d \Delta \hat{p}_{wt}[k+i|k] + D_d \hat{\mathbf{u}}[k+i|k] + K_d \hat{\mathbf{d}}[k+i|k] \quad (5.4)$$

$$\underline{\mathbf{y}} \leq \mathbf{y} \leq \overline{\mathbf{y}} \quad (5.5)$$

$$\underline{\Delta p_{wt}} \leq \Delta p_{wt} \leq \overline{\Delta p_{wt}} \quad (5.6)$$

$$\underline{\mathbf{u}} \leq \mathbf{u} \leq \overline{\mathbf{u}} \quad (5.7)$$

Where

\mathbf{y}	is the output vector with the PMA pressures,	[bar]
and Δp_{wt}	is the state which is the pressure in the WT.	[bar]

As it is shown in *Equation: (5.2)* the optimal input signal is obtained such that the cost of running the pumps is minimized. Therefore, the objective function gives a price for all the consumed power over the control horizon, which is a specific future time interval. No direct information about the flows through the pumps are available, therefore the flows need to be expressed as other variables, leading to the problem being reformulated.

The minimization is subject to the dynamics of the water distribution network, and the constraints. The constraint on the output of the system, is considered as the pressure demand for the end-users. Furthermore, two constraints to the pressure in the WT and the input signal to the pumps are present.

In the following sections the design of the control system is explained.

5.2 Model predictive control

Model predictive control is an advanced control method that depends on the dynamic model of the system. It is model based as it uses an explicit internal model to generate predictions of future system behavior. Therefore MPC allows to calculate an optimal control signal taking the future model and disturbance behavior into account. The control structure of MPC is in general:

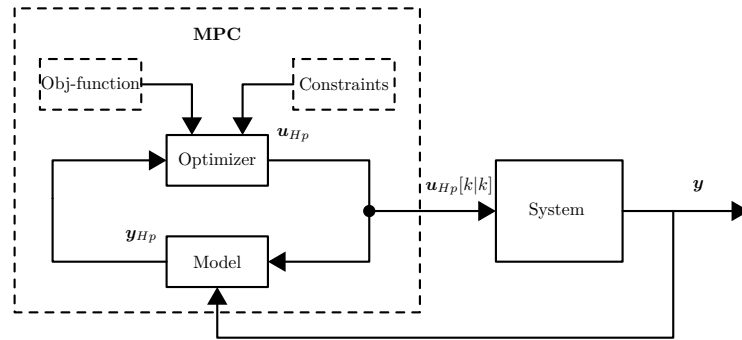


Figure 5.2. The block of MPC algorithm [28].

Figure 5.2 is of the same structure as Figure 5.1, however here the MPC block is specified. A MPC is an iterative process that can be summarized as follows:

- 1: A measurement is taken on either the outputs or directly on the states if state measurement is available. Otherwise the states are estimated.
- 2: The optimizer calculates a set of predicted values over the prediction horizon, according to the objective of the control and the constraints. The predicted inputs are defined by \mathbf{u}_{Hp} .
- 3: $\mathbf{u}_{Hp}[k|k]$, the first entry of the calculated control sequence at the current time k , is applied.
- 4: Go back to 1.

The future outputs \mathbf{y}_{Hp} and the future inputs \mathbf{u}_{Hp} are defined by:

$$\mathbf{y}_{Hp} = \begin{bmatrix} \mathbf{y}[k|k] \\ \vdots \\ \mathbf{y}[k + H_p - 1|k] \end{bmatrix} \quad (5.8)$$

$$\mathbf{u}_{Hp} = \begin{bmatrix} \mathbf{u}[k|k] \\ \vdots \\ \mathbf{u}[k + H_p - 1|k] \end{bmatrix} \quad (5.9)$$

Where

$\mathbf{y}[k|k]$ is the predicted output to time k based on the current output,
 H_p is the prediction horizon,
 and $\mathbf{u}[k|k]$ is the predicted optimal control signal to the current time k .

To calculate the matrices, H_p need to be determined. In Section *G: Electrical price* it is seen that the price fluctuates a lot but some periodicity is seen every 24 hours. Furthermore, water consumption is seen as periodic, with a periodicity of 24 hours, due to the daily rhythm of the population. Therefore, H_p is chosen to 24.

5.3 Reformulation of the objective function

The minimization problem formulated in Section 5.1: *Control Problem* describes the optimization subject to the system dynamics and constraints. In order to make this problem solvable, the objective function has to match the state-space dynamics, therefore it has to be reformulated. As it is shown in *Equation: (5.1)*, the hydraulic power is expressed with the flow through the pumps, however the dynamics include the WT pressure as a state.

The equation used for the reformulation of the pump flows is recalled *Equation: (4.128)*:

$$\hat{z} = (M_c^{-1}N_c)\hat{u} - (M_c^{-1}Q_c)\hat{d} - (M_c^{-1}B_o)\Delta\hat{p}_{wt} \quad (5.10)$$

Equation: (5.10) explains how the independent flows of the network can be calculated with the system matrices. Using this equation and substituting this into the objective function, the flows through the pumps can be obtained. Recalling that all flows can be obtained from the independent variables, the flow through the pumps is given with a linear mapping such that:

$$q_p[k] = G^T B_1^T z[k] \quad (5.11)$$

Where

$G^T \in \mathbb{R}^{(2 \times e)}$ is a matrix representing a linear mapping between the flow through the two main pumps and the edge flows in the system. The dimension e is the number of edges without the WT while the number of rows is the number of main pumps. This mapping matrix is the same as the mapping described in *Equation: (4.123)*.

The system dynamics are only valid for small-signal values of the chord flows, and therefore for the small-signal values of the pump flows. As a consequence of this, $q_p[k]$ is written as a sum of the operating point and the deviation:

$$q_p[k] = \bar{q}_p + \hat{q}_p[k] = \bar{q}_p + G^T B_1^T \hat{z}[k] \quad (5.12)$$

Where

\bar{q}_p is the operating value of the flow through the main pumps, $[\text{m}^3/\text{h}]$
and $\hat{q}_p[k]$ is the small-signal value of the flows through the main pumps. $[\text{m}^3/\text{h}]$

The operating value for the pump flows is determined by the nonlinear model of the pumps with the available pressure measurements. This is described in detail in *Appendix: H*.

Inserting the expression for the small-signal chord flows given in *Equation: (5.10)* into *Equation: (5.12)* and then into the objective function, which yields:

$$\hat{q}_p[k] = G^T B_1^T (M_c^{-1}N_c \cdot \hat{u}[k] - M_c^{-1}Q_c \cdot \hat{d}[k] - M_c^{-1}B_o \cdot \Delta\hat{p}_{wt}[k]) \quad (5.13)$$

Therefore the small-signal flow through the main pumps can be written as:

$$\hat{q}_p[k] = \Lambda_1 \hat{u}[k] + \Lambda_2 \hat{d}[k] + \Lambda_3 \Delta\hat{p}_{wt}[k] \quad (5.14)$$

Based on *Equation: (5.14)* the following is defined:

$$\begin{aligned}\Lambda_1 &= \mathbf{G}^T \mathbf{B}_1^T \mathbf{M}_c^{-1} \mathbf{N}_c \in \mathbb{R}^{(2 \times 2)} \\ \Lambda_2 &= -\mathbf{G}^T \mathbf{B}_1^T \mathbf{M}_c^{-1} \mathbf{Q}_c \in \mathbb{R}^{(2 \times 2)} \\ \Lambda_3 &= -\mathbf{G}^T \mathbf{B}_1^T \mathbf{M}_c^{-1} \mathbf{B}_o \in \mathbb{R}^{(2 \times 1)}\end{aligned}$$

Hence the objective function:

$$\frac{1}{\eta} \sum_{i=0}^{H_p-1} \left[\mathbf{u}^T[k+i|k] \cdot \left(\bar{\mathbf{q}}_p + \Lambda_1 \hat{\mathbf{u}}[k+i|k] + \Lambda_2 \hat{\mathbf{d}}[k+i|k] + \Lambda_3 \Delta \hat{p}_{wt}[k+i|k] \right) \right] \cdot c_p[k+i|k] \quad (5.15)$$

As can be seen in *Equation: (5.15)*, the objective function now includes both the full- and small-signal inputs, the small-signal disturbances and the small-signal pressure in the WT. It is important to point out that the system dynamics are described by small-signals, however as it is stated in the problem formulation, the optimization for the cost has to be according to full-signals. Since the dynamics are meant to be plugged into the objective function, the following has to be considered:

$$\mathbf{u} = \bar{\mathbf{u}} + \hat{\mathbf{u}} \quad (5.16)$$

and

$$\mathbf{d} = \bar{\mathbf{d}} + \hat{\mathbf{d}} \quad (5.17)$$

which shows that the signals are decomposed to their constant values in the operating point and the small-signal deviations.

As shown, in *Equation: (5.10)*, the WT pressure is described as a state in the model of the water distribution system. Therefore, the state-space model in *Equation: (5.3)* can be used to substitute this pressure term in *Equation: (5.15)*.

Before substituting the dynamics into the objective function, it is important to point out that an initial measurement of the states has to be available. In other words, an initial small-signal pressure value is required in the WT. The deviation from the operating point can be determined by subtracting the operating point value from the measurement. Due to the available sensors it is possible to obtain the initial WT pressure at $i = 0$.

The cost function is formulated in such a way, that from the current time step, k , the future values are iterated from $i = 0$ to $i = H_p - 1$, when calculating the price of energy usage for the whole interval. In order to replace this iterative summation with vector and matrix products, all signals and matrices are written up for the complete prediction horizon. Therefore, the elements of the input vector represent input configurations at different time steps moving towards the end of the interval, such that:

$$\mathbf{u}_{H_p} = \begin{bmatrix} \mathbf{u}[k|k] \\ \vdots \\ \mathbf{u}[k + H_p - 1|k] \end{bmatrix} \in \mathbb{R}^{(2H_p \times 1)} \quad (5.18)$$

The disturbance vector is formulated as:

$$\mathbf{d}_{H_p} = \begin{bmatrix} \mathbf{d}[k|k] \\ \vdots \\ \mathbf{d}[k + H_p - 1|k] \end{bmatrix} \in \mathbb{R}^{(2H_p \times 1)} \quad (5.19)$$

At time step k , these signals consist of the present and future input and disturbance vectors until the end of the horizon, which is $H_p - 1$, since i is iterated from zero. In the further sections the same notation is used for all signals as in *Equation: (5.18)* and *Equation: (5.19)*.

In order to substitute the system dynamics into the objective function, it has to be written up for the prediction horizon, with extended matrices and signal vectors that represent the predicted values of the inputs, states and disturbances. For $i = 1$, the iteration of the state equation gives:

$$\Delta\hat{p}_{wt}[1] = A_d\Delta\hat{p}_{wt}[0] + B_d\hat{u}[0] + E_d\hat{d}[0] \quad (5.20)$$

Now $\Delta\hat{p}_{wt}[2]$ is calculated in the same way, but with $\Delta\hat{p}_{wt}[1]$ substituted:

$$\Delta\hat{p}_{wt}[2] = A_d[A_d\Delta\hat{p}_{wt}[0] + B_d\hat{u}[0] + E_d\hat{d}[0]] + B_d\hat{u}[1] + E_d\hat{d}[1] \quad (5.21)$$

Moving further in time steps, the predicted states only depend on the past values of the input, disturbance and the initial state measurement. Writing up the matrix equation until the $i = H_p - 1$ time steps, thus until the end of the prediction horizon, the following extended matrix equation yields:

$$\underbrace{\begin{bmatrix} \Delta\hat{p}_{wt}[0] \\ \Delta\hat{p}_{wt}[k+1|k] \\ \Delta\hat{p}_{wt}[k+2|k] \\ \vdots \\ \Delta\hat{p}_{wt}[k+H_p-1] \end{bmatrix}}_{\Delta\hat{p}_{wt,H_p}} = \underbrace{\begin{bmatrix} 1 \\ A_d \\ A_d^2 \\ \vdots \\ A_d^{(H_p-1)} \end{bmatrix}}_{\Phi} \Delta\hat{p}_{wt}[0] + \underbrace{\begin{bmatrix} \mathbf{0} & \mathbf{0} & \dots & \mathbf{0} \\ B_d & \mathbf{0} & \dots & \mathbf{0} \\ A_d B_d & B_d & \dots & \mathbf{0} \\ \vdots & \vdots & \ddots & \vdots \\ A_d^{(H_p-1)} B_d & A_d^{(H_p-2)} B_d & \dots & \mathbf{0} \end{bmatrix}}_{\Gamma} \underbrace{\begin{bmatrix} \hat{u}[k|k] \\ \hat{u}[k+1|k] \\ \hat{u}[k+2|k] \\ \vdots \\ \hat{u}[k+H_p-1|k] \end{bmatrix}}_{\hat{u}_{H_p}} + \underbrace{\begin{bmatrix} \mathbf{0} & \mathbf{0} & \dots & \mathbf{0} \\ E_d & \mathbf{0} & \dots & \mathbf{0} \\ A_d E_d & E_d & \dots & \mathbf{0} \\ \vdots & \vdots & \ddots & \vdots \\ A_d^{(H_p-1)} E_d & A_d^{(H_p-2)} E_d & \dots & \mathbf{0} \end{bmatrix}}_{\Psi} \underbrace{\begin{bmatrix} \hat{d}[k|k] \\ \hat{d}[k+1|k] \\ \hat{d}[k+2|k] \\ \vdots \\ \hat{d}[k+H_p-1|k] \end{bmatrix}}_{\hat{d}_{H_p}} \quad (5.22)$$

The first line of the dynamics describes the following trivial equation:

$$\Delta\hat{p}_{wt}[0] = \Delta\hat{p}_{wt}[0] \quad (5.23)$$

The dynamics, expressed with the newly introduced vectors and matrices, are written as:

$$\Delta\hat{p}_{wt,H_p} = \Phi\Delta\hat{p}_{wt}[0] + \Gamma\hat{u}_{H_p} + \Psi\hat{d}_{H_p} \quad (5.24)$$

Where

$\Delta\hat{\mathbf{p}}_{wt,H_p} \in \mathbb{R}^{(H_p \times 1)}$	is the predicted state vector calculated for the whole prediction horizon,
$\Delta\hat{\mathbf{p}}_{wt}[0] \in \mathbb{R}^{(1 \times 1)}$	is the initial state describing the whole prediction horizon,
$\hat{\mathbf{u}}_{H_p} \in \mathbb{R}^{(2H_p \times 1)}$	is the predicted input vector consisting of all the predicted values from the current time step until $k = H_p - 1$,
$\hat{\mathbf{d}}_{H_p} \in \mathbb{R}^{(2H_p \times 1)}$	is the disturbance vector consisting of all the future values from the current time step until $k = H_p - 1$,
$\Phi \in \mathbb{R}^{(H_p \times 1)}$	is the state matrix along the prediction horizon, taking A_d into account at each time step,
$\Gamma \in \mathbb{R}^{(H_p \times 2H_p)}$	is the input matrix along the prediction horizon, taking A_d and \mathbf{B}_d matrix into account at each time step,
and $\Psi \in \mathbb{R}^{(H_p \times 2H_p)}$	is the disturbance matrix along the prediction horizon, taking the A_d and \mathbf{E}_d matrix into account at each time step.

The state, input and disturbance matrices can be calculated prior to solving the MPC optimization because they consist of the matrices describing the model. *Equation: (5.24)* defines the future state trajectories for each time step throughout the prediction horizon. Furthermore, it is noted here that these matrices now describe the variables for the whole prediction horizon, and therefore the signals are subscripted with H_p , as mentioned above.

The objective function formulated in *Equation: (5.15)* consists of the product of the $\Lambda_{1,2,3}$ matrices and the signals. In order to express the objective function in vector form, the cost function is multiplied with these $\Lambda_{1,2,3}$ matrices such that:

$$\Lambda_{1,H_p} = \begin{bmatrix} \Lambda_1 c_p[k|k] & \dots & \mathbf{0} \\ \vdots & \ddots & \vdots \\ \mathbf{0} & \dots & \Lambda_1 c_p[k + H_p - 1|k] \end{bmatrix} \in \mathbb{R}^{(2H_p \times 2H_p)} \quad (5.25)$$

$$\Lambda_{2,H_p} = \begin{bmatrix} \Lambda_2 c_p[k|k] & \dots & \mathbf{0} \\ \vdots & \ddots & \vdots \\ \mathbf{0} & \dots & \Lambda_2 c_p[k + H_p - 1|k] \end{bmatrix} \in \mathbb{R}^{(2H_p \times 2H_p)} \quad (5.26)$$

$$\Lambda_{3,H_p} = \begin{bmatrix} \Lambda_3 c_p[k|k] & \dots & \mathbf{0} \\ \vdots & \ddots & \vdots \\ \mathbf{0} & \dots & \Lambda_3 c_p[k + H_p - 1|k] \end{bmatrix} \in \mathbb{R}^{(2H_p \times H_p)} \quad (5.27)$$

All the matrices and signals are represented in vector form along with their predicted values, the objective function is written up such that:

$$\Upsilon(\hat{\mathbf{u}}_{H_p}, \Delta\hat{\mathbf{p}}_{wt,H_p}) = \frac{1}{\eta} (\bar{\mathbf{u}}_{H_p} + \hat{\mathbf{u}}_{H_p})^T \left[\bar{\mathbf{q}}_{p,H_p} + \Lambda_{1,H_p} \hat{\mathbf{u}}_{H_p} + \Lambda_{2,H_p} \hat{\mathbf{d}}_{H_p} + \Lambda_{3,H_p} \Delta\hat{\mathbf{p}}_{wt,H_p} \right] \quad (5.28)$$

The dynamics of the system is substituted into *Equation: (5.28)*:

$$\begin{aligned} \Upsilon(\hat{\mathbf{u}}_{H_p}) = \frac{1}{\eta} (\bar{\mathbf{u}}_{H_p} + \hat{\mathbf{u}}_{H_p})^T & \left[\bar{\mathbf{q}}_{p,H_p} + \Lambda_{1,H_p} \hat{\mathbf{u}}_{H_p} + \Lambda_{2,H_p} \hat{\mathbf{d}}_{H_p} \right. \\ & \left. + \Lambda_{3,H_p} \left(\Phi \Delta\hat{\mathbf{p}}_{wt,H_p}[0] + \Gamma \hat{\mathbf{u}}_{H_p} + \Psi \hat{\mathbf{d}}_{H_p} \right) \right] \end{aligned} \quad (5.29)$$

By expressing the terms in *Equation: (5.29)*, the following yields:

$$\begin{aligned} \Upsilon(\hat{\mathbf{u}}_{Hp}) = & \frac{1}{\eta} \left[\underbrace{(\bar{\mathbf{u}}_{Hp} + \hat{\mathbf{u}}_{Hp})^T \bar{\mathbf{q}}_{p,Hp}}_{\text{I}} + \underbrace{(\bar{\mathbf{u}}_{Hp} + \hat{\mathbf{u}}_{Hp})^T \mathbf{\Lambda}_{1,Hp} \hat{\mathbf{u}}_{Hp}}_{\text{II}} \right. \\ & + \underbrace{(\bar{\mathbf{u}}_{Hp} + \hat{\mathbf{u}}_{Hp})^T \mathbf{\Lambda}_{2,Hp} \hat{\mathbf{d}}_{Hp}}_{\text{III}} + \underbrace{(\bar{\mathbf{u}}_{Hp} + \hat{\mathbf{u}}_{Hp})^T \mathbf{\Lambda}_{3,Hp} \mathbf{\Phi} \Delta \hat{p}_{wt,Hp}[0]}_{\text{IV}} \\ & \left. + \underbrace{(\bar{\mathbf{u}}_{Hp} + \hat{\mathbf{u}}_{Hp})^T \mathbf{\Lambda}_{3,Hp} \mathbf{\Gamma} \hat{\mathbf{u}}_{Hp}}_{\text{V}} + \underbrace{(\bar{\mathbf{u}}_{Hp} + \hat{\mathbf{u}}_{Hp})^T \mathbf{\Lambda}_{3,Hp} \mathbf{\Psi} \hat{\mathbf{d}}_{Hp}}_{\text{VI}} \right] \end{aligned} \quad (5.30)$$

The product of the different terms with the operating and deviation values results in the following:

$$\text{I) } (\bar{\mathbf{u}}_{Hp} + \hat{\mathbf{u}}_{Hp})^T \bar{\mathbf{q}}_{p,Hp} = \bar{\mathbf{u}}_{Hp}^T \bar{\mathbf{q}}_{p,Hp} + \hat{\mathbf{u}}_{Hp}^T \bar{\mathbf{q}}_{p,Hp} \quad (5.31)$$

$$\text{II) } (\bar{\mathbf{u}}_{Hp} + \hat{\mathbf{u}}_{Hp})^T \mathbf{\Lambda}_{1,Hp} \hat{\mathbf{u}}_{Hp} = \bar{\mathbf{u}}_{Hp}^T \mathbf{\Lambda}_{1,Hp} \hat{\mathbf{u}}_{Hp} + \hat{\mathbf{u}}_{Hp}^T \mathbf{\Lambda}_{1,Hp} \hat{\mathbf{u}}_{Hp} \quad (5.32)$$

$$\text{III) } (\bar{\mathbf{u}}_{Hp} + \hat{\mathbf{u}}_{Hp})^T \mathbf{\Lambda}_{2,Hp} \hat{\mathbf{d}}_{Hp} = \bar{\mathbf{u}}_{Hp}^T \mathbf{\Lambda}_{2,Hp} \hat{\mathbf{d}}_{Hp} + \hat{\mathbf{u}}_{Hp}^T \mathbf{\Lambda}_{2,Hp} \hat{\mathbf{d}}_{Hp} \quad (5.33)$$

$$\begin{aligned} \text{IV) } (\bar{\mathbf{u}}_{Hp} + \hat{\mathbf{u}}_{Hp})^T \mathbf{\Lambda}_{3,Hp} \mathbf{\Phi} \Delta \hat{p}_{wt,Hp}[0] &= \bar{\mathbf{u}}_{Hp}^T \mathbf{\Lambda}_{3,Hp} \mathbf{\Phi} \Delta \hat{p}_{wt,Hp}[0] \\ &+ \hat{\mathbf{u}}_{Hp}^T \mathbf{\Lambda}_{3,Hp} \mathbf{\Phi} \Delta \hat{p}_{wt,Hp}[0] \end{aligned} \quad (5.34)$$

$$\text{V) } (\bar{\mathbf{u}}_{Hp} + \hat{\mathbf{u}}_{Hp})^T \mathbf{\Lambda}_{3,Hp} \mathbf{\Gamma} \hat{\mathbf{u}}_{Hp} = \bar{\mathbf{u}}_{Hp}^T \mathbf{\Lambda}_{3,Hp} \mathbf{\Gamma} \hat{\mathbf{u}}_{Hp} + \hat{\mathbf{u}}_{Hp}^T \mathbf{\Lambda}_{3,Hp} \mathbf{\Gamma} \hat{\mathbf{u}}_{Hp} \quad (5.35)$$

$$\text{VI) } (\bar{\mathbf{u}}_{Hp} + \hat{\mathbf{u}}_{Hp})^T \mathbf{\Lambda}_{3,Hp} \mathbf{\Psi} \hat{\mathbf{d}}_{Hp} = \bar{\mathbf{u}}_{Hp}^T \mathbf{\Lambda}_{3,Hp} \mathbf{\Psi} \hat{\mathbf{d}}_{Hp} + \hat{\mathbf{u}}_{Hp}^T \mathbf{\Lambda}_{3,Hp} \mathbf{\Psi} \hat{\mathbf{d}}_{Hp} \quad (5.36)$$

The objective functions is expressed with the vector of small-signal inputs. The operating values of the inputs are the operating pressures of the two main pumps. Both the small-signal and operating point values of the disturbances are present. These disturbances are the ODs of the end-user valves, therefore they describe the characteristics of water usage. From the expressions derived above it can be seen that predictions are necessary for this water usage. The operating point values are known and are constant in the whole sequence. The small signal values are the deviations from this constant OD and known, since the full-signal value of the whole disturbance sequence is known.

All matrices in the objective function are expressed using the predicted value of the electrical price which is changing over time. Therefore, the matrices need to be updated at every time step.

After rearranging the terms, it is shown in *Equation: (5.36)* that the objective function consists of quadratic and linear terms of the vector $\hat{\mathbf{u}}_{Hp}$. Furthermore, there are constant terms due to the operating values of the disturbances and inputs.

Hence the quadratic term results in:

$$\hat{\mathbf{u}}_{Hp}^T (\mathbf{\Lambda}_{1,Hp} + \mathbf{\Lambda}_{3,Hp} \mathbf{\Gamma}) \hat{\mathbf{u}}_{Hp} \quad (5.37)$$

The linear term is given by:

$$\begin{aligned} & \bar{\mathbf{u}}_{Hp}^T (\mathbf{\Lambda}_{1,Hp} + \mathbf{\Lambda}_{3,Hp} \mathbf{\Gamma}) \hat{\mathbf{u}}_{Hp} + \hat{\mathbf{u}}_{Hp}^T (\mathbf{\Lambda}_{2,Hp} + \mathbf{\Lambda}_{3,Hp} \mathbf{\Psi}) \hat{\mathbf{d}}_{Hp} \\ & + \hat{\mathbf{u}}_{Hp}^T \mathbf{\Lambda}_{3,Hp} \mathbf{\Phi} \Delta \hat{p}_{wt,Hp}[0] + \hat{\mathbf{u}}_{Hp}^T \bar{\mathbf{q}}_{p,Hp} \end{aligned} \quad (5.38)$$

And the constants are:

$$\bar{\mathbf{u}}_{Hp}^T \bar{\mathbf{q}}_{p,Hp} + \bar{\mathbf{u}}_{Hp}^T \mathbf{\Lambda}_{2,Hp} \hat{\mathbf{d}}_{Hp} + \bar{\mathbf{u}}_{Hp}^T \mathbf{\Lambda}_{3,Hp} \mathbf{\Phi} \Delta \hat{p}_{wt,Hp}[0] + \bar{\mathbf{u}}_{Hp}^T \mathbf{\Lambda}_{3,Hp} \mathbf{\Psi} \hat{\mathbf{d}}_{Hp} \quad (5.39)$$

Therefore it is shown that this optimization simplifies to a quadratic problem that can be written up in such a form as follows:

$$\Upsilon(\hat{\mathbf{u}}_{Hp}) = \frac{1}{\eta} \left(\frac{1}{2} \hat{\mathbf{u}}_{Hp}^T \mathbf{R} \hat{\mathbf{u}}_{Hp} + \mathbf{b} \hat{\mathbf{u}}_{Hp} + c \right) \quad (5.40)$$

Where

$$\begin{aligned} \mathbf{R} &\in \mathbb{R}^{(2H_p \times 2H_p)} \\ \mathbf{b} &\in \mathbb{R}^{(1 \times H_p)} \\ c &\in \mathbb{R}^{(1 \times 1)} \end{aligned}$$

The matrix \mathbf{R} in the quadratic problem is given as:

$$\mathbf{R} = 2 \left(\mathbf{\Lambda}_{1,Hp} + \mathbf{\Lambda}_{3,Hp} \mathbf{\Gamma} \right) \quad (5.41)$$

The vector \mathbf{b} is given as:

$$\mathbf{b} = \bar{\mathbf{u}}_{Hp}^T (\mathbf{\Lambda}_{1,Hp} + \mathbf{\Lambda}_{3,Hp} \mathbf{\Gamma}) + \hat{\mathbf{d}}_{Hp}^T (\mathbf{\Lambda}_{2,Hp} + \mathbf{\Lambda}_{3,Hp} \mathbf{\Psi})^T + \Delta \hat{p}_{wt,Hp}^T [0] (\mathbf{\Lambda}_{3,Hp} \mathbf{\Phi})^T + \bar{\mathbf{q}}_{p,Hp}^T \quad (5.42)$$

The constant term c is given as:

$$c = \bar{\mathbf{u}}_{Hp}^T \bar{\mathbf{q}}_{p,Hp} + \bar{\mathbf{u}}_{Hp}^T \mathbf{\Lambda}_{2,Hp} \hat{\mathbf{d}}_{Hp} + \bar{\mathbf{u}}_{Hp}^T (\mathbf{\Lambda}_{3,Hp} \mathbf{\Phi}) \Delta \hat{p}_{wt,Hp} [0] + \bar{\mathbf{u}}_{Hp}^T (\mathbf{\Lambda}_{3,Hp} \mathbf{\Psi}) \hat{\mathbf{d}}_{Hp} \quad (5.43)$$

Hence the optimization is given by:

$$\min_{\hat{\mathbf{u}}_{Hp}} \Upsilon(\hat{\mathbf{u}}_{Hp}) = \min_{\hat{\mathbf{u}}_{Hp}} \frac{1}{\eta} \left(\frac{1}{2} \hat{\mathbf{u}}_{Hp}^T \mathbf{R} \hat{\mathbf{u}}_{Hp} + \mathbf{b} \hat{\mathbf{u}}_{Hp} + c \right) \quad (5.44)$$

5.4 Constraints

The reformulation of the objective function results in a constrained quadratic problem. This problem is the process of minimizing the objective function described in *Equation: (5.44)* with respect to the input signal with the presence of constraints on the input. As shown in the control problem, constraints are defined as inequalities on the output, state and input signals respectively. Since all constraints should be set up as a constraint on the controller input, \mathbf{u}_{Hp} , these inequalities must be reformulated.

The constraints on the output signal, are the upper and lower bounds for the end-user pressures in the two PMAs. Recalling the output equation constructed for the control and extending it for the prediction horizon, similarly as it was done for the state equation, yields:

$$\hat{\mathbf{y}}_{Hp} = \mathbf{\Theta} \Delta \hat{\mathbf{p}}_{wt} + \mathbf{\Omega} \hat{\mathbf{u}}_{Hp} + \mathbf{\Pi} \hat{\mathbf{d}}_{Hp} \quad (5.45)$$

Where the output, feedforward and disturbance matrices are respectively:

$$\mathbf{\Theta} = \begin{bmatrix} \mathbf{C}_d & \dots & \mathbf{0} \\ \vdots & \ddots & \vdots \\ \mathbf{0} & \dots & \mathbf{C}_d \end{bmatrix} \in \mathbb{R}^{(2H_p \times H_p)} \quad (5.46)$$

$$\Omega = \begin{bmatrix} D_d & \dots & \mathbf{0} \\ \vdots & \ddots & \vdots \\ \mathbf{0} & \dots & D_d \end{bmatrix} \in \mathbb{R}^{(2H_p \times 2H_p)} \quad (5.47)$$

$$\Pi = \begin{bmatrix} K_d & \dots & \mathbf{0} \\ \vdots & \ddots & \vdots \\ \mathbf{0} & \dots & K_d \end{bmatrix} \in \mathbb{R}^{(2H_p \times 2H_p)} \quad (5.48)$$

Inserting the extended state equation into the output equation yields:

$$\hat{\mathbf{y}}_{Hp} = \Theta[\Phi\Delta\hat{p}_{wt}[0] + \Gamma\hat{\mathbf{u}}_{Hp} + \Psi\hat{\mathbf{d}}_{Hp}] + \Omega\hat{\mathbf{u}}_{Hp} + \Pi\hat{\mathbf{d}}_{Hp} \quad (5.49)$$

Rearranging the expression as:

$$\hat{\mathbf{y}}_{Hp} = \Theta\Phi\Delta\hat{p}_{wt}[0] + (\Theta\Gamma + \Omega)\hat{\mathbf{u}}_{Hp} + (\Theta\Psi + \Pi)\hat{\mathbf{d}}_{Hp} \quad (5.50)$$

Equation: (5.50) defines the relation between the small-signal output and small-signal inputs. Inserting the upper and lower bound values of the small-signal outputs in this equation, the inequality constraint is obtained for the outputs as an affine function of the small-signal input signals. It has to be considered, that the constraints are originally set for full-signal values. Therefore, in this case the upper and lower values are the maximum allowed and minimum required pressure values delivered to the end-users. As a consequence of this, when inserting the bounds back into *Equation: (5.50)*, the operating point has to be subtracted at both sides to transform each term to small-signals. The constraint is given as:

$$\underline{\mathbf{y}}_{Hp} - \bar{\mathbf{y}}_{Hp} \leq \Theta\Phi\Delta\hat{p}_{wt}[0] + (\Theta\Gamma + \Omega)\hat{\mathbf{u}}_{Hp} + (\Theta\Psi + \Pi)\hat{\mathbf{d}}_{Hp} \leq \overline{\mathbf{y}}_{Hp} - \bar{\mathbf{y}}_{Hp} \quad (5.51)$$

Where

$\overline{\mathbf{y}}_{Hp}$ is the upper bound of the end-user pressure, [bar]
 and $\underline{\mathbf{y}}_{Hp}$ is the lower bound of the end-user pressure. [bar]

The constraint on the states can be reformulated using the same idea as for the output, except that it is sufficient to use the extended state dynamic equation such that:

$$\underline{\Delta\mathbf{p}_{wt,Hp}} - \overline{\Delta\mathbf{p}_{wt,Hp}} \leq \Phi\Delta\hat{p}_{wt}[0] + \Gamma\hat{\mathbf{u}}_{Hp} + \Psi\hat{\mathbf{d}}_{Hp} \leq \overline{\Delta\mathbf{p}_{wt,Hp}} - \underline{\Delta\mathbf{p}_{wt,Hp}} \quad (5.52)$$

Where

$\overline{\Delta\mathbf{p}_{wt,Hp}}$ is the upper bound of the WT pressure, [bar]
 and $\underline{\Delta\mathbf{p}_{wt,Hp}}$ is the lower bound of the WT pressure. [bar]

The constraint for the input signals are given by:

$$\underline{\mathbf{u}} - \bar{\mathbf{u}} \leq \hat{\mathbf{u}}_{Hp} \leq \overline{\mathbf{u}} - \bar{\mathbf{u}} \quad (5.53)$$

Where

$\overline{\mathbf{u}}$ is the upper bound of the control input, [bar]
 and $\underline{\mathbf{u}}$ is the lower bound of the control input. [bar]

All constraints are setup as constraints on the input signal in *Equation: (5.51)*, *Equation: (5.53)* and in *Equation: (5.52)*. In order to formulate all the constraints as one affine

inequality system, the three constrain inequalities are divided into six inequalities such that the lower bound for the input is given by:

$$\underbrace{\underline{u} - \bar{u}_{Hp}}_{\hat{u}_1} \leq \hat{u}_{Hp} \quad (5.54)$$

The upper bound of the input is given by:

$$\underbrace{\bar{u} - \bar{u}_{Hp}}_{\hat{u}_2} \geq \hat{u}_{Hp} \quad (5.55)$$

The lower bound of the output is given by:

$$\underbrace{\underline{y}_{Hp} - \bar{y}_{Hp} - \Theta\Phi\Delta\hat{p}_{wt}[0] - (\Theta\Psi + \Pi)\hat{d}_{Hp}}_{\hat{y}_1} \leq \underbrace{(\Theta\Gamma + \Omega)}_{L_y} \hat{u}_{Hp} \quad (5.56)$$

The upper bound of the output is given by:

$$\underbrace{\bar{y}_{Hp} - \bar{y}_{Hp} - \Theta\Phi\Delta\hat{p}_{wt}[0] - (\Theta\Psi + \Pi)\hat{d}_{Hp}}_{\hat{y}_2} \geq \underbrace{(\Theta\Gamma + \Omega)}_{L_y} \hat{u}_{Hp} \quad (5.57)$$

The lower bound of the state is given by:

$$\underbrace{\Delta p_{wt,Hp} - \Delta \bar{p}_{wt,Hp} - \Phi\Delta\hat{p}_{wt}[0] - \Psi\hat{d}_{Hp}}_{\Delta\hat{p}_{wt,1}} \leq \Gamma\hat{u}_{Hp} \quad (5.58)$$

The upper bound of the state is given by:

$$\underbrace{\Delta p_{wt,Hp} - \Delta \bar{p}_{wt,Hp} - \Phi\Delta\hat{p}_{wt}[0] - \Psi\hat{d}_{Hp}}_{\Delta\hat{p}_{wt,2}} \geq \Gamma\hat{u}_{Hp} \quad (5.59)$$

Collecting all the constraints, the following affine constraint inequality is obtained:

$$\begin{bmatrix} I \\ -I \\ L_y \\ -L_y \\ \Gamma \\ -\Gamma \end{bmatrix} \hat{u}_{Hp} \geq \begin{bmatrix} \hat{u}_1 \\ \hat{u}_2 \\ \hat{y}_1 \\ \hat{y}_2 \\ \Delta\hat{p}_{wt,1} \\ \Delta\hat{p}_{wt,2} \end{bmatrix} \quad (5.60)$$

5.5 Convexity

In the following section convexity of the objective function is examined. Due to the reformulation of the objective function and constraints, the MPC optimization problem becomes the following:

$$\min_{\hat{u}_{Hp}} \Upsilon(\hat{u}_{Hp}) = \min_{\hat{u}_{Hp}} \frac{1}{\eta} \left(\frac{1}{2} \hat{u}_{Hp}^T R \hat{u}_{Hp} + b \hat{u}_{Hp} + c \right) \quad (5.61)$$

$$s.t. \quad \begin{bmatrix} I \\ -I \\ L_y \\ -L_y \\ \Gamma \\ -\Gamma \end{bmatrix} \hat{u}_{Hp} \geq \begin{bmatrix} \hat{u}_1 \\ \hat{u}_2 \\ \hat{y}_1 \\ \hat{y}_2 \\ \Delta\hat{p}_{wt,1} \\ \Delta\hat{p}_{wt,2} \end{bmatrix} \quad (5.62)$$

Objective function

The objective function and the constraints are all written up according to the small-signal value of the control signal. The difficulty of solving this optimization problem simplifies however, if Υ is convex. This is due to the fact that if the objective function is convex then any local minimum is also the global minimum [29].

The function, Υ , defines a quadratic surface. If this surface is convex, then it can be visualized as in *Figure 5.3*. If the objective function is non-convex, the surface has a form such as in *Figure 5.4*.

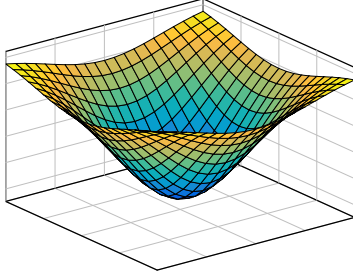


Figure 5.3. Quadratic convex surface.

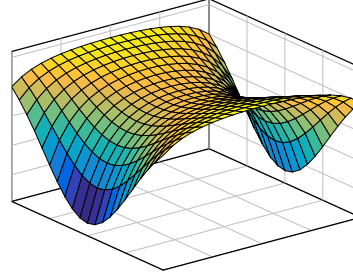


Figure 5.4. Quadratic non-convex surface.

Figure 5.3 and *Figure 5.4* points out the differences between the two minimization problems. Solving the convex quadratic problem will result in obtaining the global minimum, which can be found determining the first derivative of the function and solving it when equal to zero. In order to ensure convexity, the objective function must have a positive semi-definite Hessian matrix. The Hessian is a square matrix of second order partial derivatives of a scalar valued function or scalar field. To obtain an expression that fulfills this condition, the Hessian for *Equation: (5.61)* is analyzed:

$$\Upsilon(\hat{\mathbf{u}}_{Hp}) = \frac{1}{\eta} \left(\frac{1}{2} \hat{\mathbf{u}}_{Hp}^T \mathbf{R} \hat{\mathbf{u}}_{Hp} + \mathbf{b} \hat{\mathbf{u}}_{Hp} + c \right) \quad (5.63)$$

$$\frac{\partial \Upsilon(\hat{\mathbf{u}}_{Hp})}{\partial \hat{\mathbf{u}}_{Hp}} = \frac{1}{\eta} (\mathbf{R} \hat{\mathbf{u}}_{Hp} + \mathbf{b}) \quad (5.64)$$

$$\frac{\partial^2 \Upsilon(\hat{\mathbf{u}}_{Hp})}{\partial \hat{\mathbf{u}}_{Hp}^2} = \frac{1}{\eta} \mathbf{R} \quad (5.65)$$

Equation: (5.65) shows that convexity is ensured if:

$$\mathbf{R} \geq 0 \quad (5.66)$$

For all $\hat{\mathbf{u}}_{Hp}$, since the efficiency, η is a positive constant, therefore does not change the convexity of the function.

Recalling *Equation: (5.41)*, \mathbf{R} depends on $\mathbf{\Lambda}_1$ from *Equation: (5.14)*, which is defined as $\mathbf{\Lambda}_1 = \mathbf{G}^T \mathbf{B}_1^T \mathbf{M}_c^{-1} \mathbf{N}_c$.

Bringing back the structure of $\mathbf{N}_c = \mathbf{B}_1 \mathbf{G}$, the above equation can be rewritten as:

$$\mathbf{\Lambda}_1 = \mathbf{N}_c^T \mathbf{M}_c^{-1} \mathbf{N}_c \quad (5.67)$$

In *Equation: (4.67)* \mathbf{M}_c has been defined as a symmetric positive-definite matrix, the same procedure as in *Equation: (4.68)* is followed. The above equation is multiplied by a non-zero vector column \mathbf{x} and its transpose \mathbf{x}^T

$$\mathbf{x}^T \mathbf{N}_c^T \mathbf{M}_c^{-1} \mathbf{N}_c \mathbf{x} \quad (5.68)$$

A new variable is defined $\mathbf{y} = \mathbf{N}_c \mathbf{x}$, now making use of the definition of positive definiteness:

$$\mathbf{y}^T \mathbf{M}_c^{-1} \mathbf{y} \geq 0 \quad (5.69)$$

With \mathbf{M}_c fulfilling the requirements for positive definiteness, the Hessian of \mathbf{R} can be certified to be greater than zero, hence convex.

Constraints

The constraints are given by linear inequalities which define half-spaces that are contained in the quadratic function. A half-space is a set of points that satisfy a single inequality constraint, hence, each constraint defines a half-space [30]. Every half-space is a convex set and the intersection of any number of convex sets is convex [29].

5.6 PI controller

As described in Section 5.1: *Control Problem* the two PMA pumps should generate a constant differential pressure. Furthermore Section 5.1: *Control Problem* concludes that a simple PI controller, reacting to a reference calculated by the MPC, should be used to control the pressure generated by the main pumps.

In *Appendix: H* a linearized pump model is derived. With the operating point of the four pumps and their respective parameters shown in *Appendix: C*, four different models are derived, and given as:

$$G_{C2}(s) = 0.966 \quad G_{C16}(s) = 0.976 \quad G_{C18}(s) = 0.217 \quad G_{C25}(s) = 0.546$$

The controllers are design through the Matlab toolbox *Control System Designer App*[31], with the approach of the same control characteristics. Since the time constant of the water system is measured to be 1155 seconds, see Section I.1: *System time constant*. The settling time of the PI controllers is chosen to be under 10 seconds, which is deemed sufficient. The steady state error and the overshoot should not exceed 5% as this in the worst case will saturate the differential pressure sensors.

The controllers are designed as:

$$\begin{aligned} PI_{c2} &= \frac{1.39s + 1.39}{s} & PI_{c18} &= \frac{5.89s + 5.89}{s} \\ PI_{c16} &= \frac{1.39s + 1.39}{s} & PI_{c25} &= \frac{2.57s + 2.57}{s} \end{aligned}$$

From the design and test conducted in *Appendix: H*, it is shown that the controllers meet the desired requirements and thus can be implemented on the test setup.

Control System Implementation

6

This chapter explains how the controller designed in Chapter 5: *Controller* is desired to be implemented on the scaled system at Aalborg university.

6.1 Simulink implementation

In the implementation of the control, the model estimated in Section 4.6.3: *Linear Estimation Outcomes* is used. Although the fit percentage differs from the real data, the behavior and dynamics of the WT are qualitatively correct, making this model the most suitable and realistic one to work with. *Figure 6.1* shows the implementation strategy for the control design on the model of the water distribution system.

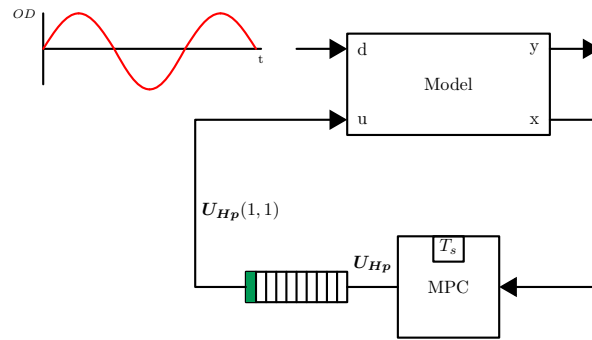


Figure 6.1. Sketch of the control implementation.

In the block diagram, the state-space box represents the estimated plant with inputs defined by the control, u , and disturbance signals, d . The output of the state-space model is the pressure around the end-user valves, y . In Simulink, the state of the system, i.e. the WT pressure is also defined as an output. As the current value of the initial state is measured, it is sent to the MPC block at each iteration step. This iteration step is defined by the sampling time, T_s of the MPC block which runs the minimization algorithm at each of this time steps. When the algorithm is done, the control signal for the prediction horizon is saved as u_{HP} . Although the prediction is calculated for the future price scenarios, only the first element in u_{HP} is picked for control. After applying the first entry of u_{HP} , the iteration continues with the next time step. In the next step the price and disturbance sequences are shifted one time step further and then a new measurement is carried out on the model again.

In order to solve the optimization and find a global minimum for the problem specified in *Equation: (5.61)*, Quadratic Programming(QP) is used. Solvers for QP problems in Matlab are well developed and available in a wide range, therefore in this project the *quadprog* function in the control toolbox is used. This function minimizes the problem subject to the specified constraints to the convex objective function. The method chosen

is interior point convex algorithm which solves the problem by simplifying the constraints and then iterates in the interior of the feasible set [32].

In previous sections, the length of the prediction horizon, H_p , is introduced. It is decided to predict 24 hours forward due to the periodicity of the electricity price and the behavior of the end-user consumption. Therefore, the control input to the state-space model is updated every hour. The sampling time for the control input differs from the sample time determined for the discrete time state-space model, which is $T_s = 87.5s$.

In *Appendix: G*, the electric price model is shown. For the implementation of the control not only the electric price model is needed but also a model for the end-user water consumption. This model can be seen in *Figure 6.2*.

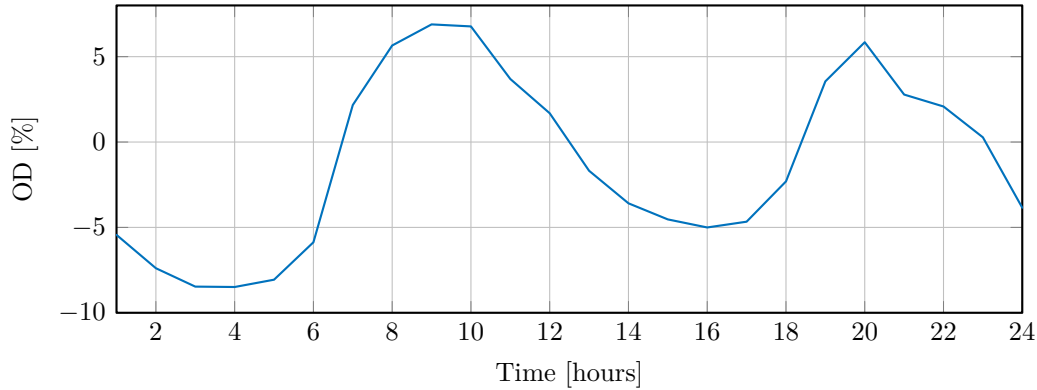


Figure 6.2. End-users water consumption, with acts as a disturbance to the system.

In this case the model is created to last for a week based on the 24 hours data and then it repeats.

6.2 Implementation goals

The convexity of the objective function has been developed and verified in Section 5.2: *Model predictive control* and in Section 5.5: *Convexity*.

Although the objective function for the minimization is convex, difficulties with infeasibility occur while solving the constrained problem. When constraints for the pressure in the WT and for the pressure in the PMAs are included, there are not any feasible solutions existing for the problem. Infeasibility means that no solution of \mathbf{u}_{hp} exists which could satisfy all the constraints defined by the measurements carried out on the test setup. However, when constraints only on the input signals are included, the algorithm can find a global minimum of the objective function. The QP solver detects this problem automatically at the presolve phase of each optimization run, thus in these cases the MPC box does not give a solution.

In Section 4.8: *Verification of model*, the model is verified, however in some respects lacks the ability to give back the real world behavior of the system. As described in Section 4.6.3: *Linear Estimation Outcomes*, the estimation has been carried out so the dynamics of the WT reflect the same behavior as the real world system. Considering the differences between the model and the test setup, the conclusion can be made that the model is qualitatively correct but quantitatively incorrect. Although the physical limitations are calculated from the measurements on the real test setup, it should still be possible to solve the optimization with the defined constraints.

Considering the fact that in real world completely perfect models are nearly impossible to make, blaming the accuracy of the model for infeasibility is not the right argument. It is assumed that there is a qualitative error in the two constraints concerning the WT and the output pressures. A reason could be that there is an error in the reformulation of the original constraints for the control signal, u_{Hp} . It is a reasonable assumption, since the two inequality constraints can be modified such that the optimization problem becomes feasible. However the prediction does not work as expected due to varying electricity prices not having the expected effect on the optimal control solution.

In order to present the implementation of the controller, some of the incorrect constraints are modified to show that the algorithm works and keeps the control values within the upper and lower bounds. In order to show the deficiencies of the optimization with the incorrect constraints, several results are compared and a conclusion is made concerning the expected behavior of the control.

6.3 Implementation with input constraint

For initial testing, the MPC is implemented such that only the constraint on the input is kept with the appropriate low and upper bounds. An implementation of such would make no sense on the test setup since the constraints on the WT are the most important boundaries concerning the control problem. In a real life scenario, leaving out the pressure constraint in the WT would mean that the optimal input empties the tower, disregarding what the price is. However, this test is suitable for verifying whether the minimization works correctly or not. It is expected to see that the input signal is constant and as low as possible during operation. This behavior, compared to the real system, is expected because the cheapest way of running the pumps is the slowest as possible.

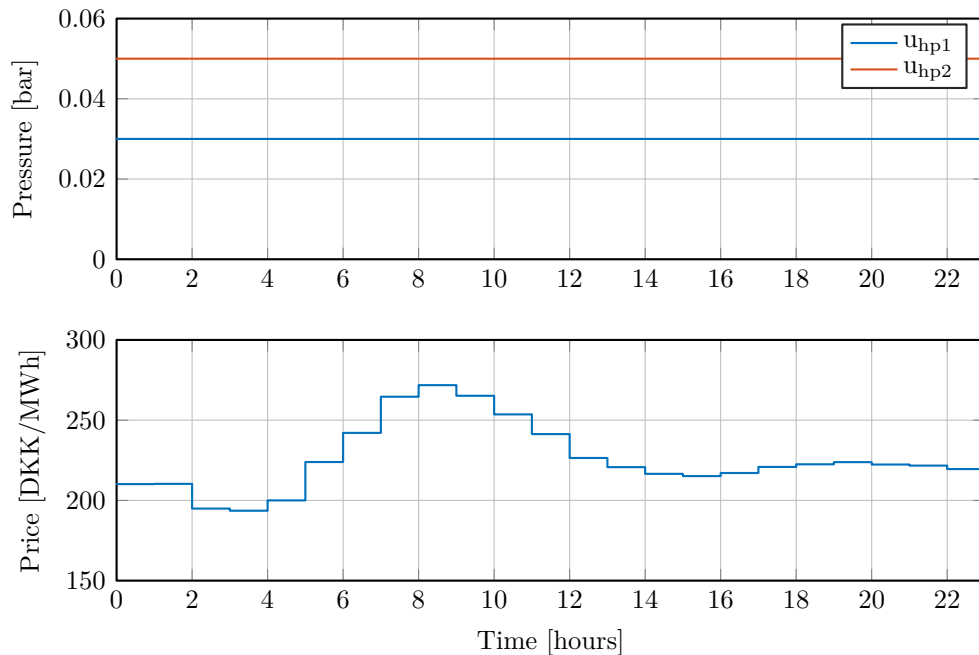


Figure 6.3. Optimization only with input constraints. The first figure shows the two control inputs for the pumps. Pump one can be seen in red and pump two in blue. The second figure shows the cost of electricity for the first 24 hours.

In *Figure 6.3* it can be seen that the full-signal input to pumps is constant at 0.05 and 0.03 [bar], which are the two different lower bounds for the pumps, respectively. Constraints

on the pumps are set in order to avoid the lower bound hysteresis of the pumps and not to exceed the upper bound.

As the input drops down to its minimum value, the WT level is expected to follow the same behavior and empty the water inside. In the following figure it can be seen how the WT pressure decreases until it reaches the steady-state for the input signal.

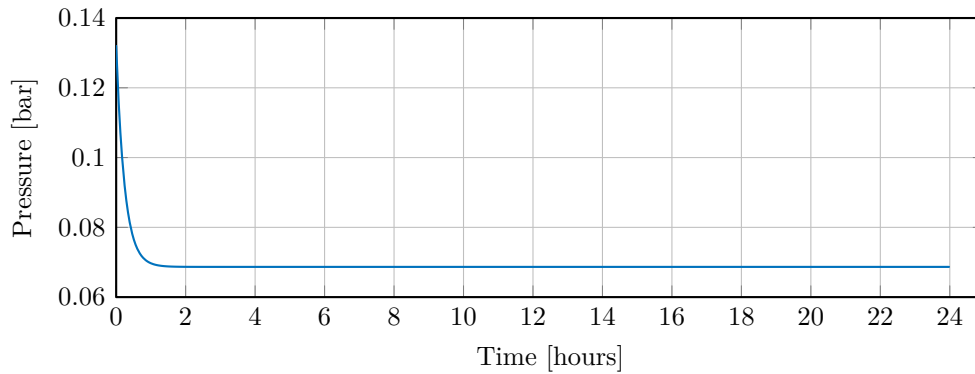


Figure 6.4. WT pressure for simulation with input constraint.

The initial pressure in the WT from 0.132 [bar] drops and shows the dynamics of how the tank is being emptied. Since the optimal solution for the control signal is bounded by the lower constraint, the WT is not emptied completely. This result is reasonable and expected, as the lower constraints for the pumps are small values and the initial condition set for the WT is significantly high. The pressure in the WT is dominant in the system, compared to the pressure provided by the pumps, thus the water level decreases.

The PMA pressures also experience a pressure drop due to the decrease in the control input in the pumps, as seen in *Figure 6.8*.

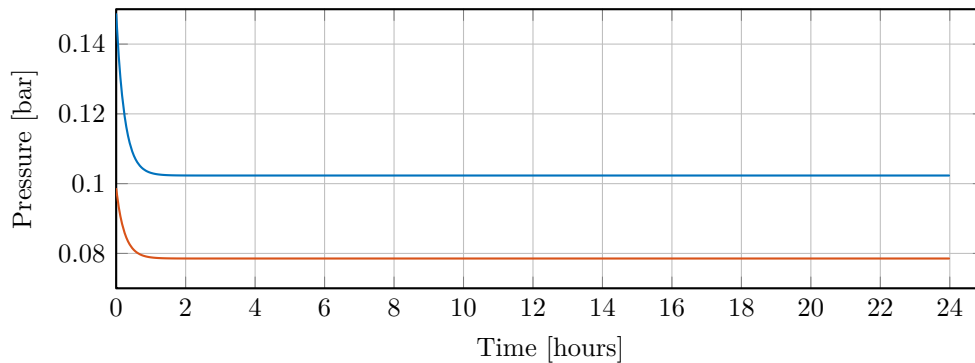


Figure 6.5. PMA pressures for simulation with input constraint.

As it is seen in the previous figures, when only the state constraint is added, the behavior of the state, inputs and outputs is as expected.

In the introduction of the section it is explained how the QP solver cannot find any feasible solution when the output and state constraints are inserted. Nevertheless, in order to show implementation of the MPC, the constraints regions are shifted so the problem becomes feasible. Therefore, it can be guaranteed that the input, state and output constraints are respected in spite of the constraints regions not being the original ones.

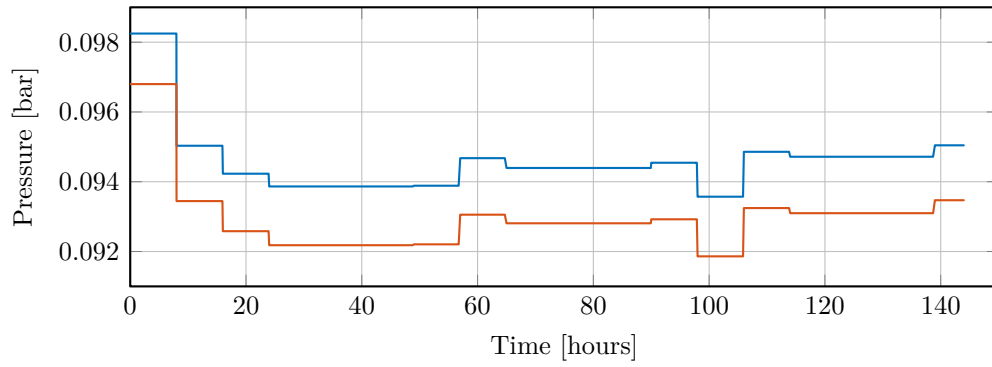


Figure 6.6. Input pressures for simulation with all the constraints.

The controller inputs are no longer in the lower bound values of the constraints, as seen in *Figure 6.3*, and they vary over time. However, the behavior shown in *Figure 6.8* is not expected, since the path followed by the input has nothing to do with the price curve shown in *Figure 6.3*. It would be expected that the input is maximized when the price is low and the opposite with high prices. Considering the unsatisfactory behavior for the input, the same is anticipated for the state and output values.

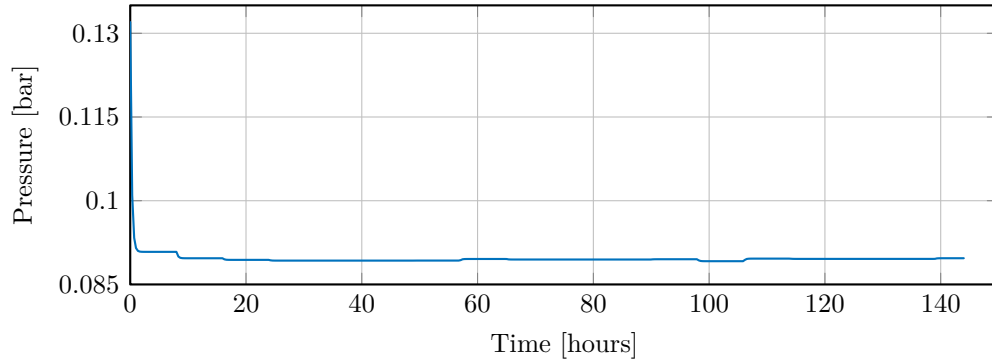


Figure 6.7. WT pressure with all the constraints.

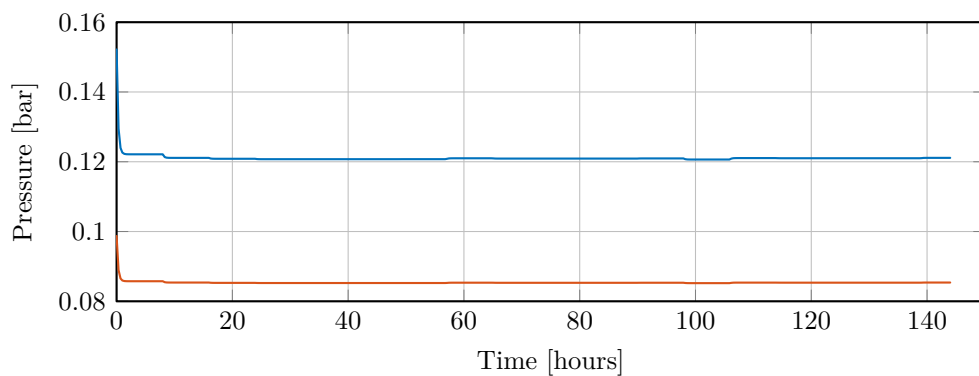


Figure 6.8. Output pressures with all the constraints.

It is shown that the output and WT pressure outcomes of the optimizations with and without the inequality constraints are the same.

The optimizing problem designed is hereby finished as the MPC control has been implemented together with the estimated model. On the one hand, it is shown that

the constrained problem for the input is solvable and expected values are obtained. On the other hand, the problem cannot be completed due to the incapability to calculate a control input once the constraints of the system are set. Thereby, it has been proved that by expanding the region of the constraints, the problem is proved to be solvable, although the results obtained are not the expected ones.

Part III

Conclusion and verification

The current system model of the water distribution network is based on a parameter estimated linearized model. This is due to the inaccurate results from the nonlinear parameter estimation but also due to the fact that the implemented MPC only handles linear models. This property of the MPC implies that even if a nonlinear model was obtained, it should be linearized in order to be used in the MPC. The advantage of a nonlinear model is that it can be linearized online at different operating points, and applied in the MPC. This procedure avoids operation far from the desired range of the model as the chosen operating point for the linearization is constantly varied. Therefore the precision of the MPC is improved, as a linearized model is generally only valid close to the operating point.

When only constraints for the input to the pumps are present, the MPC acts as supposed, as the input reference is set to the minimum value no matter what the price is. However, when the rest of the constraints are added, the optimization fails to find a solution in the feasible region. Changing the upper and lower bounds of the WT and output pressure constraints, the global minimum can be found. A possible argumentation why the constraints do not work, can be explained by the reformulation of them. As the minimization is done over the control input, the constraints on the output and the WT pressure are transformed to the control input. The reformulation is done by using the extended system dynamics in Section 5.3: *Reformulation of the objective function*. The system matrices for the control horizon take part directly in the inequality constraints when the transformation is done e.g. from y_{Hp} to u_{Hp} . Infeasibility can be caused by the trivial equation introduced in the first row of the extended matrix. The trivial entry of the matrix is introduced in order to match the indexing in the objective function. By using this matrix in the reformulated constraints, the first row zeros out the first optimal solution of u_{Hp} . Therefore, no matter what the optimal control value is, the lower bound of the small-signal constraint must be lower than zero and the upper bound must be positive. If it does not apply for the first entry of u_{Hp} , then the introduced constraint can result in infeasibility.

The model subject to MPC control in a real world water distribution network is affected by uncertainties concerning the prediction e.g. estimations of electricity price and water consumption. At some point the model can deviate from the actual plant, especially in the presented case where a small-signal model has been derived around a specific operating point. Therefore, the state of the WT will be affected by these uncertainties e.g. in a situation where the consumption is highly unexpected, the MPC could violate the constraints.

In a situation where prediction error, model deviation and uncertainty due to disturbance is present, constraints can be violated despite to the priori calculations made by MPC. In case of the water distribution system, extended with the WT, the states are measured. However, there are not any information about the outputs although they are affected by disturbances. Therefore, if the output pressure violates the constraints on the output,

there will not be any direct information about it. Violation of the constraints can happen on both the inputs and outputs.

A method to avoid this situation is to soften the constraints. Changing constraints from hard to soft can be done by having requirements that must be satisfied changed to be dependent on a variable that will be penalized by the cost function, if the variable is outside a desired range. Thus infeasibility can not occur and the MPC will instead try to bring the solution inside the optimal constraint region due to the penalized variable. Introducing such a variable is not always possible as some constraints are bound by physical parameters ensuring system safety, but can be applied to other constraints.

Another approach could be to include adaptive control to the MPC. This could tune the parameters in the controller, such that when deviations in e.g. water consumption, electrical prices or the WT level are appearing, the adaptive part would adjust the parameters such that the deviation would become smaller.

Conclusion 8

In this project the main focus has been on deriving, estimating and controlling the water distribution system with an attached water tower located at the control and automation department in Aalborg University. Multiple models that describe the pressure loss over different components in the system have been used, in order to obtain a detailed description of the water distribution system. Due to the uncertainties introduced by the pipe model parameters, parameter estimations have been carried out.

Hydraulic model

The water distribution network consists of four main components, pipes, pumps, valves and a water tower (WT). A detailed dynamical model is derived for each of the components and gathered together into a complete final expression. This expression is used to describe the nonlinear relation between flows and pressure in each individual component.

Graph representation

In order to represent the water network in a mathematical way, a Graph Theory approach is used. Once the network is described, the analogy between hydraulic and electrical circuits is conducted.

Parameter estimation

Certain parameters, corresponding to the pipes dynamics, are unknown, therefore a nonlinear parameter identification toolbox is utilized. This estimation is deemed unsuccessful due to the dynamics of the valves and pumps being slower than the dynamics of the pipes, thus the system desired information is hidden in the slower dynamics.

Alternatively, a linearized approach is attempted, resulting in an improved model in comparison to the nonlinear model.

Following the linear parameter estimation a verification of the model is carried out. This validation shows that the model behaves correctly and consists of the same dynamic as the system setup.

Control problem

A model predictive control(MPC) problem is designed in order to reduce the power consumption of the pumps, taking into account the electrical price and the physical constraints of the system. By controlling the main pumps and using the WT, the pressure at the end-users is maintained within the desired constraints. A minimization problem is set up, which is subject to the dynamics of the water distribution network, and the constraints. Furthermore, constraints to the pressure in the WT, the pressure demand for the end-users and the input signal to the pumps are set.

Control System Implementation

The MPC problem is implemented in Matlab Simulink. For initial testing, only the constraints in the inputs are kept, where the obtained results are as expected. Furthermore, when adding the remaining constraints of the system, there are not any feasible solutions existing for the problem. Therefore, the constraints regions are shifted

so the problem is again feasible, in order to show that the control is implemented correctly.

Part IV

Appendices

Unit Conversion



Unit transformation for the pipe model

Due to the large difference between the SI-units of flow, $[m^3/s]$, and pressure, $[Pa]$, a conversion from seconds to hours and pascal to bar is made.

The final pipe model from *Equation: (4.21)*, is shown below.

$$\begin{aligned} \frac{L\rho}{A} \frac{dq}{dt} &= \Delta p - \frac{8fL}{\pi^2 g D^5} \rho g |q|q - k_f \frac{8}{\pi^2 g D^4} \rho g |q|q - \Delta z_h \rho g \\ &= \Delta p - \left(\frac{8fL}{\pi^2 g D^5} + k_f \frac{8}{\pi^2 g D^4} \right) \rho g |q|q - \Delta z_h \rho g \end{aligned} \quad (A.1)$$

$1[\text{bar}] = 10^5[\text{Pa}]$. Therefore *Equation: (A.1)* can be rewritten as:

$$\begin{aligned} \frac{L\rho}{A \cdot 10^5} \frac{dq}{dt} &= \frac{\Delta p}{10^5} - \left(\frac{8fL}{\pi^2 g D^5 \cdot 10^5} + k_f \frac{8}{\pi^2 g D^4 \cdot 10^5} \right) \rho g |q|q - \frac{\Delta z_h \rho g}{10^5} \\ \frac{L\rho}{A \cdot 10^5} \frac{dq}{dt} &= \Delta p_{bar} - \left(\frac{8fL}{\pi^2 g D^5 \cdot 10^5} + k_f \frac{8}{\pi^2 g D^4 \cdot 10^5} \right) \rho g |q|q - \frac{\Delta z_h \rho g}{10^5} \end{aligned} \quad (A.2)$$

The coordinate transformation from $[\frac{m^3}{s}]$ to $[\frac{m^3}{h}]$ can be done by multiplying by 3600 on the left-hand side. *Equation: (A.1)* can be written as:

$$\frac{L\rho}{A \cdot 10^5} \frac{d}{dt} \frac{q}{3600} = \frac{\Delta p}{10^5} - \left(\frac{8fL}{\pi^2 g D^5 \cdot 10^5} + k_f \frac{8}{\pi^2 g D^4 \cdot 10^5} \right) \rho g \frac{|q|}{3600} \frac{q}{3600} - \frac{\Delta z_h \rho g}{10^5} \quad (A.3)$$

There is not any need to apply unit conversion to the final valve model described in *Equation: (4.29)*, since the parameter, k_v , being designed for the water flow in $[m^3]$ taking into account one hour at a pressure drop across the valve of 1 [bar].

In the pump final model *Equation: (4.32)*, the constants are scaled so the pump equation has the units in $[bar]$ and the flow has the units in $[\frac{m^3}{h}]$.

Water Tower Hydraulic Capacitance Unit Transformation

In Section 4.1.4: *Water Tower*, the unit of the WT hydraulic capacitance, C_H is shown. This unit is given in SI which makes it necessary to convert it into the unit system followed throughout the project. Below the procedure of the unit conversion for C_H is shown:

$$C_H \left[\frac{A}{\rho g} \right] = C_H \left[\frac{\frac{m^2}{kg \cdot \frac{m}{s^2}}}{\frac{m^3}{m^3 \cdot s^2}} \right] = C_H \left[\frac{\frac{m^2}{N \cdot \frac{1}{m}}}{\frac{m^2}{m^2 \cdot m}} \right] = C_H \left[\frac{\frac{m^2}{Pa}}{\frac{m^2}{m}} \right] = C_H \left[\frac{m^3}{Pa} \right] \quad (A.4)$$

As well as with the pipes equation, the pressure needs to be converted from $[Pa]$ to $[bar]$, applying unit conversion to *Equation: (A.4)*:

$$C_H \left[\frac{m^3}{Pa} \right] = K \cdot C_H \left[\frac{m^3}{Bar} \right] \quad (A.5)$$

Where $K = 10^5$, which converts the pressure to $[bar]$.

Assumption List

B

Number	Assumptions	Section reference
1	The fluid in the network is water.	Section 4.1.1: <i>Pipe model</i>
2	All pipes in the system are filled up fully with water at all time.	Section 4.1.1: <i>Pipe model</i>
3	The pipes have a cylindrical structure and the cross section, $A(x)$, is constant for every $x \in [0, L]$.	Section 4.1.1: <i>Pipe model</i>
4	The flow of water is uniformly distributed along the cross sectional area of the pipe and the flow is turbulent.	Section 4.1.1: <i>Pipe model</i>
5	Δz_h , the change in elevation only occurs in pipes.	Section 4.1.2: <i>Valve model</i>
6	The pumps in the network are centrifugal pumps.	Section 4.1.3: <i>Pump model</i>
7	The storage of the WT has a constant diameter. In other words, the walls of the WT are vertical.	Section 4.1.4: <i>Water Tower</i>
8	Valves in the water distribution system are modelled according to the assumption that the length, L , is zero.	Section 4.1.2: <i>Valve model</i>
9	\mathcal{G} is a connected graph.	Section 4.3: <i>Graph representation</i>
10	The pipe volume is assumed to be known to an accuracy where there is not any benefit from estimating it. Thereby the estimation problem is simplified.	Section 4.4: <i>Nonlinear Parameter identification</i>
11	Functions describing the pressure drops across the elements of the system are continuously differentiable. Therefore can be approximated with their Taylor-series.	Section 4.5.1: <i>Taylor expansion on a simple example</i>
12	The operating point for the system is chosen such that $f(\bar{x}, \bar{u}) = 0$.	Section 4.5.1: <i>Taylor expansion on a simple example</i>
13	The efficiency of the main pumps are considered constant for small deviations around the same operating point.	Section 5.1: <i>Control Problem</i>

Table B.1. List of assumptions.

System Description



C.1 Components of the System

Part	Component	Length	Diameter	Material	ϵ	Δz	Fittings	Σk_f
Ring	C_4	5m+0.3m	20 mm	25 mm PEM	0.01 mm	0 m	b,c,c,a,a	4.42
	C_8	10 m	20 mm	25 mm PEM	0.01 mm	0 m	c,b,a,c,b	3.92
	C_9	10 m	20 mm	25 mm PEM	0.01 mm	0 m	c	0.51
	C_{10}	10 m	20 mm	25 mm PEM	0.01 mm	0 m	c,a,a	3.11
	C_{11}	10 m	20 mm	25 mm PEM	0.01 mm	0 m	c,a	1.81
	C_{12}	10 m	20 mm	25 mm PEM	0.01 mm	0 m	c,c,a,c,b	3.63
	C_{13}	10 m	20 mm	25 mm PEM	0.01 mm	0 m	c	0.51
	C_{14}	5m+4m	20 mm	25 mm PEM	0.01 mm	0 m	a,c	1.81
PMA1	C_{19}	2 m	10 mm	15 mm PEX	0.007 mm	0 m	b,c,d,c,e,a	3.57
	C_{21}	1 m	10 mm	15 mm PEX	0.007 mm	0 m	c,d,b	1.46
	C_{22}	1 m	10 mm	15 mm PEX	0.007 mm	0 m	c,d,b,e,b	7.68
	C_{23}	2 m	10 mm	15 mm PEX	0.007 mm	0 m	a,b,d,e	2.55
PMA2	C_{23}	3 m	10 mm	15 mm PEX	0.007 mm	0.5 m	d,c,a,c,e	2.77
	C_{23}	1 m	10 mm	15 mm PEX	0.007 mm	0 m	c,e	0.81
	C_{23}	1 m	10 mm	15 mm PEX	0.007 mm	0 m	b,d,c,b	2.26
	C_{23}	2 m	10 mm	15 mm PEX	0.007 mm	0 m	b,a	2.10
-	C_{42}	2 m	10 mm	15 mm PEX	0.007 mm	0.5 m	c,c,a,d,e	2.77
-								
-								

Table C.1. Table with details about the pipes in the water system, shown in *Figure C.2*. Note that Σk_f is an initial guess for the parameter estimation in Section 4.4: *Nonlinear Parameter identification*.

Fitting	Symbol	k_f
Tee - Over all loss	$k_{f,a}$	1.3
Tee - Straigh through	$k_{f,b}$	0.8
90° bend - Diameter/radius ration 1:1	$k_{f,c}$	0.51
Sudden enlarger - Diameter ratio 1:2	$k_{f,d}$	0.15
Sudden contractor - Diameter ratio 1:2	$k_{f,e}$	0.3

Table C.2. Table with details about the fittings in the water system. The fittings are not shown in *Figure C.2*. The values are found in [33, 34].

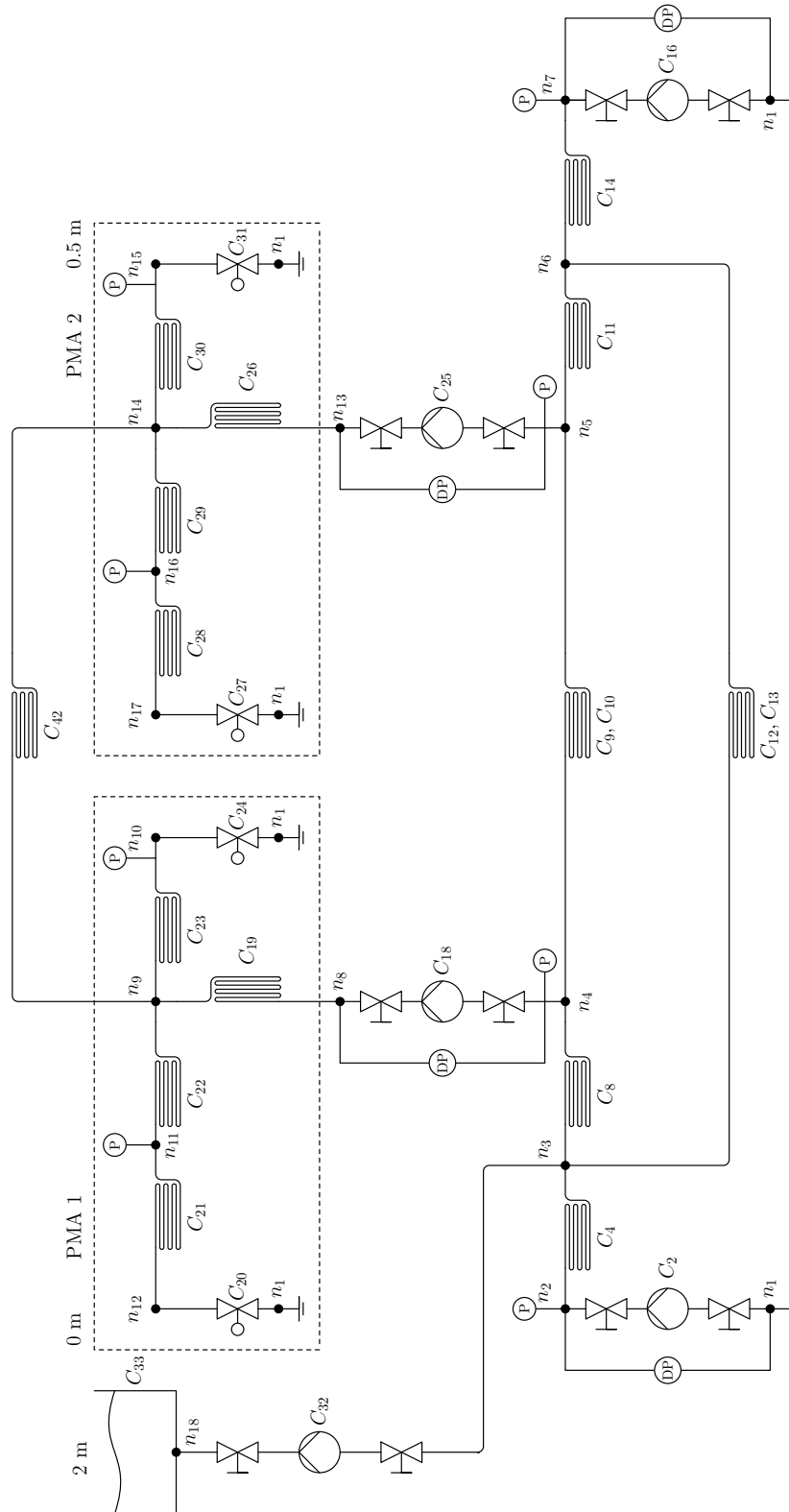
Part	Component	Valve fitting	k_{vs}	n_{gl}	θ_{off}	θ_{max}	Valve motor
PMA1	C_{20}, C_{24}	Belimo R2015-1-S1	1	3.2	15°	90°	Belimo LRQ24A-SR
PMA2	C_{27}, C_{31}	Belimo R2015-1-S1	1	3.2	15°	90°	Belimo LRQ24A-SR

Table C.3. Table with details about the valves in the water system, shown on *Figure C.2*. The parameters are found in [35, 36].

Part	Component	Pump type	Constants
Ring	C_2, C_{16}	Grundfors UPMXL GEO 25-125 180	$a_{h0} = 1.2024$ $a_{h1} = 0.0098$ $a_{h2} = 0.0147$ $B_0 = 9.8924$
PMA(1,2)	C_{18}, C_{25}	Grundfors UPM2 25-60 180	$a_{h0} = 0.6921$ $a_{h1} = -0.0177$ $a_{h2} = 0.0179$ $B_0 = 0.0698$

Table C.4. Table with details about the pumps in the water system, shown in *Figure C.2*. The parameters are provided by Grundfos.

C.2 System Topology










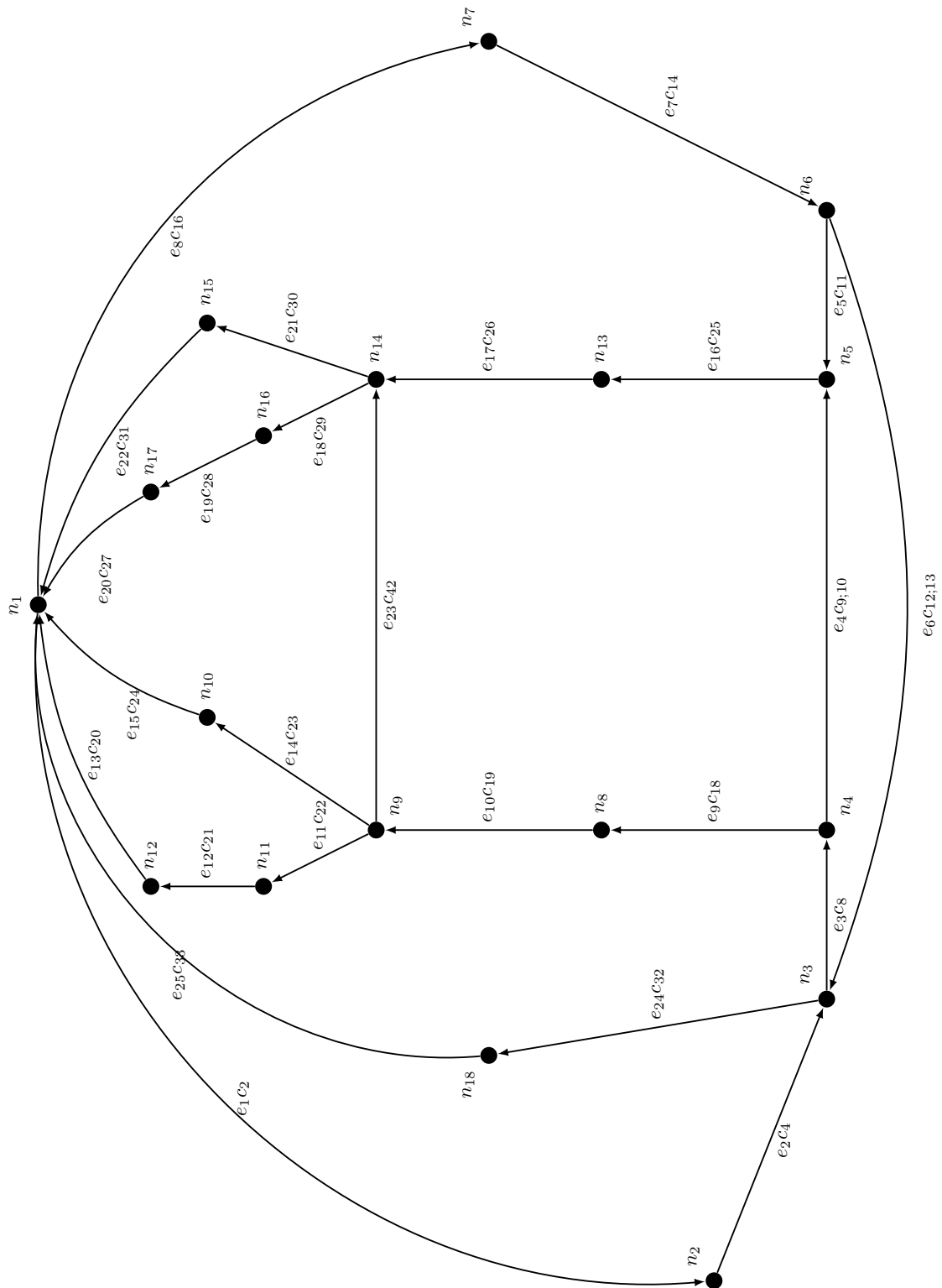
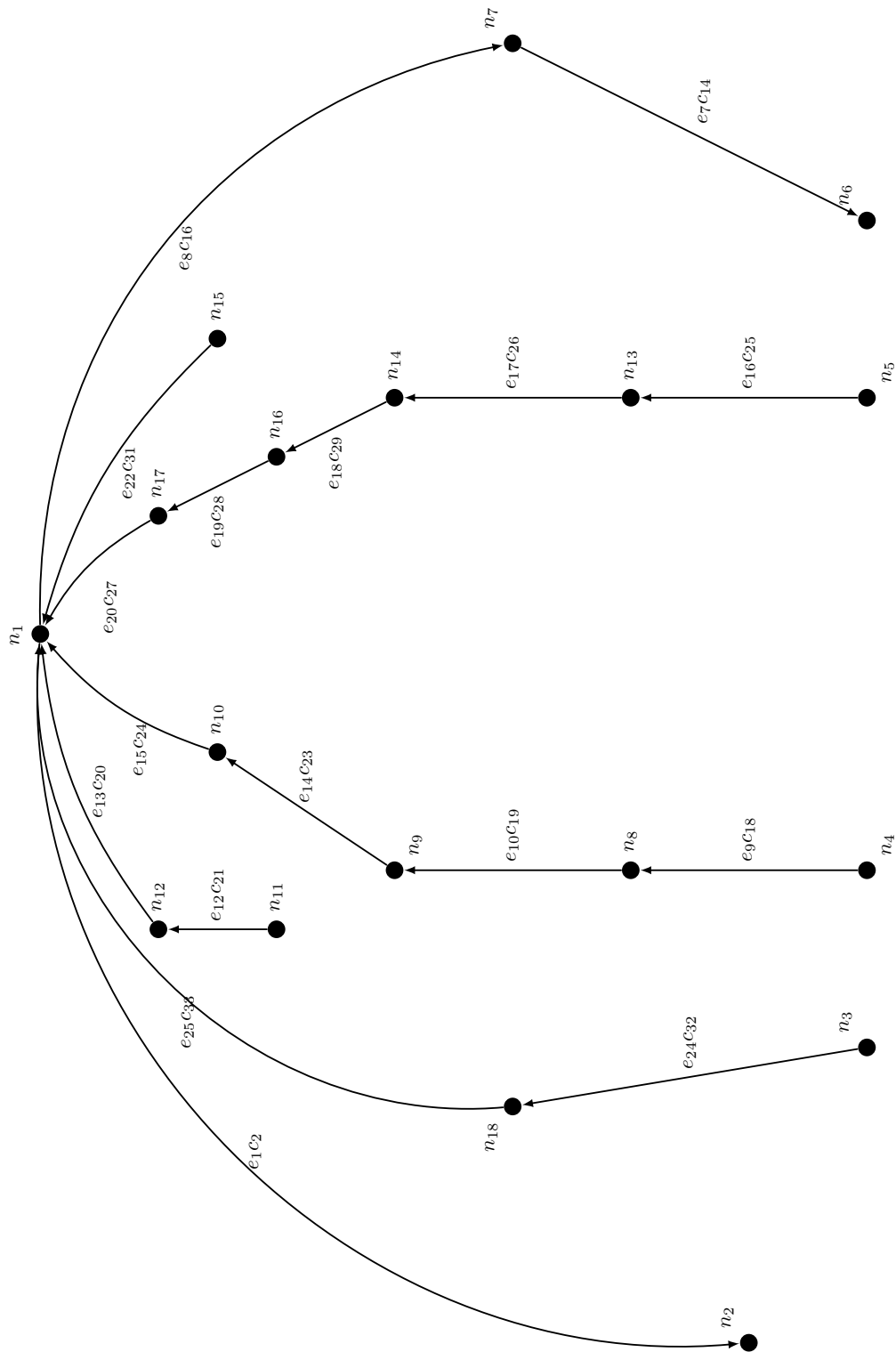
Symbol	Name
	Pump
	Manual valve
	Electronic valve
	Pipe segment
	Pressure sensor
	Differential pressure sensor
	Gnd

Table C.5. Symbol and name for component in the water network.

C.3 System Graph



C.4 Spanning Tree



C.5 Incidence Matrix

[illegible]

C.6 Cycle Matrix

$$B = \begin{bmatrix} 1 & 0 & 0 & 0 & 0 & 0 & 0 & 0 & 1 & 0 & 0 & 0 & 0 & 0 & 0 & 0 & 0 & 0 & 0 & 1 & 1 \\ 0 & 1 & 0 & 0 & 0 & 0 & 0 & 0 & 0 & 0 & 1 & 1 & 0 & 0 & 1 & 1 & 0 & 0 & 0 & -1 & -1 \\ 0 & 0 & 1 & 0 & 0 & 0 & 0 & 0 & 0 & 0 & 0 & -1 & -1 & 0 & 0 & -1 & -1 & 1 & 1 & 1 & 1 & 1 & 0 & 0 & 0 \\ 0 & 0 & 0 & 1 & 0 & 0 & 0 & 0 & 0 & 1 & 1 & 0 & 0 & 0 & 0 & 0 & 1 & 1 & 1 & 1 & 1 & 1 & 0 & 0 & 0 & 0 \\ 0 & 0 & 0 & 0 & 1 & 0 & 0 & 0 & 0 & 1 & 1 & 0 & 0 & 0 & 0 & 0 & 0 & 0 & 0 & 0 & 0 & 0 & 0 & 1 & 1 & 1 \\ 0 & 0 & 0 & 0 & 0 & 1 & 0 & 0 & 0 & 0 & 0 & 0 & 0 & 1 & 1 & -1 & -1 & 0 & 0 & 0 & 0 & 0 & 0 & 0 & 0 & 0 \\ 0 & 0 & 0 & 0 & 0 & 0 & 1 & 0 & 0 & 0 & 0 & 0 & 0 & 0 & 0 & 0 & 0 & 0 & -1 & -1 & -1 & 1 & 0 & 0 & 0 & 0 \\ 0 & 0 & 0 & 0 & 0 & 0 & 0 & 1 & 0 & 0 & 0 & 0 & 0 & 0 & 0 & -1 & -1 & 0 & 0 & 1 & 1 & 1 & 0 & 0 & 0 & 0 \end{bmatrix} \quad (\text{C.2})$$

Valve equation

The Kv value as a function of the opening degree above 35° is for a valve in the system given by:

$$Kv(OD) = kv_{100}e^{(n_{gl}(\gamma-1))} \quad (D.1)$$

The pressure across the valve as a function of the flow is given by:

$$\mu(q) = \frac{1}{(Kv)^2}q|q| \quad (D.2)$$

Gathering the two previous equations allows to describe the pressure across the valve as a combined function of both the flow and the opening degree.

$$M(q, OD) = \frac{1}{(kv_{100}e^{(n_{gl}(\gamma-1))})^2}q|q| \quad (D.3)$$

The linerization of the function $M(q, OD)$ by multi variable Taylor expansion in the operating points \bar{q} and \bar{OD} is given by the form

$$\begin{aligned} M(q, OD) &\approx M(a, b) + \frac{\partial}{\partial x}(M(a, b))(x - a) + \frac{\partial}{\partial y}(M(a, b))(y - b) \\ &\approx e^{\frac{2(\theta_{off} - \bar{OD})n_{gl}}{\theta_{max} - \theta_{off}} + 2} \bar{q}|\bar{q}| - 2 \frac{e^{\frac{2(\theta_{off} - \bar{OD})n_{gl}}{\theta_{max} - \theta_{off}} + 2} n_{gl} \hat{OD} \bar{q}|\bar{q}|}{\theta_{max} - \theta_{off}} + 2e^{\frac{2(\theta_{off} - \bar{OD})n_{gl}}{\theta_{max} - \theta_{off}} + 2} \hat{q}|\bar{q}| \end{aligned} \quad (D.4)$$

Where

$$\begin{aligned} a &= \bar{q} \\ x &= \bar{q} + \hat{q} \\ b &= \bar{OD} \\ \text{and } y &= \bar{OD} + \hat{OD} \end{aligned} \quad \begin{aligned} &\left[\frac{\text{m}^3}{\text{s}} \right] \\ &\left[\frac{\text{m}^3}{\text{s}} \right] \\ &\left[0 \right] \\ &\left[0 \right] \end{aligned}$$

Pipe equation

The pressure across a pipe as a function of the flow is given by:

$$\mu(q) = C_p q|q| \quad (D.5)$$

The first order linear Taylor expansion in the operating point \bar{q} is given as:

$$\begin{aligned} \mu(x) &\approx \mu(a) + \frac{\partial}{\partial x}\mu(a)(x - a) \\ &\approx C_p \bar{q}|\bar{q}| + 2C_p \bar{q}\hat{q} \end{aligned} \quad (D.6)$$

Pump equation

Concerning the pump that connects the WT with the remaining system the rotational speed is zero. Therefore will the pumps influence be described by a resistive term which gives a differential pressure drop as a function of the flow.

$$\Delta p = (\frac{2}{kv_{100}^2} - a_{h2})q|q| \quad (D.7)$$

The first order linear Taylor expansion in the operating point \bar{q} is given as:

$$\begin{aligned} \Delta p(x) &\approx \Delta p(a) + \frac{\partial}{\partial x} \Delta p(a)(x - a) \\ &\approx (\frac{2}{kv_{100}^2} - a_{h2})\bar{q}|\bar{q}| + 2(\frac{2}{kv_{100}^2} - a_{h2})\bar{q}\hat{q} \end{aligned} \quad (D.8)$$

Estimation data

In order to estimate accurately the unknown parameters of the system, adequate input signals have to be applied to the model. In this way, the system will work on different scenarios regarding the different combination of inputs signals.

Figure E shows the different combination between the OD of the PMA valves, and the steps applied to the main pumps.

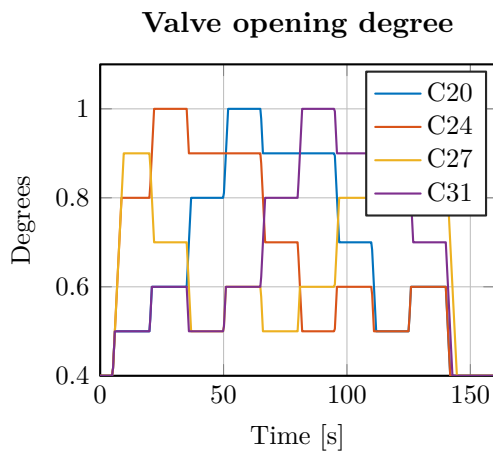


Figure E.1. Inputs to the parameter identification

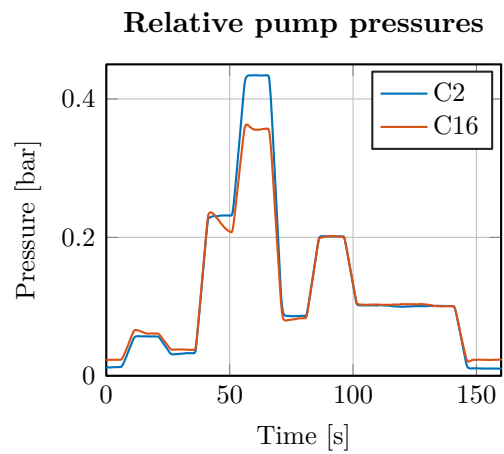


Figure E.2. Output pressure measurements

Together with the inputs from the lab and the nonlinear differential model the nonlinear parameter estimation is carried out.

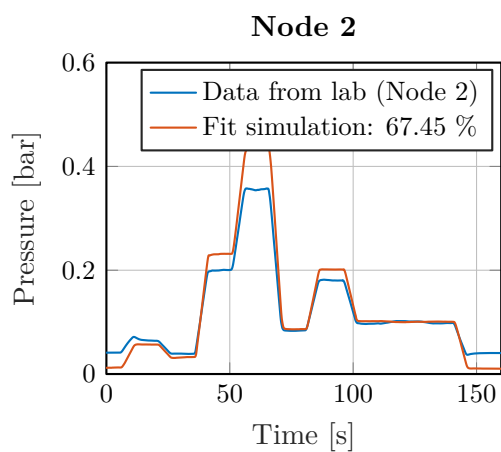


Figure E.3. Estimation comparison for node 2.

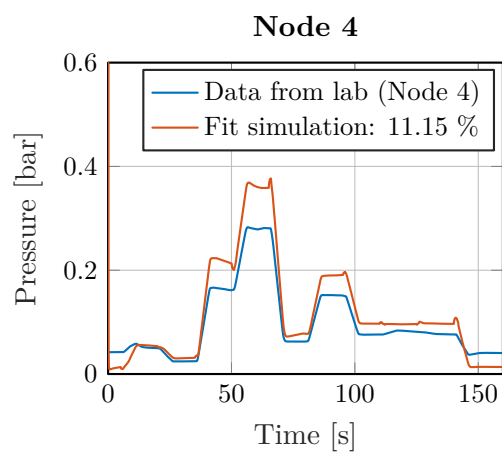


Figure E.4. Estimation comparison for node 4.

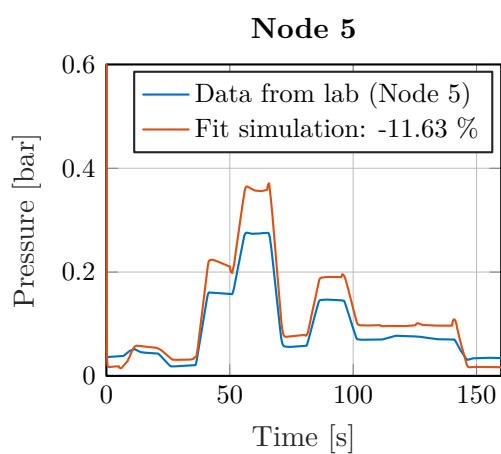


Figure E.5. Estimation comparison for node 5.

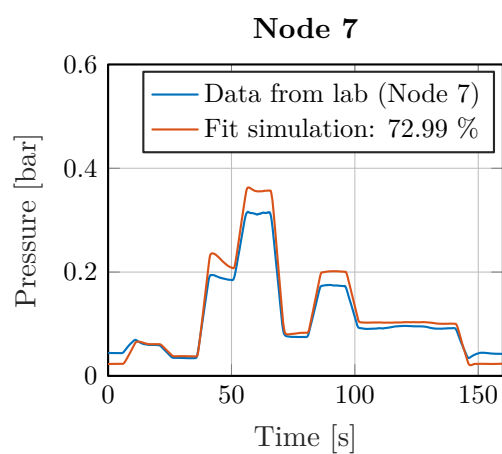


Figure E.6. Estimation comparison for node 7.

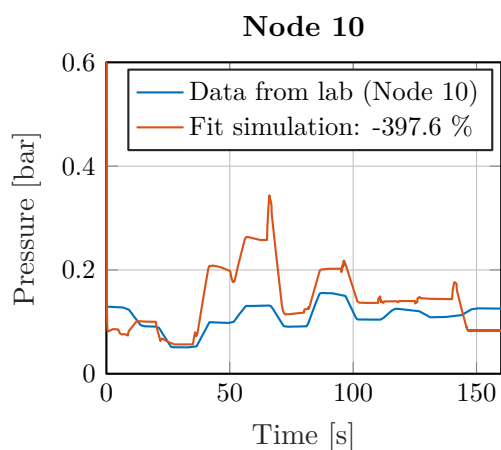


Figure E.7. Estimation comparison for node 10.

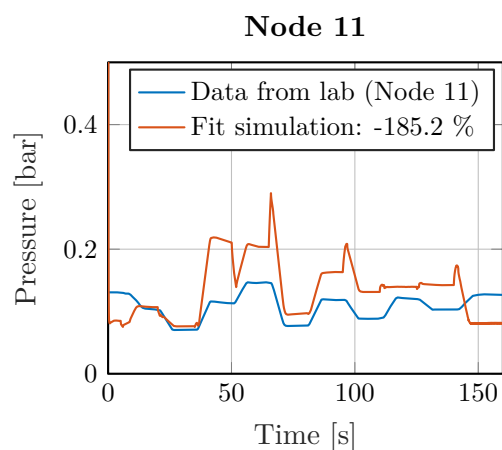


Figure E.8. Estimation comparison for node 11.

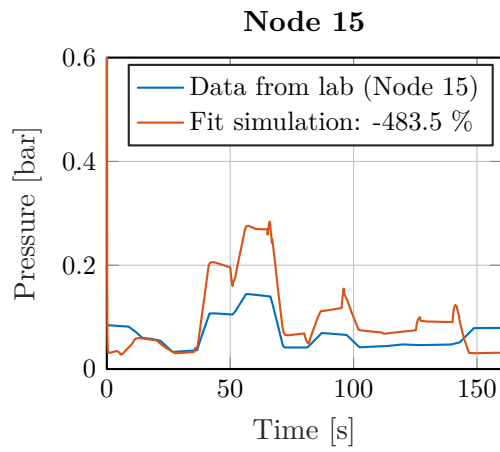


Figure E.9. Estimation comparison for node 15.

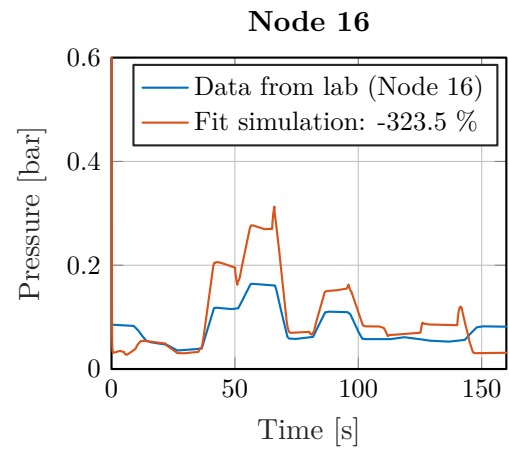


Figure E.10. Estimation comparison for node 16.

In this chapter the linear parameter estimation results, deemed insufficient, are presented.

Estimation Method

The estimation of the unknown parameters is carried through Matlab Linear Grey-Box model estimation toolbox. This toolbox allows to estimate continuous-time grey-box models for differential equations using multiple input/output time-domain data [37]. The numerical search method used for the estimation of the unknown parameters is the *Subspace Gauss-Newton least squares* search.

This method is automatically set by the parameter estimation process, thus any further understanding regarding the estimation method is considered out of scope of this project.

F.1 First linear parameter estimation

Estimation Data

The input signals used for the linear parameter estimation are presented in this section. The inputs to the end-user vales are shown in *Figure F.1* and the inputs to the pumps are shown in *Figure F.2*.

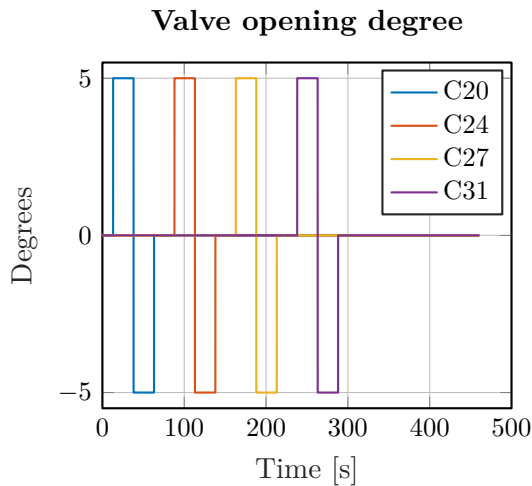


Figure F.1. Small-signal values of the opening degrees of the pma valves.

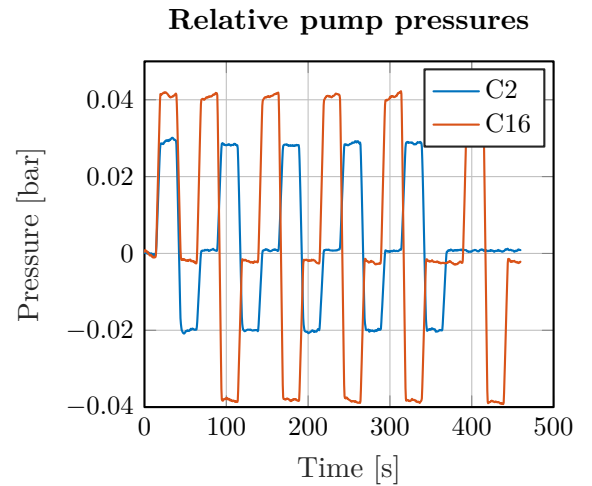


Figure F.2. Small-signal values of the angular velocity of the two main pumps.

Estimation Result

The following figures show the comparison between the data obtained from the lab and the estimated outputs of the model.

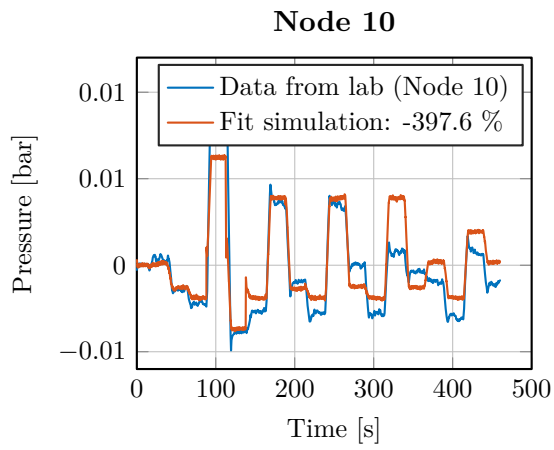


Figure F.3. Estimation comparison for node 10.

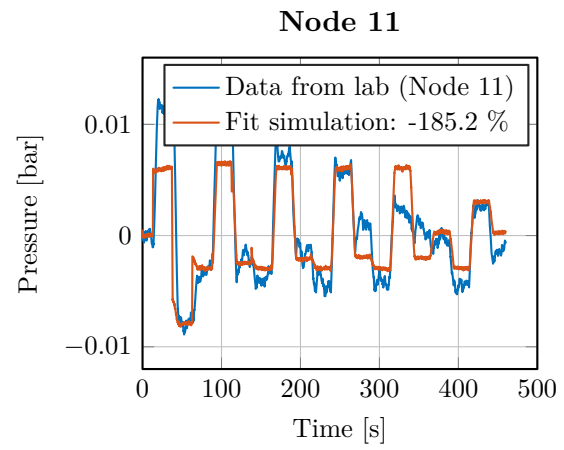


Figure F.4. Estimation comparison for node 11.

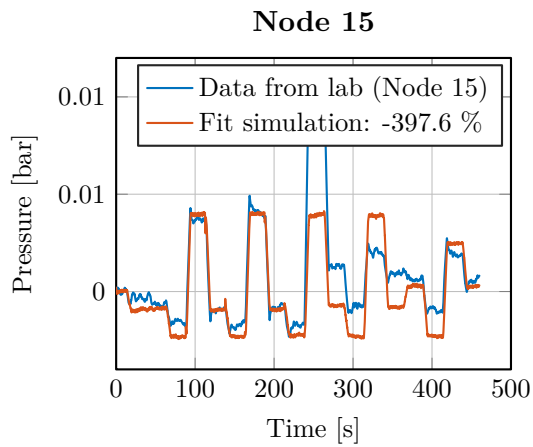


Figure F.5. Estimation comparison for node 15.

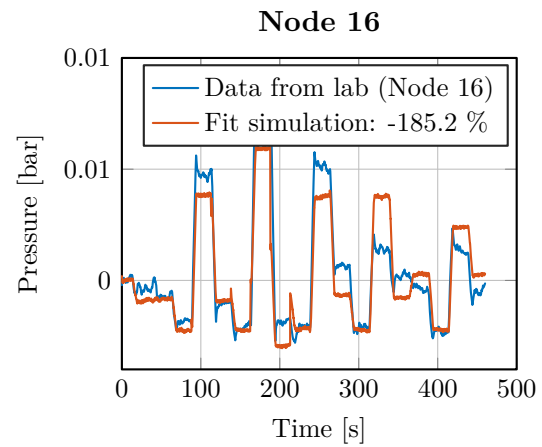


Figure F.6. Estimation comparison for node 16.

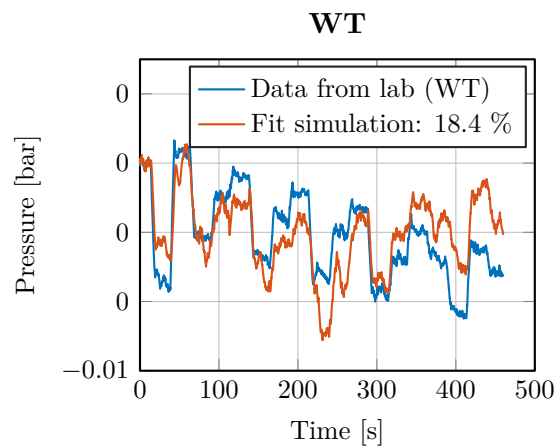


Figure F.7. Estimation comparison for WT.

F.2 Second linear parameter estimation

Estimation Data

The input signals used for the linear parameter estimation are presented in this section. The inputs to the end-user vales are shown in *Figure F.8* and the inputs to the pumps are shown in *Figure F.9*.

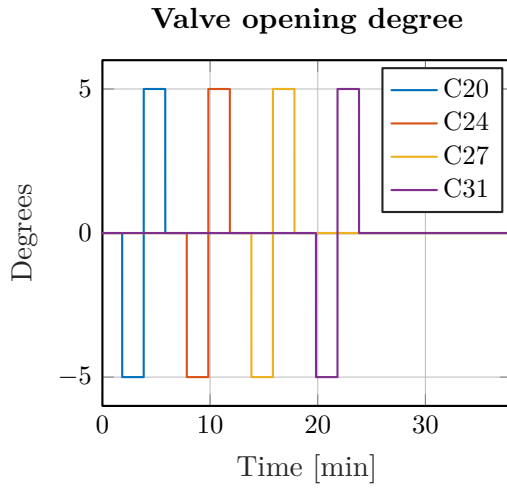


Figure F.8. Small-signal values of the opening degrees of the pma valves.

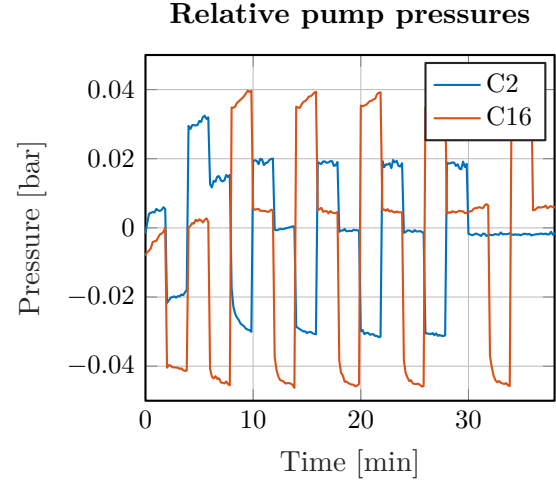


Figure F.9. Small-signal values of the angular velocity of the two main pumps.

Estimation Result

The following figures show the comparison between the data obtained from the lab and the estimated outputs of the model.

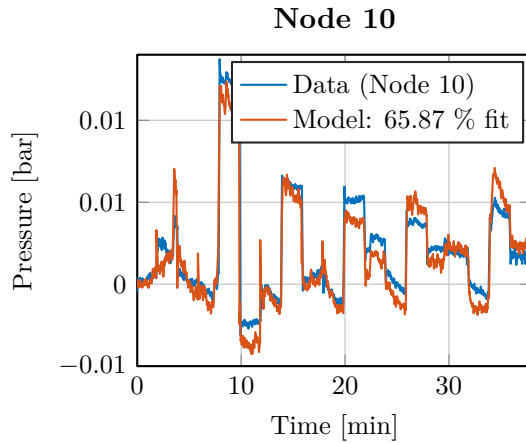


Figure F.10. Estimation comparison for node 10.

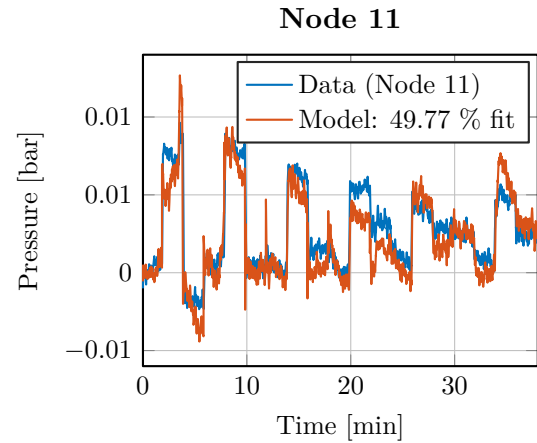


Figure F.11. Estimation comparison for node 11.

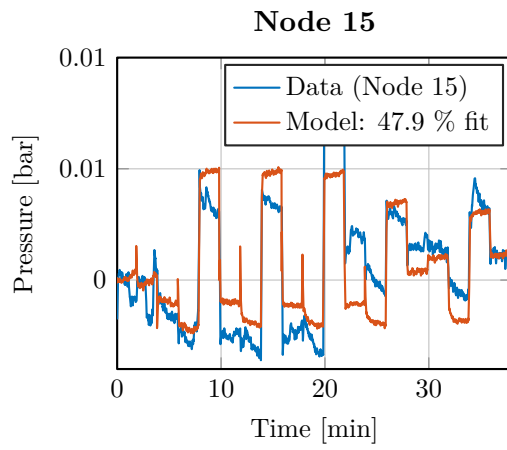


Figure F.12. Estimation comparison for node 15.

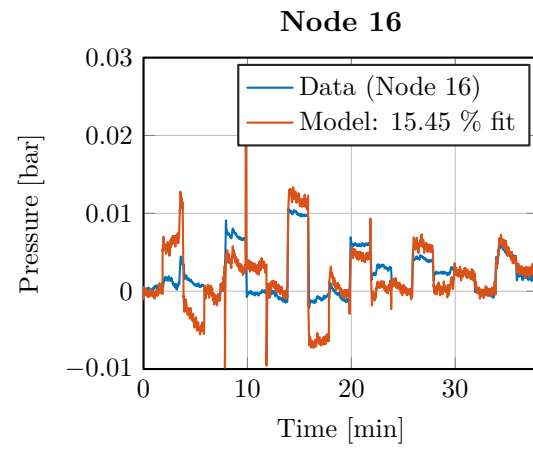


Figure F.13. Estimation comparison for node 16.

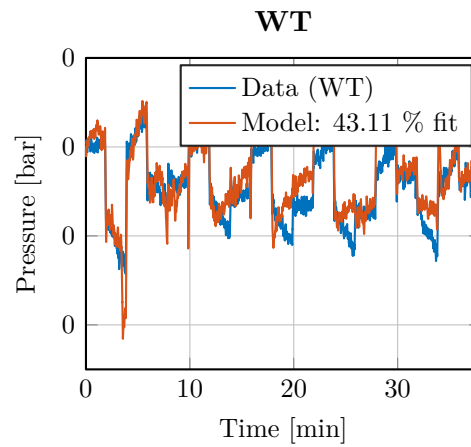


Figure F.14. Estimation comparison for WT.

To minimize the running cost of the system, the power consumption of the pumps, P_e Cf. Section 4.1.3: *Pump model*, and the electrical price, $c_p[k]$, is considered. Predicting future prices is an extensive task that depends on many factors e.g user consumption and weather conditions. Due to the fact that the main focus of this project is not to derive a high precision predictive model that describe future electrical prices, data is used from [38] instead. The price function can be seen in *Figure G.1*.

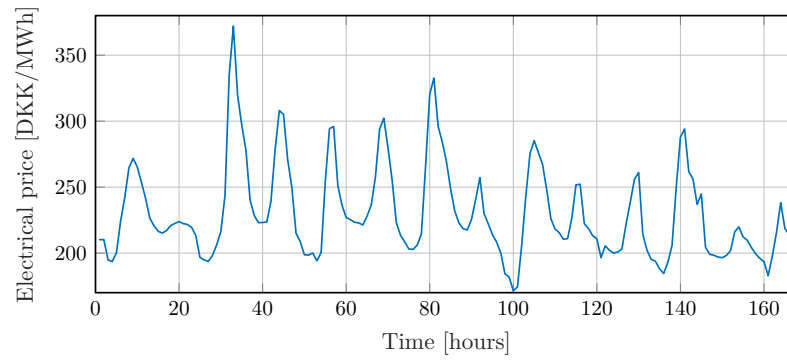


Figure G.1. $c_p[k]$, describing the electricity prices in Denmark from the 27-03-2017 to 02-04-2017.

As this is a real data from a given period, most likely it does not fit the pricing in any other given week, as the pricing is fluctuating a lot from day to day. However, the data indicates that the pricing is higher in the morning and evening which is applicable for any given week and thereby is a general property of the time dependent pricing. This behavior can be seen as the periodicity of the data with two peaks a day. The chosen data thus gives a realistic idea of the improvement of the controller which can be achieved in a real world scenario based on the week on which the data is recorded.

Pump linearization and PI controller



The control structure chosen in Chapter 5.1: *Control Problem* and Figure 5.1 includes a PI controller, which is to be designed. The PI controllers purpose is to accommodate the pressure reference from the MPC controller.

The control focus of this project has been on the model predictive control, see Section 5.2: *Model predictive control*. Therefore a simple PI controller has been designed, where the control structure can be seen on Figure H.1.

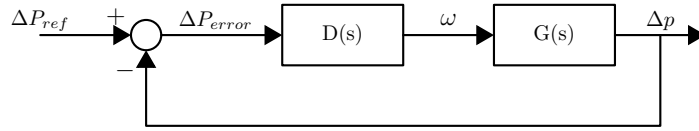


Figure H.1. The structure of the PI controller and the plant, where $D(s)$ is the PI controller and $G(s)$ is the plant i.e the two valves and the pump. The input is the pressure differential reference.

The reference from the MPC is a differential pressure, which is to be controlled through the rotational speed of the pumps. The model for the pumps is seen in Section 4.1.3: *Pump model* and is given by:

$$\Delta p = -a_{h2}q_i^2 + a_{h1}\omega_r q_i + a_{h0}\omega_r^2$$

By the assumption that the flow is constant, the expression can through a Taylor expansion be linearized, with respect to ω , to a small-signal model as seen in Equation: (H.1).

$$\begin{aligned} \Delta \hat{p} &= a_{h1}q\hat{\omega} + 2a_{h0}\omega_r\hat{\omega}_r \\ &= (a_{h1}q + 2a_{h0}\omega_r)\hat{\omega}_r \end{aligned} \tag{H.1}$$

By Laplace transform and solving for the input output relation of the plant $G(s)$, the linearized pump model can be found as seen in Equation: (H.2).

$$G(s) = \frac{\Delta \hat{p}}{\hat{\omega}} = a_1q + 2a_0\bar{\omega} \tag{H.2}$$

The chosen pump speed operating points, seen in H.3, are applied to the related pumps and the differential pressure over the pumps and their respective valves, as seen on Figure C.2, are measured. The data can be found on the attached storage under the path: CD:/Data/Steadystate and seen in H.3.

$$\begin{aligned}
\bar{\omega}_{C18} &= 0.16 & \Delta \bar{P}_{C18} &= 0.0877 \\
\bar{\omega}_{C25} &= 0.4 & \Delta \bar{P}_{C25} &= 0.2598 \\
\bar{\omega}_{C2} &= 0.4 & \Delta \bar{P}_{C2} &= 0.2008 \\
\bar{\omega}_{C16} &= 0.4 & \Delta \bar{P}_{C16} &= 0.1960
\end{aligned} \tag{H.3}$$

From this the flow in the operating point through the pumps can be estimated by *Equation: (4.43)* as the respective pump parameters are found in *Appendix: C* and thus q is the only unknown variable. Solving for \bar{q} yields two results due to the second order equation, thus only the positive results is used as negative flow through the pump is infeasible combined with positive differential pressure. The flow can be seen in H.4.

$$\begin{aligned}
\bar{q}_{C2} &= 0.442 & \bar{q}_{C16} &= 0.440 & \bar{q}_{C18} &= 0.229 & \bar{q}_{C25} &= 0.430
\end{aligned} \tag{H.4}$$

By inserting the values for the linearized model in *Equation: (H.2)*, the final models ends up as gains, see H.5, where $G_{c(n)}$ is the different linearized pump models.

$$\begin{aligned}
G_{C2}(s) &= 0.966 & G_{C16}(s) &= 0.976 & G_{C18}(s) &= 0.217 & G_{C25}(s) &= 0.546
\end{aligned} \tag{H.5}$$

PI controller

As it can be seen in *Appendix: I.1* the time constant of the WT is 1155 seconds. Therefore a controller that can settle within 10 seconds will be considered fast enough for the system. Furthermore the input to the pumps have to be within 0 - 1.0 bar, due to saturation, see [39] "DPI, 0 - 1.0 bar". Due to this constraints, the upper bound of the differential pressure over the main pumps is set to 0.95 bar, which is 0.05 bars below the maximum. Therefore the overshoot and steady state error should not exceed 5% of the reference value as this will saturate the differential sensors. The transfer function for a PI controller can be described by *Equation: (H.6)*

$$PI = K_p + \frac{K_i}{s} \tag{H.6}$$

Where

PI	is the proportional integral controller,	$[\cdot]$
k_p	is the proportional gain,	$[\cdot]$
K_i	is the integral gain	$[\cdot]$

Using the Matlab design tool box for dynamical systems, the PI controller can be found. The proportional and integral gains for the pumps are shown in *Equation: (H.7)*.

$$\begin{aligned}
k_{p,c2} &= 1.39 & k_{p,c16} &= 1.39 & k_{p,c18} &= 5.89 & k_{p,c25} &= 2.57 \\
k_{i,c2} &= 1.39 & k_{i,c16} &= 1.39 & k_{i,c18} &= 5.89 & k_{i,c25} &= 2.57
\end{aligned} \tag{H.7}$$

A step response of the different controllers with their respective linearized pump models, see H.5 is shown in *Figure H.2*, where it can be seen that they settle within ten seconds and have no overshoot.

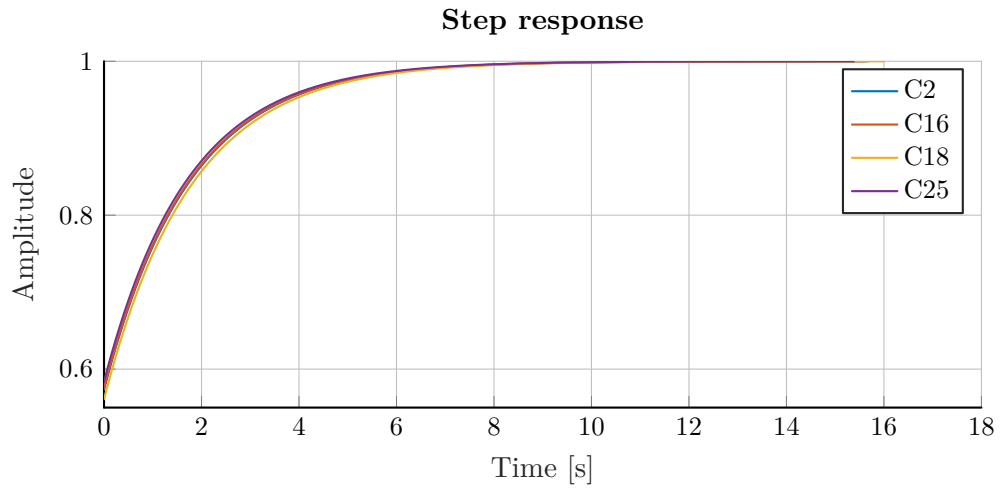


Figure H.2. Closed loop step response of the PI controllers and models.

The PI controller are implemented on the water system described in Chapter 2.1: *System overview* and tested. In *Figure H.3* the step response of the pumps can be seen. The system is starting in a steady state position of 0.15 bars and is then giving a step increase of 0.15 bars to each pump at different times. It can be seen that the pumps have some small deviations compared to the desired steady state value. This is however deemed sufficient, since the largest deviations are between ± 1.5 [mbar].

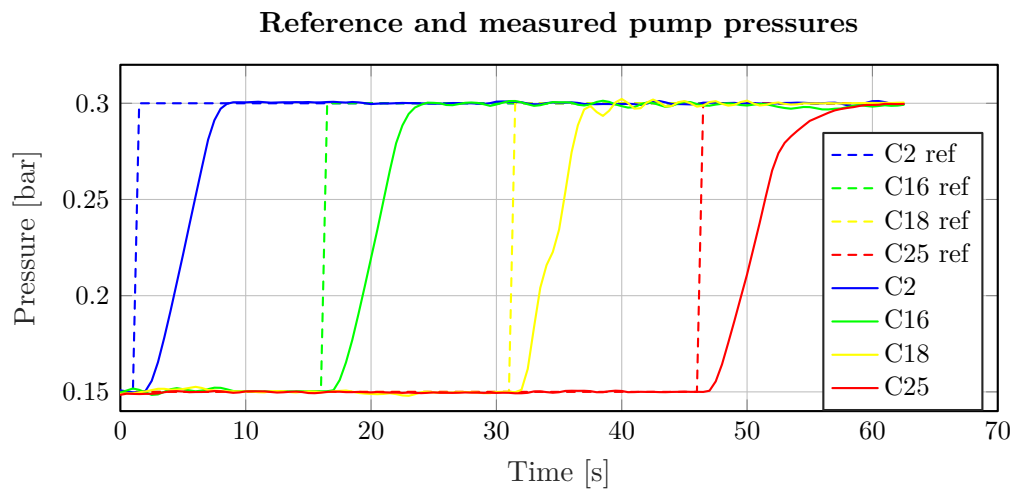


Figure H.3. Step response of the water system, where the different PI controllers are implemented on the respective pumps.

I.1 System time constant

Purpose:

The purpose of this test is to determine the time constant and settling time of the water distribution network.

Test equipment:

- The water distribution system at AAU [AAU No: 100911]

Procedure:

The following procedure was made for finding the time constant:

1. Wait for the system to get into a steady state position with the following system setup: valve opening at 0.7% for all consumer valves and differential pressure over pumps at $C2 = C16 = 0.2[\text{bar}]$, $C18 = 0.1[\text{bar}]$, $C25 = 0.25[\text{bar}]$.
2. Increase the differential pressure over C2 with $0.1[\text{bar}]$.
3. Wait 1.5 hour for the level in the WT to settle.

Measuring data:

The measurements data can be found on the attached storage under the path: CD: /Data/WTtimeconstant, a plot of the data is shown in *Figure I.1*.

Results:

The time constant of the system can be found through the linear differential equation shown in *Equation: (4.108)*. By Laplace transform and solving for the input output relation, the standard form of the transfer function for the system can be derived as seen in *Equation: (I.1)*

$$\begin{aligned}\Delta \dot{p}_{wt} &= A_p \Delta \hat{p}_{wt} + B_p \hat{u} \\ s \Delta p_{wt}(s) &= A_p \Delta \hat{p}_{wt}(s) + B_p \hat{u}(s) \\ \frac{\Delta p_{wt}(s)}{u(s)} &= \frac{B}{s - A} = \frac{\frac{B}{A}}{\frac{1}{A}s + 1}\end{aligned}\tag{I.1}$$

From the denominator, the time constant of the system can be directly read as seen in *Equation: (I.2)*

$$\tau s + 1\tag{I.2}$$

Since A in *Equation: (4.108)* is a scalar, due to the first order model only having one state, the system has one time constant.

As the dynamics of the water distribution network are described by a first order system, the time constant can be found as the time the system uses to reach 63.2% of the steady state pressure. This pressure at 63.2% of the steady state values is based on the minimum and maximum pressure values during the step and determined to:

$$(0.137 - 0.127) \cdot 63.2\% = 0.0063 \rightarrow 0.127 + 0.0063 = 0.133 \quad [\text{bar}] \quad (\text{I.3})$$

Based on the data it is determined that at a pressure of 0.133 bar has 1155 seconds passed which corresponds to 19,25 minutes, thus the time constant is determined. On *Figure I.1* the measurement data used to determine the time constant of the WT is shown. A small red dot indicates the time constant for the tank.

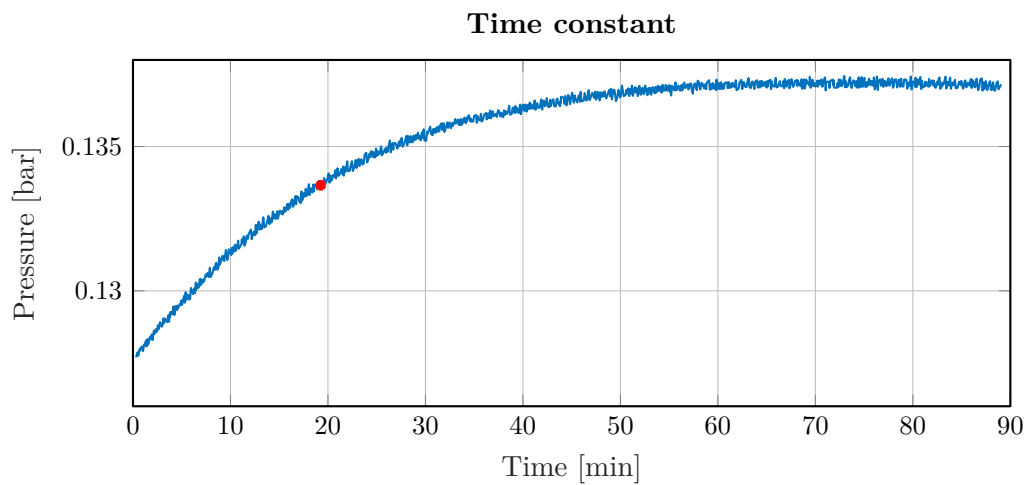


Figure I.1. The WT pressure during a step and a red dot indicating the time constant.

Uncertainties of measurement:

- The settling time for the initial state was not reached after 1.5 hours, which would affect the calculated time constant.

Conclusion:

From this test the time constant is determined. The results is based on the fact that the water distribution network dynamics can be described by a first order system, thereby is the time constant found by applying a step to the system and determined to be 19,25 minutes.

I.2 System dynamics

In this section the speed of dynamics for the test setup without the WT is investigated.

Test equipment:

- The water distribution system at AAU [AAU No: 100911].

Procedure:

The following procedure was made for finding the time constant:

1. Disconnect the WT from the test setup.
2. The initial setup of the system at time $t=0$ is chosen as, the valve opening at 0.7 for all consumer valves and the rotational speed of the pumps set to $C2 = C16 = 3$, $C18 = 0.7$, $C25 = 4.2$.
3. Reduce the rotational speed of C2 and C16 to 1.2 at time $t=30$.
4. Increase the rotational speed of C2 and C16 to 2.5 at time $t=45$.
5. Reduce the rotational speed of C2 and C16 to 1.5 at time $t=60$.
6. Increase the rotational speed of C2 and C16 to 3 at time $t=75$.

Measuring data:

The measurements data can be found on the attached storage under the path: CD:/Data/systemdynamics.

Results:

The step input given to the rotational speed of the two main pumps results in a change of differential pressure across the pumps. The measured differential pressure is shown in *Figure I.2*.

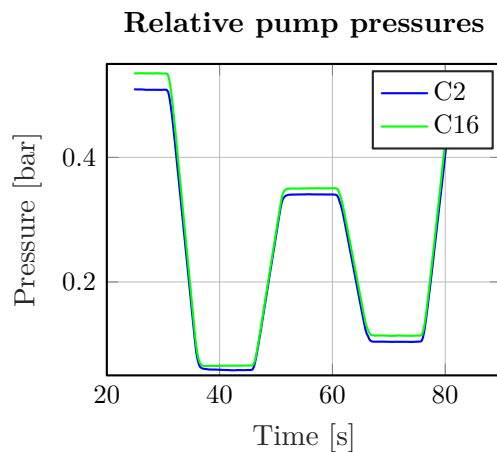


Figure I.2. The measured differential pressure across the pumps.

The differential pressure change across the pumps affects the remaining system and the resulting pressures in the main ring and the PMA's. The pressure in the ring is measured at node 4 and node 5, the measurements are shown in *Figure I.3*. The pressure in the pma is measured at node 10 and node 15, the measurements are shown in *Figure I.4*.

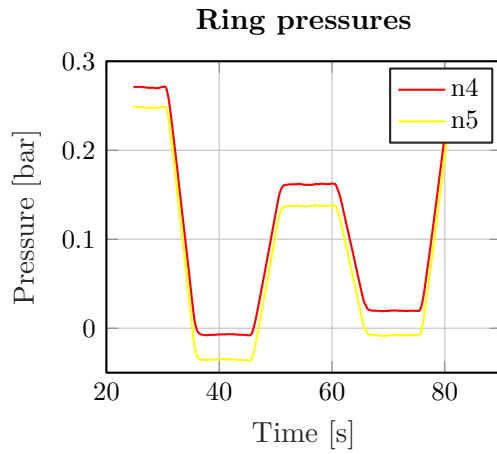


Figure I.3. Estimation comparison for node 10.

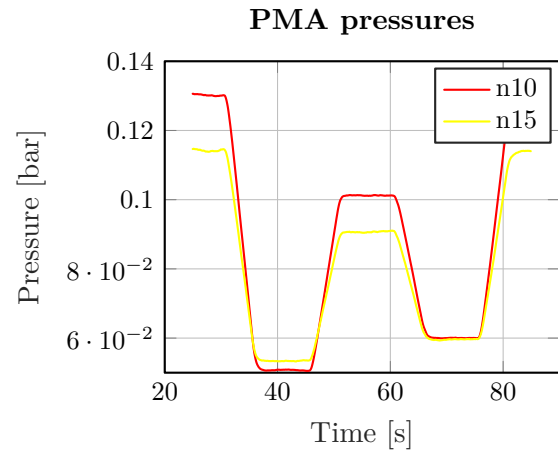


Figure I.4. Estimation comparison for node 11.

From the measurement data it is seen that the pressure in both the PMA and the main ring follows the pressure changes across the main pumps. Furthermore it is seen that this is happening without noticeable time delay. An absent time delay between the change in pump pressure and the pressure in the systems suggest that the dynamics of the system describing flow and pressure in the pipes is faster than the pump dynamics. This is furthermore indicated by the pressure in the system, which settles with the pumps and thus the true pipe dynamics are not exposed at the system cannot be excited sufficiently.

Based on these results it can be concluded that the dominating timeconstant in the full system is the one of the WT which is determined to approximately 20 minutes and further described in *Appendix: I.1*.

Conclusion:

From this test the dynamics of the system without the WT are tested. It is found that the pressure in the nodes settles almost simultaneously with the pump pressure, thus indicating that the observable dynamics found in this test are bound by the pump dynamics.

Test considerations



In this section some considerations about how the controller, designed in Chapter *II: Control Design*, should have been tested on the available test setup are given. These are based on the desire to verify if the requirements are met, these are described in Chapter *3: Requirements and Constraints* as keeping the pressure at each CP above the desired minimum while minimizing the running cost of the system.

The MPC is designed with a receding horizon control with a 24 hour control horizon due to the behavior of the electrical price and the water consumption which both have a periodicity of 24 hours. Based on this, a test conducted over a 24 hour period would allow to investigate the main characteristics of the MPC when price and consumption deviations during a day occur due to the periodicity of the data. The controller will be tested according to the requirements found in Chapter *3: Requirements and Constraints*, these are:

- Pressure at CP, $0.08 < y < 0.14$ [bar]
- Minimizing the total cost of running the system

A results of such a test could then be compared to a system without MPC in order to verify if the MPC is capable of saving money, and in what degree.

Bibliography

- [1] N. R. Council *et al.*, *Public Water Supply Distribution Systems: Assessing and Reducing Risks—First Report*. National Academies Press, 2005.
- [2] B. Appelbaum, “Water & sustainability (volume 4): Us electricity consumption for water supply & treatment—the next half century,” 2002.
- [3] Y. X. J.N. Tsitsiklis, “Pricing of fluctuations in electricity markets,” *European Journal of Operational Research*, 2015.
- [4] M. Feldman, “Aspects of energy efficiency in water supply systems,” in *Proceedings of the 5th IWA Water Loss Reduction Specialist Conference, South Africa*, pp. 85–89, 2009.
- [5] Watts, “Water pressure regulators frequently asked questions.” Last visited 14-02-2017, <http://www.watts.com/pages/faq.asp?catId=64&faqId=7>.
- [6] Lenntech, “Why oxygen dissolved in water is important.” Last visited 14-02-2017, http://www.lenntech.com/why_the_oxygen_dissolved_is_important.htm.
- [7] S. Murphy, “General information on dissolved oxygen.” Last visited 14-02-2017, <http://bcn.boulder.co.us/basin/data/NEW/info/DO.html>.
- [8] Grundfos, “Upml geo and upmxl geo oem.” Last visited 02-03-2017, <http://www.grundfos.com/products/find-product/upml-geo-upmxl-geo-oem.html#overview>.
- [9] Grundfos, “Upm2, upm geo, upm2k.” Last visited 02-03-2017, net.grundfos.com/Apl/WebCAPS/Grundfosliterature-4927111.pdf.
- [10] PE100, “What is the meaning of the designations pe80 and pe100.” Last visited 02-03-2017, <https://www.pe100plus.com/PE-Pipes/PE-technical-guidance/model/Materials/mrs/What-is-the-meaning-of-the-designations-PE80-and-PE100-i254.html>.
- [11] M. MØlgaard and B. G. Pétursson, *Energy Optimization of Water Distribution Networks*. 2015. Master thesis, Aalborg University.
- [12] C. Kallesøe and C. Persis, “Pressure regulation in nonlinear hydraulic networks by positive controls,” *Proceedings of the European Control Conference Budapest, Hungary*, 2009.
- [13] B. Hunt, *Fluid Mechanics for Civil Engineers*. University of Canterbury, 1995.
- [14] A. K. S. Prabhata K. Swamee, *Design of Water Supply Pipe Networks*. John Wiley & Sons, 2008.
- [15] Y. Nakayama, *Introduction to Fluid Mechanics*. Butterworth Heinemann, 1999.
- [16] N. Trifunovic, *Introduction to uUrban Water Distribution*. Balkema, 2006.
- [17] H. Boysen, *k_v:what,why,how,whence?* Danfoss A/S, 2011.

- [18] U. Keller, *Method for the Hydraulic Compensation and Control of a Heating or Cooling System and Compensation and Control Valve Therefor*. BELIMO Holding AG, Hinwil(CH), 2009.
- [19] C. Kallesøe, *Fault Detection and Isolation in Centrifugal Pumps*. 2005. Ph.D. thesis, Aalborg University.
- [20] W. Borutzky, *Bond Graph Methodology*. Springer London, 2010.
- [21] C. D. Persis and C. S. Kallesøe, “Pressure regulation in nonlinear hydraulic networks by positive and quantized controls,” *IEEE TRANSACTIONS ON CONTROL SYSTEMS TECHNOLOGY*, vol. 19, November 2011.
- [22] N. Deo, *Graph Theory with Applications to Engineering and Computer Science*. 2004.
- [23] C. K. J. L. Maryamsadat Tahavori, Tom Nørgaard Jensen and R. Wisniewski, “Toward model-based control of non-linear hydraulic networks,” July 2012.
- [24] M. S. P. Kaare Brandt Petersen, *The Matrix Cookbook*. 2012.
- [25] PE100, “Nonlinear grey-box models.” Last visited 07-04-2017, <https://se.mathworks.com/help/ident/nonlinear-grey-box-models.html>.
- [26] MathWorks, “Compare.” Last visited 07-05-2017, <https://se.mathworks.com/help/ident/ref/compare.html>.
- [27] G. F. Franklin, J. D. Powell, and A. Emami-Naeini, *Feedback control of dynamic systems*, vol. 7.
- [28] E. F. Camacho and C. Bordons, *Generalized Predictive Control*, pp. 47–79. London: Springer London, 2007.
- [29] M. I. of Technology, *Introduction to Convex Constrained Optimization*. 2004.
- [30] B. Van Roy and K. Mason, “Formulation and analysis of linear programs,” *Unpublished manuscript*, 2005.
- [31] MathWorks, “Getting started with the control system designer.” Last visited 07-05-2017, <https://se.mathworks.com/help/control/examples/getting-started-with-the-control-system-designer.html?prodcode=ML>.
- [32] K. Hauser, *Convex Optimization and Interior-Point Methods*. 2012.
- [33] Polypipe, “Effast pvcu and abs - high performance pvcu and abs pressure pipe systems. 2008.” Last visited 07-05-2017, <http://www.sbsdownloads.co.uk/Supplier/Polypipe%20Terrain/Product%20%20Installation%20Guides/Installation%20Guides/Effast%20PVCu%20and%20ABS%20Technical%20Installation%20Guide.pdf>.
- [34] G. Fischer, “For pe piping systems in utilities.” Last visited 07-05-2017, <http://www.gfps.com/content/dam/gfps/master%20Content/Documents/EN/Planning%20Fundamentals/PL%20VS%20en.pdf>.
- [35] Belimo, “Technical databook.” Last visited 07-05-2017, http://www.belimo.com.cn/pdf/CCV_databook%5B15.04.2011%5D.pdf.
- [36] Belimo, “2-way and 3-way characterised control valves.” Last visited 07-05-2017, http://www.belimo.ch/pdf/e/project_2-way_3-way_Characterised%20control%20valves.pdf.

- [37] MathWorks, “Estimate linear grey-box models.” Last visited 07-05-2017, <https://se.mathworks.com/help/ident/ug/estimating-linear-grey-box-models.html>.
- [38] “Elspot prices.” Last visited 19-04-2017, <http://www.nordpoolspot.com/Market-data1/Elspot/Area-Prices/DK/Hourly/?dd=DK2&view=chart>.
- [39] Grundfos, “Pressure transmitters and sensors.” Last visited 22-05-2017, http://www.grundfos.com/content/dam/Global%20Site/direct-sensors/Databooklets/97790251_1216_Pressure%20transmitters%20and%20sensors_DB_GB.PDF.